TECHNISCHE UNIVERSITÄT WIEN
Vienna University of Technology

Diplomarbeit

Soil to Oil: Comparative Analysis of the Processing of Soybean Oil and Palm Oil in an Internally Circulating FCC Pilot Plant

ausgeführt zum Zwecke der Erlangung des akademischen Grades eines Diplom-Ingenieurs
am Institut für Verfahrenstechnik, Umwelttechnik und Technische Biowissenschaften E166

unter der Leitung von

Ass. Prof. Dipl.-Ing. Dr.techn. Alexander Reichhold

eingerichtet an der Technischen Universität Wien
Fakultät für Technische Chemie

von

Cornelius Kipyego Lagat
Pappenheimgasse 8/23
A-1200
Matr. Nr.: 1228403

Wien, am 01.04.2015 Cornelius Kipyego Lagat

…….To Sr. Ali,

for journeying with me.

ACKNOWLEDGEMENT

I would like to express my sincere gratitude to all those who made the culmination of this work possible.

My utmost appreciation first and foremost goes to Ass. Prof. Dipl.-Ing. Dr.techn. Alexander Reichhold for the opportunity he afforded me to join his working group and for the invaluable ideas that I learnt during my time in the group. Professor Reichhold´s intellectual heft is matched by his friendly nature and I was honoured to have worked with him.

I would like to express my warm thanks to my supervisors in the working group, Dipl.-Ing. Josef Fimberger and Dipl.-Ing. Mark Berchtold, for their support, patience and guidance throughout the course of the project and in the writing of this thesis. I would also thank my fellow colleagues in the office for their input in this work and for the great atmosphere in the office. I would especially like to thank Dipl.-Ing Gerhard Hofer for the encouragement and above all the collegiality.

Finally, my special appreciation goes to my family, friends and benefactors for making this journey a success. I would be remiss if I did not acknowledge your contribution. Words cannot express my gratitude but I must say I am truly indebted to you for your advice, financial support, input and prayers. May the Lord bless you abundantly.

ABSTRACT

The Intergovernmental Panel on Climate Change (IPCC) in its latest synthesis report paints a gloomy picture of the years ahead if the current greenhouse gas emission levels are not arrested. The major contributor to the rising emissions is fossil fuels with the transport sector being the major driver of spiralling $C0_2$ emissions. It is on this premise that the growth of the biofuels sector is thus based.

Fluid Catalytic Cracking (FCC) is a refinery process that can be employed to produce biofuels. Vienna University of Technology has established a fully continuous FCC pilot plant with a compact design that can be used to process various feedstocks at a comparable industrial level. This present study investigated the cracking of vegetable oils.

The gist of this study was twofold: The first was the cracking of vegetable oils at low temperatures and second to compare the product spectrums obtained when palm oil and soybean oil are cracked. The former makes this study stand out since catalytic cracking at low temperatures has not been performed before in the pilot plant. Selection of the two vegetable oils was based on their structure and market share. Palm oil is composed majorly of saturated fatty acids (50%) whilst soybean oil of polyunsaturated fatty acids (61%). Together, the two vegetable oils command a market share of about 65% of the total vegetable oils production.

The processing temperatures ranged from 430 – 550°C (Standard FCC). An effect of the unsaturation content on the product spectrum was observed with a higher unsaturation content increasing the effect of secondary transformations. Both oils showed good conversion yields with gasoline posting an optimum output at around 515°C. The gasoline also recorded high octane numbers (RON circa 100) with no oxygenates present. A substantial amount of economically viable olefin gases was also yielded. In addition Light Cycle Oil (LCO) was maximized at low temperatures.

KURZFASSUNG

Der Intergovernmental Panel on Climate Change (IPCC, der Zwischenstaatliche Ausschuss für Klimaänderungen) zeichnet in seinem jüngsten Synthesebericht ein düsteres Bild der kommenden Jahre, wenn die aktuellen Treibhausgas-Emissionswerte nicht reduziert werden. Die Hauptursache für die steigenden CO_2 Emissionen fossiler Brennstoffe stellt der Verkehrssektor dar. Das Wachstum des Biokraftstoffsektors beruht auf dieser Prämisse.

Fluid Catalytic Cracking (FCC) ist ein Raffinerieprozess, der zur Herstellung von Biokraftstoffen verwendet werden kann. Die Technische Universität Wien hat eine voll kontinuierliche FCC Pilotanlage mit einer kompakten Bauweise etabliert, die verwendet werden kann, um verschiedene Rohstoffe vergleichbar zum Industriemaßtab zu verarbeiten. Die vorliegende Studie untersuchte das Cracken von Pflanzenölen.

Das Ziel dieser Studie war einerseits das Cracken von Pflanzenölen bei niedrigen Temperaturen und andererseits der Vergleich der für Palmöl und Sojaöl erhaltenen Produktspektren. Der erster Teil dieser Studie ist einzigartig, da das katalytische Cracken bei so niedrigen Temperaturen in der Pilotanlage noch nie durchgeführt wurde. Die Auswahl der beiden Pflanzenöle wurde von ihrer Struktur und ihrem Marktanteil beeinflusst. Palmöl besteht hauptsachlich aus gesättigten Fettsäuren (50%), Sojaöl aus mehrfach ungesättigten Fettsäuren (61%). Die zwei Pflanzenöle haben einen Marktanteil von etwa 65% der gesamten Pflanzenöl-Produktion.

Die Verarbeitungstemperaturen lagen im Bereich von 430 bis 550°C. Der Grad der Ungesättigtheit hatt einen signifikanten Einfluss auf das Produktspektrum. Bei einem höheren Grad treten sekundäre Umwandlungsprozess verstärkt auf. Beide Öle zeigten gute Gesamtkonversionsraten mit einer optimalen Benzin Ausbeute bei etwa 515°C. Das erhaltene Benzin ist qualitativ hochwertig mit Oktanzahlen (ROZ) von ca. 100 und ohne sauerstoffhaltige Verbindungen. Ebenso konnte auch ein hoher Anteil an den wirtschaftlich bedeutenden gasförmigen Olefinen erzielt werden. Zusätzlich wurde der Anteil von Light Cycle Oil (LCO) bei niedrigen Temperaturen maximiert.

TABLE OF CONTENTS

1 INTRODUCTION

1.1 Energy Demand

It is envisaged that in the coming years the energy demand in the world will be driven by an increasing population and economic growth. According to projections from UNPD[1], the world's population is expected to hit the 8.1 billion threshold by the year 2025 and 9.6 billion by 2050 [1]: An increase from the 6.8 billion estimated in 2010 with India and China accounting for about a third of this population. Increased population in the urban areas will see a concomitant increase in the energy demand to satiate this population. The bulk of this energy will be supplied by fossil fuels with crude oil playing a central role due to the strong impetus from the transportation sector. Crude oil falls into the category of fossil fuels alongside coal and natural gas with IEA[2] statistics for 2012 indicating that fossil fuel accounted for 81.7% of the total energy supply [2].

According to the IEA, as of 2011, 32 million barrels of oil were produced with the major oil producers being Russia, Saudi Arabia and the USA. Spurred by the boom in extraction of tight oil, the USA is on a cusp of a new era of oil production and projections by IEA will see her overtake Russia and Saudi Arabia to become the leading producer of oil by the year 2015. On her part BP3, in its energy outlook released in January 2014 [3], projects that by the year 2035, the renaissance of this energy sector will see the USA becoming energy self-sufficient.

The domino effects of the shale revolution which has seen a sudden surge in US oil production are being felt at the moment with prices of crude oil tumbling down from 110 USD per barrel to values below 50 USD per barrel recorded in January 2015. This slump has had repercussions on businesses and oil exporting countries´ economies that have been riding on the crest of high oil prices. Analysts are predicting though that the price will inevitably rebound.

Though there will be an increase in fossil fuel production in the coming years, BP in its forecast as captured in Figure 1.1, gives a trajectory where oil will only account for about 27% of the total energy supply in the year 2035, a drop of about 5% when compared to the year 2012 as a result of an increased use of renewables, nuclear and hydro power.

[1] United Nations Population Division
[2] International Energy Agency
[3] British Petroleum

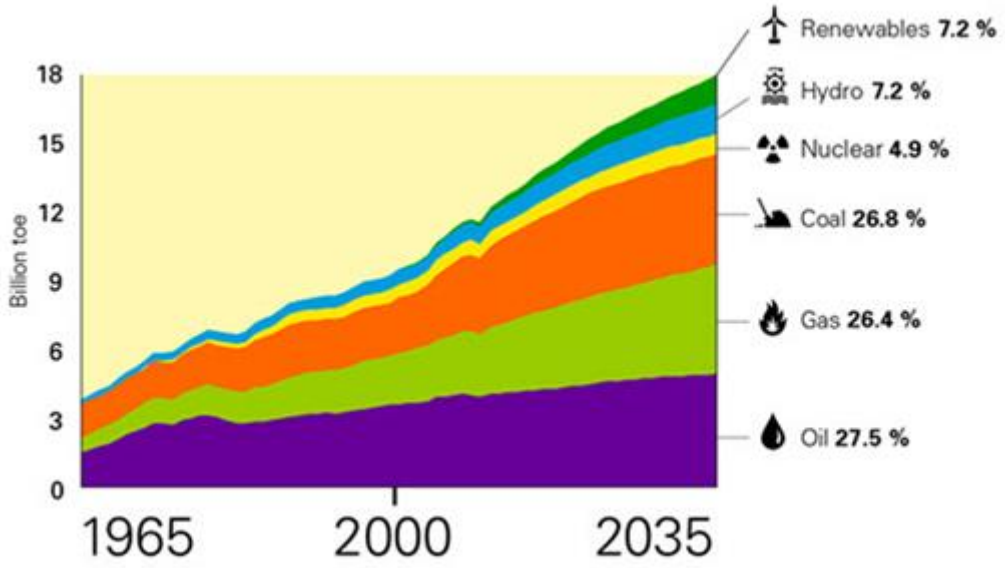

Figure 1.1 *Energy projections [4].*

1.2 Rationale for Alternative Fuels

The concerns over the effects of fossils fuels on climate change coupled with the unpredictability of oil prices as a consequence of volatile political climates especially in the oil rich Middle East, have spawned the need to seek alternative methods to produce transport fuel. Gasoline and diesel are by far the most commonly used fuels in the transportation sector and their availability at reasonable prices will always have a ripple effect on the economy.

The subject of increased CO_2 emissions, needless to say is germane to our society today. Since the Mauna Loa Observatory was set up in 1958, CO_2 emissions – the primary driver of climate change – have increased by 24% with record levels reached in May 9, 2013 when the daily mean concentration surpassed the 400 ppm[4] mark for the first time in history [5]. According to preliminary estimates as published by the IEA, energy related CO_2 emissions as of 2011 peaked 31.2 Gt[5] which accounted for about 60% – the largest – of the global GHG[6] emission sources [6].

In the latest IPCC synthesis report released on November 2, 2014 as the final part of the IPCC's Fifth Assessment Report (AR5) [7], emphasis on reduction of greenhouse gas emissions has been put at the forefront so as to scale down the impacts to levels that we can comprehensively deal with:

[4] Parts per million
[5] Gigatonnes
[6] Greenhouse gas

'' Substantial emissions reductions over the next few decades can reduce climate risks in the 21st century and beyond, increase prospects for effective adaptation, reduce the costs and challenges of mitigation in the longer term, and contribute to climate-resilient pathways for sustainable development. ''

The report ends with the clarion call that the world needs to change its fuelish ways.

Spurred by such reports, public debate has crystalized the belief that there is a pressing need to shift from fossil fuels to non-fossil fuels in order to mitigate the profound effects of climate change. This explains the need to look for alternative sources of fuel that are sustainable, renewable and eliminate or at the very least reduce green gas house emissions. This is where biofuels come in as one of the alternative fuels since they are considered carbon neutral fuels.

Suffice it to say that the biofuel industry is primed for future growth. Biofuels is not a delusion: it's a solution to an emerging crisis. Though it may not be the silver bullet that will solve the energy crisis, it should be looked at as something that is poised to make major strides towards augmenting the fight against climate change.

1.3 Scope of Thesis

This thesis thus seeks to present the case of biofuels obtained from two types of vegetable oil: palm and soybean oil, by means of catalytic cracking. **Chapter 2** of this study will focus on vegetable oils with regard to their structure, yields, production outlook and market trends. An in-depth look on soybean oil and palm oil apropos of the crop cultivation to the processing of the oils will also be given. The different types of biofuels, their production and future outlook, market trends, their use as fuels as well as the various policies that govern their use as fuels will also be discussed. Finally fluid catalytic cracking as a means of production of biofuels will be covered. **Chapter 3** will dwell on the FCC pilot plant at the Vienna University of Technology with an overview on the feedstocks processed, catalyst used, plant operation and product analysis. The discussion of results obtained from the two vegetable oils processed with emphasis on the effect of the unsaturation content on the yields of various product lumps obtained will be tackled in detail in **Chapter 4**. Finally, **Chapter 5** will offer a summary of the results obtained and a few suggestions on future projects.

2 SOIL TO OIL

This chapter begins by covering various perspectives on the feedstock – vegetable oils – used during this study. A few biofuels will then be covered with the policies that govern their production being spelt out. Finally the chapter will dwell on catalytic cracking as a way of producing biofuels from vegetable oils. Soil to oil thus describes the cycle of biofuel production via the catalytic cracking of vegetable oils.

2.1 Vegetable Oil

2.1.1 Structure

Vegetable oils are referred to as triacylglycerols (TAGs) or commonly as triglycerides due to the fact that they are the major constituents of vegetable oils. A triglyceride is a compound consisting of three fatty acid molecules and glycerol, a trihydric alcohol. Vegetable oils can be both edible and non-edible with palm, soybean, coconut, olive , nut oils et cetera being paradigms of edible oils whereas examples of non-edible oils include Jatropha, *Madhuca indica* and *Pongamia pinnata*.

Rapeseed oil can be both edible and non-edible based on the amount of erucic acid. Industrial rapeseed has high levels of erucic acid and is thus non-edible whereas canola oil refers to rapeseed oil with low levels of erucic acid which makes it edible. The vegetable oil structure is shown in Figure 2.1.

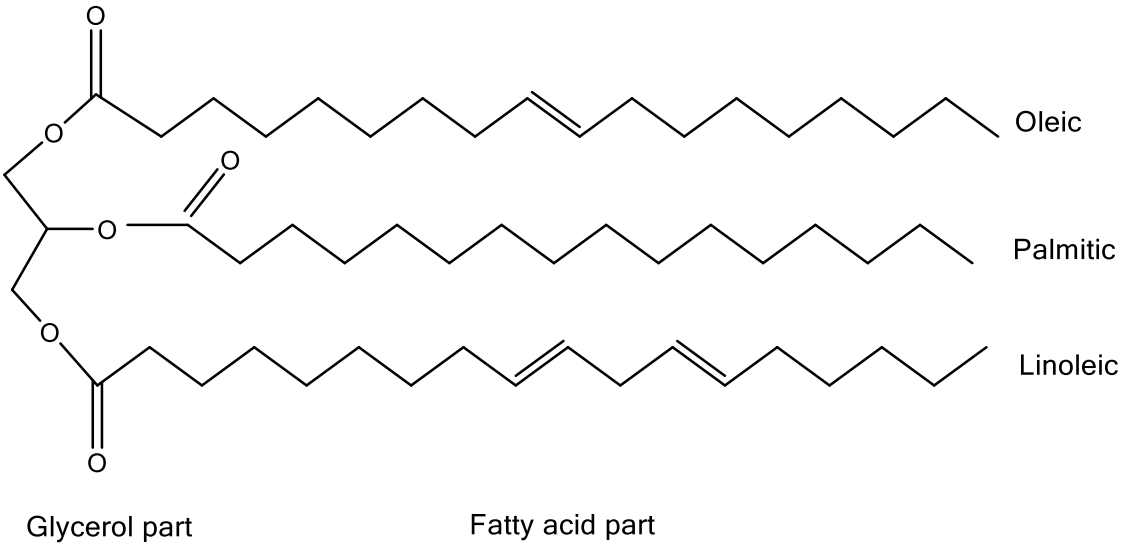

Figure 2.1 *Vegetable oil structure.*

2.1.2 Vegetable Oil Yields

Vegetable oils are obtained from various energy crops and their yields vary from one crop to another. Some of the vegetable oil yields of common energy crops are depicted in Table 2.1. It can be inferred that palm oil produces the most oil per hectare of land and can be estimated as having a production of approximately tenfold more than soybean. The downside of palm oil however, is that palm trees can only thrive in tropical areas and this explains why Malaysia and Indonesia are the dominant palm oil producers.

Table 2.1 *Vegetable oil yields of common energy crops [8].*

Energy crop	Kg oil / Hectare
Corn (maize)	145
Hemp	305
Soybean	375
Mustard seed	481
Safflower	655
Sunflowers	800
Peanuts	890
Opium poppy	978
Rapeseed	1,000
Jatropha	1,590
Coconut	2,260
Oil palm	5,000
Microalage	40,000 – 120,0000

2.1.3 Vegetable Oil Production and Outlook

It is estimated that global vegetable oil production will increase by 28% or 48 Mt by the year 2023 based on the base period 2011-2013 catapulted mainly by improved crop yields and aggressive planting [9]. The bulk of this projected production will come from the major producing countries comprising Indonesia, Malaysia, China, the European Union, the United States, Argentina, Brazil and India with their contribution totalling roughly 77% during the outlook period. A commensurate increase in the use of vegetable oils as biodiesel feedstock within the same outlook period from 10 Mt to 28.8 Mt will likewise be witnessed representing a 50% increase. This will account for approximately 15% of the total vegetable oil consumption. Argentina for instance is expected to consume almost 74% – approximately 3 Mt – of its vegetable oil for biodiesel production.

Figure 2.2 gives a glimpse of the share different types of vegetables contributed towards the total global production in the year 2013/2014. As is plain to see, palm oil is now the leading type vegetable oil produced after wrestling the title from soybean oil some years back. The total vegetable oil production was 171 million metric tons [10].

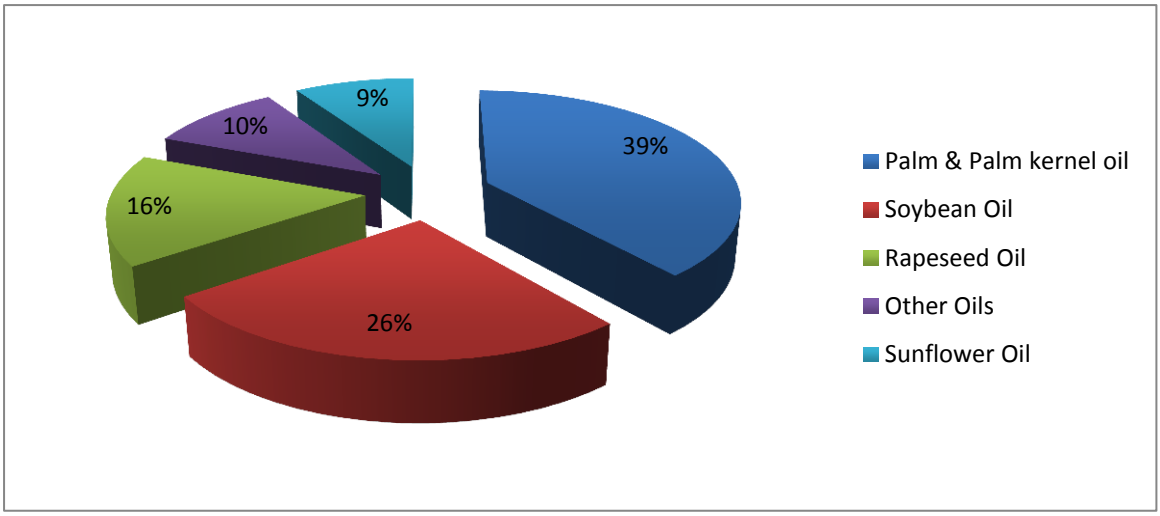

Figure 2.2 *Global vegetable oil production in 2013/2014.*

2.1.4 Vegetable Oil Prices

The price of vegetable oil over the last couple of years has shown some signs of tightening after fluctuations in the period covering the years 2008-2009 as a consequence of the concurrence of several factors. Chief among these factors was the adverse weather conditions which led to a decreased oilseed output and the increased demand for vegetable oil from the biodiesel sector. From the highs of 2010 when the price rocketed to 1150.76 USD/t, global prices of vegetable oil have been on a progressive decline with a price of 804.48 USD/t posted in 2013 whereas the forecast for the outlook period 2014-2023 expects that the price will slump to 740.50 USD/t at the close of the period [9]. These price trends are captured in Figure 2.3.

The declining global vegetable oil prices have been brought about by the sprawling palm plantations and an increased oilseed crop output with another record crop expected in 2014. This should provide a good stock buffer for any unforeseen shortfalls within the outlook period. Underpinned by the different biodiesel policies that will witness various countries seek to attain the quotas set aside for biodiesel coupled with an increase in income and population, the demand for vegetable oil will continue to grow thus averting prices spiralling down further.

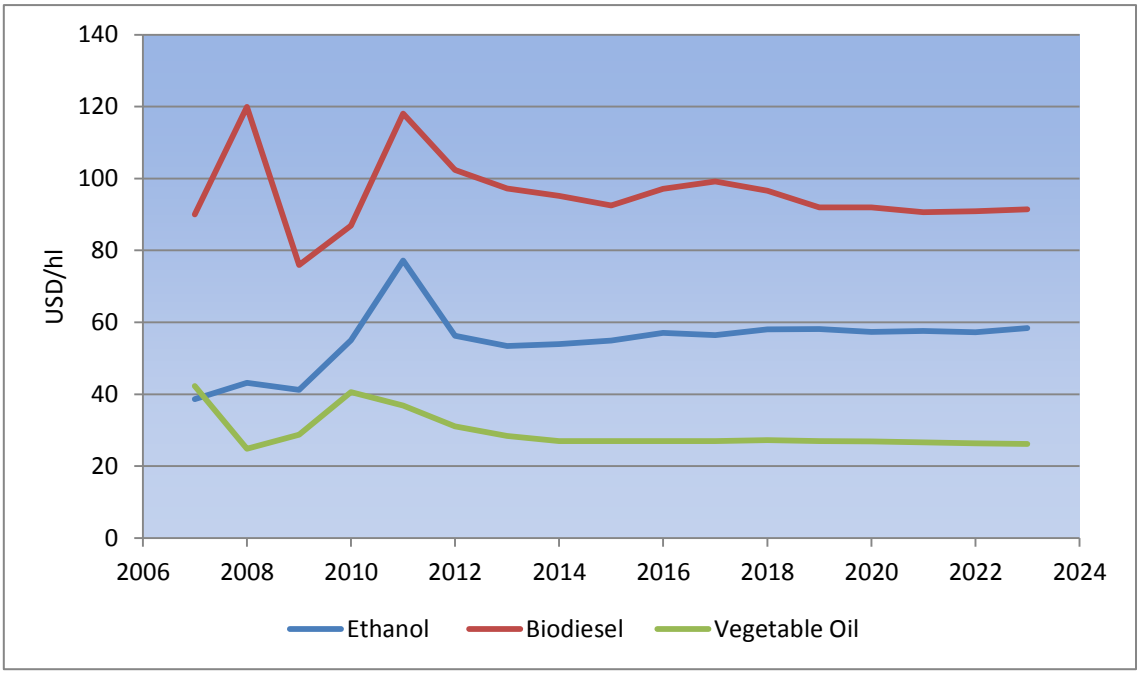

Figure 2.3 *Ethanol, biodiesel and vegetable oil prices [9].*

2.1.5 Soybean Oil

2.1.5.1 Introduction

Due to its numerous uses the soybean has been aptly dubbed the wonder bean or the Cinderella crop. The scientific name of soybean is *Glycine max*. It is a leguminous crop with the highest protein source per gram – 43 grams per 100 grams – and is rich in omega 3 and omega 6 fatty acids essential for the regulation of lipid and cholesterol levels in the body.

The origin of the soybean can be traced back to China and aside from its valuable edible oil, it is also used in the production of soy protein meal which is in turn used in the manufacture of feeds for poultry, cattle and swine.

Major soybean producing countries are captured in Figure 2.4 with the United States leading the pack with an output of 82 million metric tonnes followed by the MERCUSOR[7] countries of Brazil and Argentina. The production in Brazil is expected to reach 105 million metric tonnes by the year 2020 driving force being the availability of large potential arable land.

[7] Mercado Común del Sur

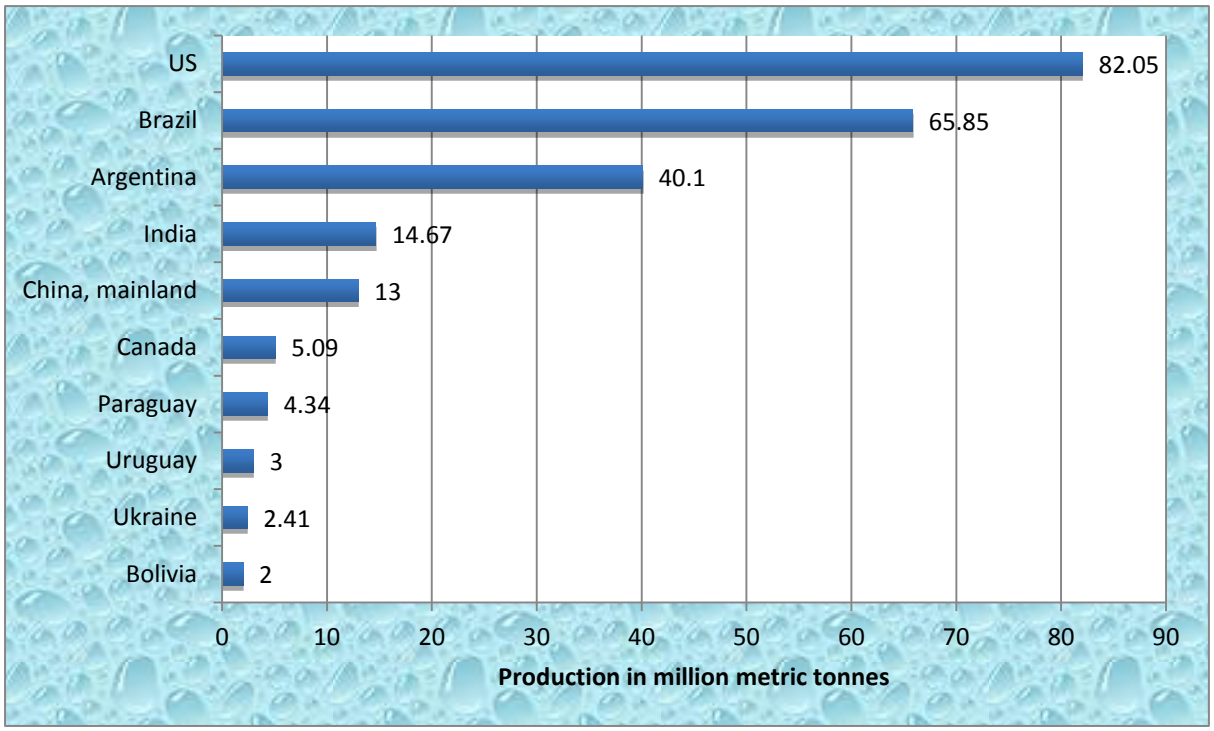

Figure 2.4 *Major soybean producing countries in the year 2012 [11].*

2.1.5.2 Planting and Harvesting

Loose, well drained loam soils are best suited for the planting of soybeans with the soil temperature required for germination being a minimum of 15°C. A good population density for the crop is in the region of 100,000 plants per acre with the spacing varying from 0.4 to 0.6 m.

The maturity time for the soybean crop is usually between 100 to 130 days depending on the variety, the climatic conditions and the region in which it is planted. Most of the plantations the world over are usually rain fed with the average rainfall expected so as to ensure a maximum yield ranging from 450 – 700 mm per season with temperatures ranging from 18 – 35°C considered ideal.

Harvesting of the crop is mechanised and the yield will vary depending on whether the crop was rain fed or irrigated with rain fed giving a yield of 1.5 – 2.5 ton/ ha seed whereas an irrigated crop will yield between 2.5 and 3.5 ton/ha seed.

2.1.5.3 Oil Extraction

The processing and extraction of soybean oil involves a number of procedures. Once the beans arrive at the extraction plant, they are passed through a rotary magnet to remove any tramp metals and thereafter the beans are screened and sieved. After cleaning, the beans are then cracked and dehulled prior to being conditioned which is normally carried out at temperatures of about 70°C. The flaking process then follows before the oil is extracted either mechanically by means of screw presses or by use of solvents – hexane – which is the

choice method in most scenarios. Thereafter the miscella which contains about 70% solvent is passed through a 2 or 3 stage distillation process to recover the solvent followed by drying of the oil. It is worth noting that the use of vacuum distillation is the norm in order to prevent the oil going rancid as a result of the presence of oxygen.

The identity characteristics of soybean oil are tabulated below.

Table 2.2 *Soybean oil identity characteristics [12].*

Identity Characteristic	Observed min. – max.
Relative density, x° C/water at 20°C	0.919 – 0.925 x=20°C
Refractive index, n_D 40°C	1.466 – 1.470
Saponification value, mg KOH g^{-1} oil	189 – 195
Unsaponifiable matter, g/kg	≤ 15
Iodine value, (Wijs)	124 – 139
Flash Point, °C	317
Melting Point, °C	0.6

2.1.6 Palm Oil

2.1.6.1 Introduction

Palm oil biological name *Elaeis guineensis*, is one of the most ubiquitous substances in the global arena. Native to Africa, the palm oil tree is now synonymous with Malaysia and Indonesia due to the fact that they play host to around 85% of the total land – 16.4 million hectares – under palm oil. The major producing countries are captured in Figure 2.5.

The versatility of palm oil is behind its growing production since it can be found in almost 50% of all products in the supermarket and the coming years will see more plantations being added.

The portfolio of palm oil products ranges from food products such as cooking oil, chocolate products as a substitute for cocoa butter, ice cream and processed foods. Palm kernel oil has also similar uses to palm oil though it is used mostly in the production of non-food items such as candles, cosmetics and detergents. Aside from the above mentioned, palm oil is also growingly being used in the energy sector for generation of electricity and in the biofuels sector. Figure 2.6 shows the palm oil consumption in terms of the aforementioned uses.

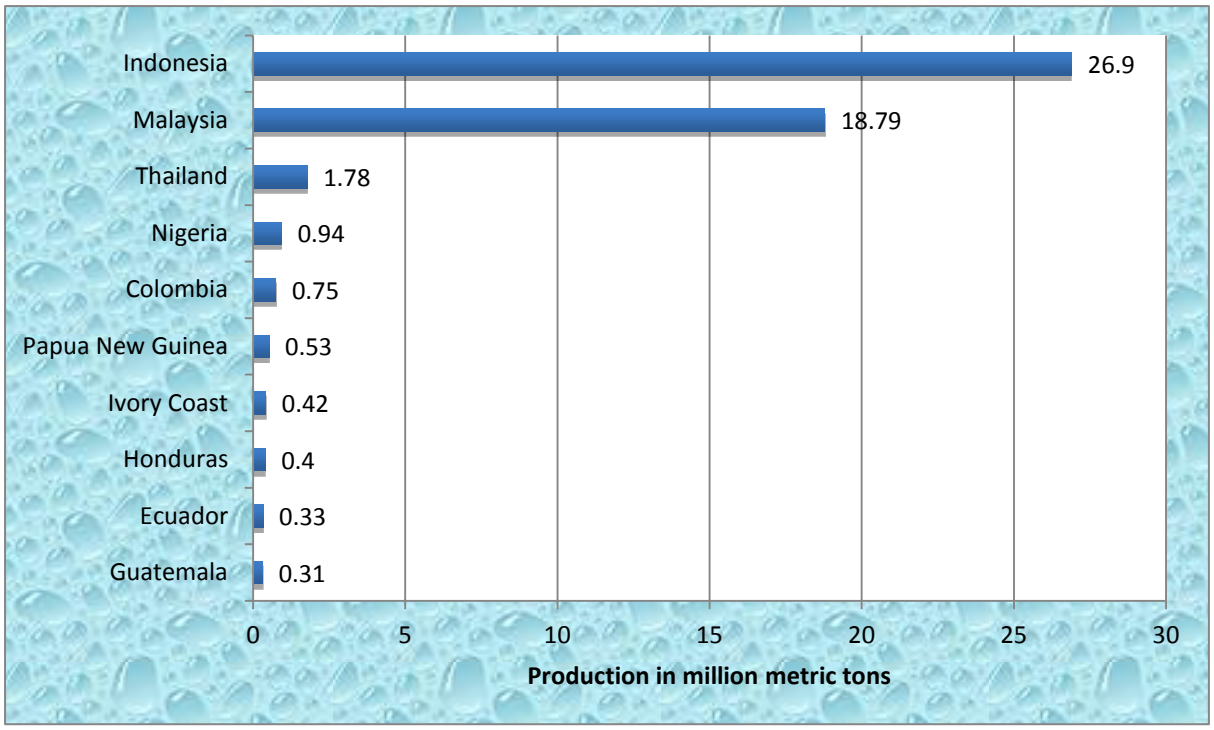

Figure 2.5 *Major palm oil producing countries in the year 2012 [11].*

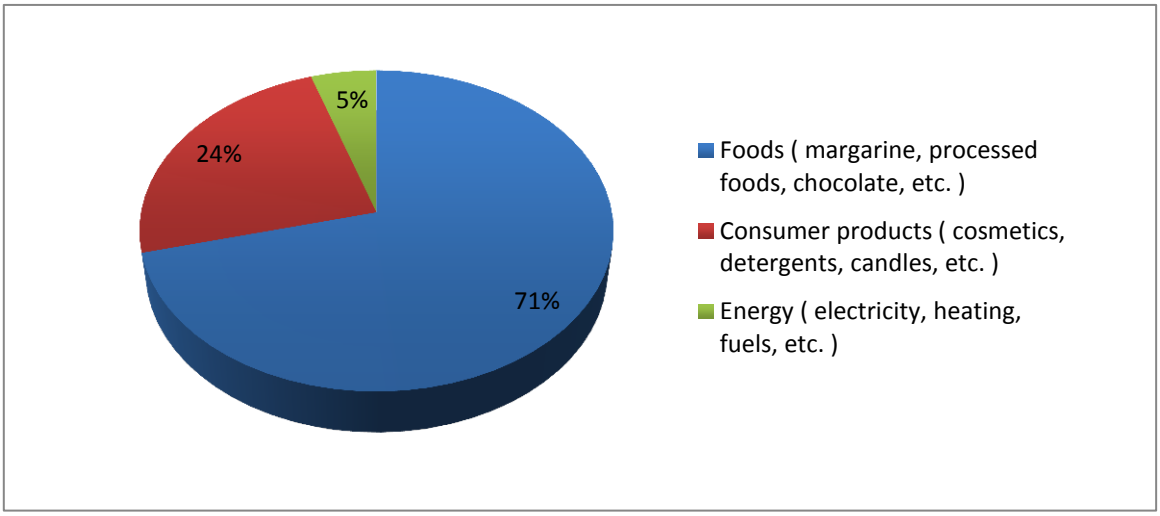

Figure 2.6 *Palm oil consumption by use [13].*

2.1.6.2 Planting and Harvesting

The oil palm thrives in almost all types of soil but the best suited are well-drained deep loamy to loamy-clay fertile soils with growth favoured by humid climates found mostly in the tropics. Germinated seeds are planted in a nursery and after a year the seedlings are transplanted to the palm groves measuring 60*60*60 cm with the seedlings being planted 9m apart in a triangular form. The optimum population density of the young palms per hectare is about 140.

Fruit production begins about 30 months after the planting with the harvesting following six months later. At the onset of harvesting the yield is low but it gradually increases and it peaks between the years 7 to 18 and then it begins to exhibit a decline until the lifespan of the tree is reached which is usually at the age of 25 years.

The yield for a mature palm tree is between 18 – 30 metric tonnes FFBs[8] per hectare with the yield hedging on a number of factors such as climatic conditions, variety of palm tree, age and the timely harvesting and processing of the fruit clusters.

2.1.6.3 Oil Extraction

The prompt processing of the FFBs after harvesting is critical in ensuring a maximum yield of oil and in most cases they need to be processed within 24 hours after the harvest to avoid the build-up of fatty acids which tend to lower the quality of palm oil extracted. Once the FFBs arrive at the mills, they are taken to a sterilizer where high pressure steam is used to sterilize the bunches so as to prevent further build-up of FFAs and to deactivate enzymes (lipases). From the sterilization chamber the FFBs are transferred to the stripping drum where the fruits are stripped from the bunch stalks. Thereafter the fruits are moved to the digesters which are steam heated cylindrical vessels that are used to remove the oil from the oil bearing cells. The digested product is then taken through a pressing machine which squeezes out the oil before finally the mixture of crude palm oil, water, and fibre goes through the processes of clarification, decanting and centrifugation to obtain the oil.

The identity characteristics of palm oil are captured below.

Table 2.3 *Palm oil identity characteristics [14].*

Identity Characteristic	Observed min. to max.
Apparent density, g ml^{-1} at 50°C	0.8889 – 0.8896
Refractive index, n_D 50°C	1.4521 – 1.4541
Saponification value, mg KOH g^{-1} oil	194 – 205
Unsaponifiable matter, % by weight	0.19 – 0.44
Iodine value, Wijs	50.4 – 53.7
Slip melting point, °C	33.8 – 39.2
Flash Point, °C	314
Total carotenoids as (β-carotene), mg kg^{-1}	474 – 689

2.1.6.4 Sustainable Palm Oil

The aggressive destruction of pristine tropical rainforests and peat swamps to pave way for sprawling palm oil plantations has generated a heated debate as a consequence of the spill over effects of these expansive plantations. Oil palms are grown in industrial plantations by multinational companies and most prefer the cutting down of the rain forests compared to the degraded land available. This is due to the economic advantage brought about by the

[8] Fresh Fruit Bunches

sale of timber. Some of the negative effects include, the pushing to the brink of extinction of some species more so the eponymous Sumatran orang-utan, rhinoceros and tiger; destruction of wildlife habitat; displacement of indigenous people; and the pollution of the environment by herbicides and fertilizers used in the plantations

In order to address the thorny issue of the effect of the spawning palm oil plantations, RSPO[9] was established in the year 2004 [15]. RSPO is a non-profit organisation that seeks to promote the production and use of sustainable palm oil by uniting stakeholders from the palm oil industry to develop and implement global standards for sustainable palm oil. Palm oil that has the RSPO certification implies that the grower of the palm oil has adhered to the 8 Principles and Criteria that govern the cultivation of palm oil.

With the advent of RSPO, since the year 2005 primary and HCV[10] forests have been designated as off limits to palm plantations thus helping to protect these pristine ecosystems.

2.2 Biofuels

The term biofuels refers to solid, liquid or gaseous fuels that are derived from bio renewable or renewable combustible feedstock [16]. Interest in biofuels in recent years has perked up due to the necessity to wean the world off the addiction to crude oil.

There are quite a number of diverse ways of production of biofuels based on the type of feedstock used and the production process employed. This section delves into some of the biofuels in the market, their production and the policies that govern their use as fuels. Catalytic cracking, upon which this thesis is based on, will be dealt with later.

2.2.1 Biodiesel

Biodiesel is a diesel equivalent fuel that meets the specifications of ASTM[11] D6751 or EN[12] 14214. It is composed of FAME[13] mixtures that are obtained from lipids feedstock (animal fat and vegetable oil) through a transesterification (also termed alcoholysis) reaction. In the transesterification reaction the lipids feedstock is reacted with an alcohol either ethanol or methanol – with methanol being the preferred alcohol due to its relatively cheap cost – in the presence or without the presence of a catalyst yielding fatty acid methyl esters and a valuable by product, glycerine. The transesterification reaction is reversible and therefore to promote the forward reaction, excess alcohol is used.

[9] Roundtable on Sustainable Palm Oil
[10] High Conservation Value
[11] American Society for Testing and Materials
[12] European Standards
[13] Fatty Acid Methyl Esters

2.2.1.1 Biodiesel Production

Catalysts that can be employed for the transesterification reactions range from alkali, acids such as sulphuric acid and enzymes, example being lipase. Alkali catalysed transesterification is the most commonly used method of biodiesel production with the catalyst of choice being KOH or NaOH. The reaction mechanism for the production of biodiesel using a catalyst is shown below.

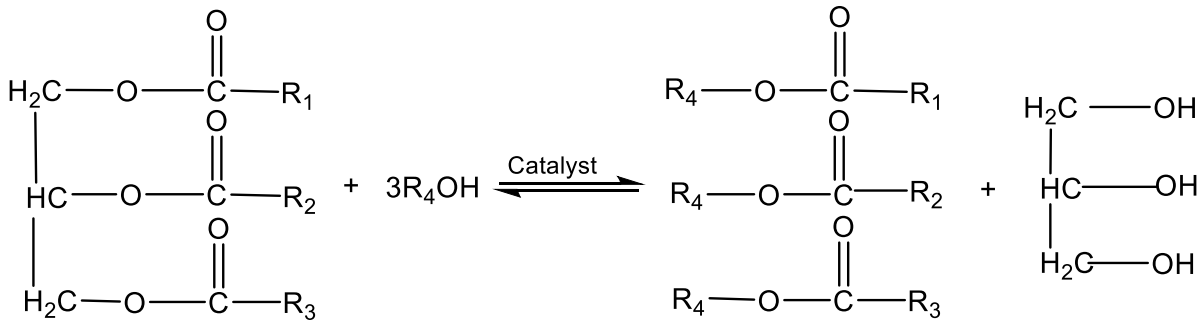

The BIOX process is a paradigm of a non-catalysed transesterification process and it uses an inert co-solvent to convert low cost feedstock – feedstock with high FFAs[14] – into biodiesel [17]. Conceived in the University of Toronto Chemical Engineering Department, the BIOX process was later transformed to industrial scale and has the capacity to produce 67 million litres of biodiesel per annum. The co-solvents first convert the FFAs and subsequently the triglycerides are converted with a yield of > 99% being achieved and hence the need of a pre-treatment step to solve the FFA issue is eliminated. The co-solvent and the methanol are also recovered and recycled back to the process.

2.2.1.2 Major Producers and Biodiesel Outlook

In its Agricultural Outlook 2014 – 2023 [9], OECD[15] and FAO[16] envisage that the global biodiesel will expand and will hit the 40 billion L mark by the year 2023 akin to a 54% growth from the year 2013; with the biodiesel market being dominated by the major producers comprising of the European Union followed by the United States, Argentina and Brazil.

The various policies that have been set up by various countries in a bid to decarbonize the transport sector will play a major role in pushing production and consumption. Buoyed by its RED[17] policy, the production in the EU is projected to hit 16 billion L by the year 2023 whereas developing countries will rack up a production totalling 16 billion L.

[14] Free Fatty Acid
[15] Organisation for Economic Co-operation and Development
[16] Food and Agriculture Organization
[17] Renewable Energy Directive

It is worth pointing out, that the dwindling vegetable oil price over the same outlook period as depicted in Figure 2.3 is expected to have a knock-on effect on world biodiesel prices with a decrease of 6% projected: the prices will witness a drop from 97.19 USD/hl posted in 2013 to an expected price of 91.47 USD/hl at the close of the outlook period. It is expected that the plummeting oil prices will not have an adverse effect on biodiesel given the fact that biofuels sector is mainly cushioned by the policies set by various governments.

Figure 2.7 and Figure 2.8 capture the outlook of biodiesel production and the anticipated biodiesel production per region in 2023 respectively.

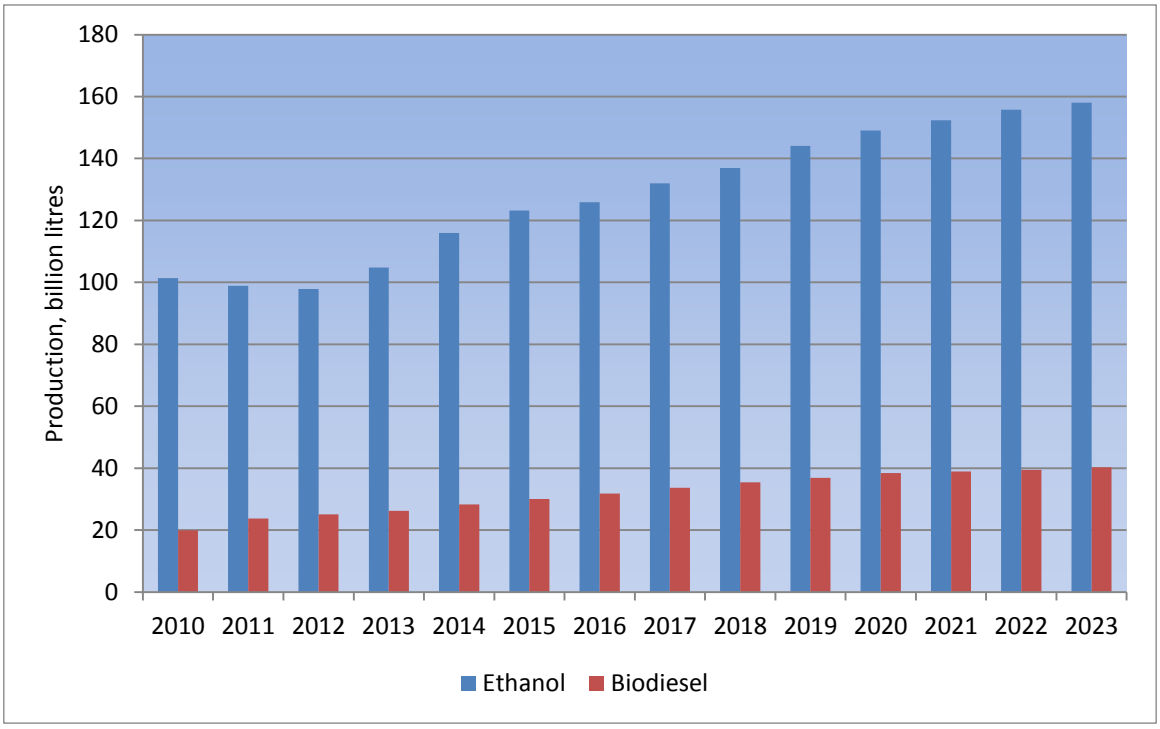

Figure 2.7 *Ethanol and biodiesel production outlook [9].*

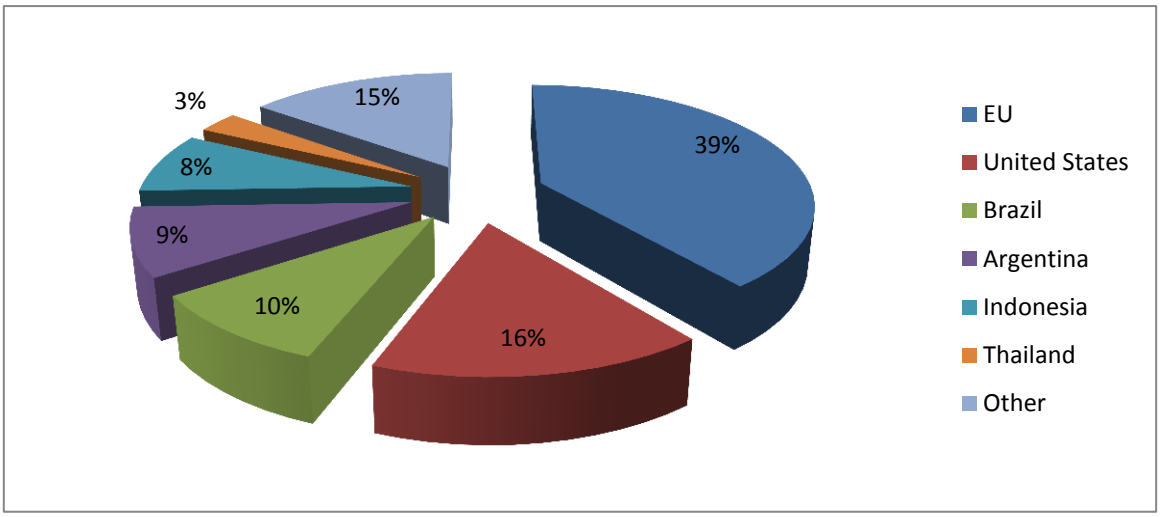

Figure 2.8 *Anticipated regional production of biodiesel in the year 2023 [9].*

2.2.1.3 Use of Biodiesel as a Fuel

Biodiesel can be used either as a neat fuel referred to as B100 or as a blend fuel. Biodiesel B100 has a lower heating value compared with low sulphur diesel but on the other hand it boasts of better cetane numbers. The lower heating value of low sulphur diesel is 35.8 MJ/kg while that of B100 is 33.3 MJ/kg. Likewise, the cetane numbers are 40 – 55 and 48 – 65 for low sulphur diesel and B100 respectively [18].

The blending of biodiesel aids in improving its performance in cold weather with the blending of biodiesel varying from one region to another. In the USA for instance the B20 (20% biodiesel, 80% petroleum diesel) blend is commonly used since this and other lower-level blends do not need any engine modifications [19]. The B20 blend provides the same engine power and consumption rate as the conventional diesel with the added advantage of a higher cetane number and lubricity as compared to petroleum diesel.

In the EU the B5 blend is used and as of June 2012, the B100 blend can be used in new agri-power engines developed by the firm DEUTZ AG in Germany. The imposition of anti-dumping duties on its biodiesel exports to Europe forced Argentina to raise its blending to 10% beginning February 2014 while Indonesia expects to be using biodiesel blends of up to 25% by the year 2025.

2.2.2 Bioalcohols

Bioalcohols refer to alcohols that are produced from biological feedstock as opposed to alcohols derived from the petrochemical industry. Though there are a number of alcohols that can be used in the auto industry, methanol (wood alcohol) and ethanol (grain alcohol) are the predominant ones based on the fact that they are better suited for internal

combustion engines and most importantly on their economic viability. Of the two however, ethanol is the most commonly employed.

2.2.2.1 Ethanol Production

"To build a vehicle affordable to the working family and powered by a fuel that would boost the rural farm economy."

Those were the words of Henry Ford in 1908 when he built the Ford T model which had a carburettor that could run on ethanol produced by the American farmers. Little did he know that his vision would be taken up once more but with the mission being to mitigate the ramifications of GHG emissions.

There are quite a number of ways of producing ethanol from biomass feedstock such as sugar, starch and lignocellulosic. Ethanol production by fermentation of grains and sugar are by far the most developed methods. The following equations depict the production from ethanol from sugars.

$$C_{12}H_{22}O_{11} + H_2O \xrightarrow{\text{Invertase}} C_6H_{12}O_6 + C_6H_{12}O_6$$

Sucrose — Fructose — Glucose

$$C_6H_{12}O_6 \xrightarrow{\text{Zymase}} 2C_2H_5OH + 2CO_2$$

Fructose / Glucose — Ethanol

2.2.2.2 Major Producers of Ethanol and Outlook

As per the OEACD-FAO outlook for the period 2013-2023 [9], ethanol production is expected to be dominated by the three major producing countries comprising the United States, Brazil and the EU. The global ethanol output is expected to reach 158 billion L by 2023 as captured in Figure 2.9. Production in the US is expected to grow from 50 to 70 billion within the outlook period and thereafter it is expected to grow marginally as a consequence of the blend wall reaching its maximum value of 14%. The EU will see its output surpass 12 billion L within the same projected time while Brazil will witness a doubling of its production to 50 billion up from 25 billion as recorded in 2013. The increased production in Brazil will be driven by the 25% blending requirement and a developing flexi-fuel auto industry coupled with an increased demand from the US to achieve its biofuel mandate.

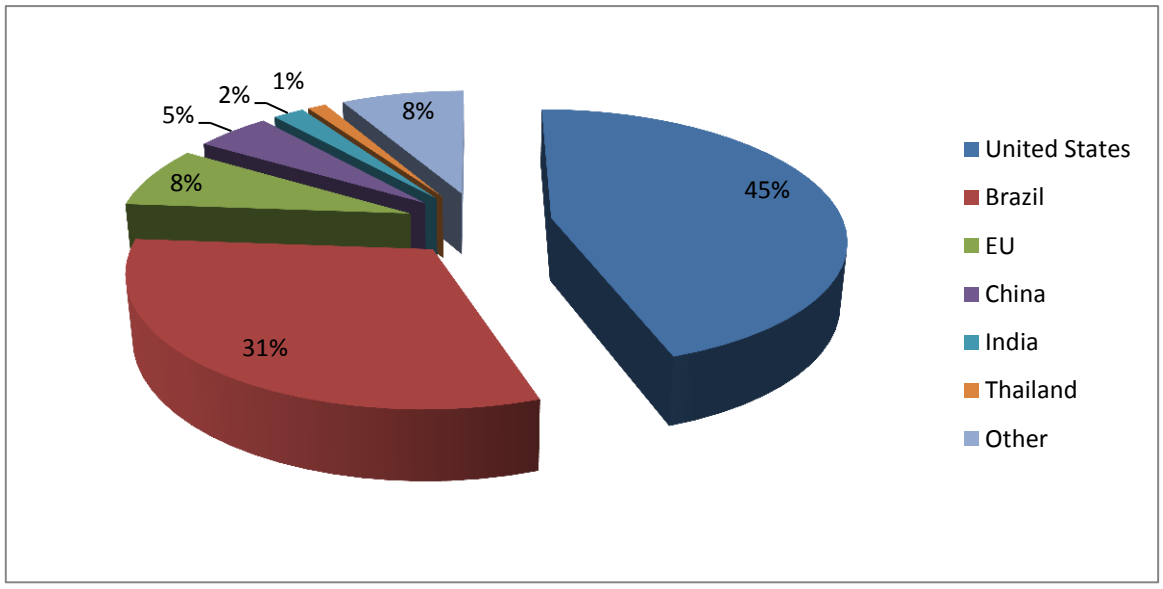

Figure 2.9 *Anticipated regional ethanol production in the year 2023 [9].*

The increased demand of ethanol in Brazil as well as the 25% mandatory blending requirement will have a domino effect on world ethanol prices as shown in Figure 2.3. Prices are projected to rise from 53.41 USD/hl to 58.37 USD/hl corresponding to an increase of 9% over the outlook period. It is expected also that the plummeting oil prices will not have an adverse effect on ethanol given the fact that biofuels sector is safeguarded the policies set by various governments.

2.2.2.3 Use of Ethanol as a Fuel

Ethanol use as fuel varies from country to country with the type of vehicle also having a major say on the range of concentration that can be used. In the EU countries low blends of ethanol and petrol are available in the market with the blends being E5 and E10. It is usually stored as E95 with blending being done at the load rack to yield the desired blend. As concerns its properties, E100 has a lower heating value of 21.3 MJ/kg but this is compensated by its high octane number of 110 [18].

FFVs[18] have the ability to run on pure gasoline to blends of gasoline and ethanol or pure ethanol depending on the location. In Brazil and The USA FFVs are common with the vehicles in the USA designed that they can run on pure gasoline up to the E85 blend without any complications while in Brazil they can run from pure gasoline to pure ethanol. They are able to function well due to the presence of a microprocessor that helps adapt the engine to the type of fuel with up to 86% of the cars sold in Brazil in the year 2006 being FFVs [20].

[18] Flexible Fuel Vehicles

Ethanol may also be reacted with isobutylene to produce ETBE[19] an oxygenate additive that is used to upgrade lower octane gasoline grades and lower aromatic contents hence improving the combustion and knock properties of the gasoline.

2.2.3 Ecofining

Ecofining is a process jointly developed by UOP and ENI companies the gist being the conversion of vegetable oil to green fuel using existing refinery infrastructure [21]. The Ecofining process is essentially a hydroprocessing technology where the vegetable oil is reacted with hydrogen in the process of a bimetallic catalyst in a dedicated reactor. The aim of the reaction is the removal of oxygen from the triglyceride molecule. A simplified flow diagram for the process is shown in Figure 2.10.

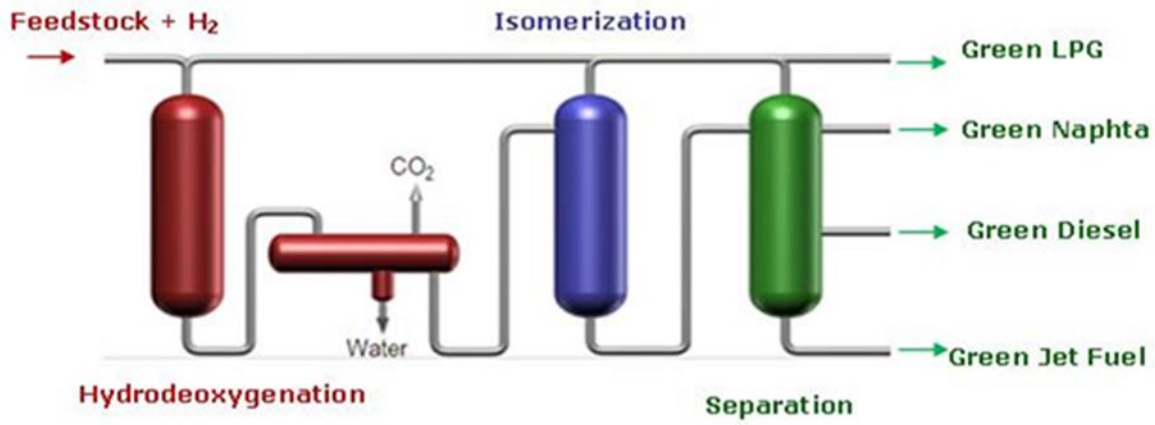

Figure 2.10 *The Ecofining process [22].*

Three competing reactions are responsible for the removal of the oxygen: hydrodeoxygenation, decarbonylation and decarboxylation. Catalytic saturation of olefinic bonds together with the hydroisomerization reaction results in an iso-paraffin rich diesel identical to traditional diesel fuel that can be used as drop-in replacement. The green diesel is also referred to as HVO- Hydrotreated Vegetable Oil. The global mechanism is depicted below [23].

$$RCOO{-}CH_2CH({-}OOCR')CH_2{-}OOCR'' \xrightarrow{H_2} C_3H_8 + \begin{matrix} RCH_3 + 2H_2O \\ R'H + CO + H_2O \\ R''H + CO_2 \end{matrix}$$

[19] Ethyl Tertiary Butyl Ether

2.2.3.1 Fuel Use

Jet fuel obtained from the process was used by GOL airlines the official airline of the Seleção – Brazil National Soccer Team – to power 200 commercial flights during the 2014 world cup including those of the national team across the various host cities [24]. Additionally, the Honeywell Green Jet Fuel blended to 50% with petroleum based fuel reduces GHG emissions by 60 to 85% compared with the petroleum based fuels with the added advantage that no modifications to the aircraft technology is required.

2.2.4 Biofuels Policies

In a concerted drive to curb the spiralling trend in GHG from the transport sector, several countries have put in place measures that will endeavour to curb or bring the emissions to levels that will not have profound effects on the environment. The results are a spawning in the quest to ensure a considerable use of renewable fuels is realized.

In the USA, EPA[20] is tasked with the development and implementation of regulations that sets a minimum volume of renewable fuels that should be sold in the USA. The RFS2[21] program under the Energy Independence and Security Act (EISA) of 2007 has for instance set a target of 36 billion gallons of renewable fuel that ought to be blended into transportation fuel by the year 2022. This is aimed at reducing the GHG emissions significantly through the use of renewable fuels [25].

In the same vein, the EU Renewable Energy Directive (RED) formerly known Directive 2009/28/EC, which advocates the use of renewable energy in the transport sector, a target minimum from every state of 10% contribution from the renewables energy to the transport industry by the year 2020 has been set; which is an increase from the 5.75% target set under the Directive 2003/30/EC which was to be attained by the year 2010 [26]. It is envisaged that biofuels will meet the bulk of this target. In a bid to stem the use of food crops as feedstock for biofuels, the EU has also set a quota of the amount of biofuels that ought to be produced from foodstocks to meet the 10% renewable energy target and this currently stands at 5%.

[20] Environmental Protection Agency
[21] Renewable Fuel Standard 2

2.3 Fluid Catalytic Cracking

2.3.1 Introduction

The refining of crude oil involves the use of several processing units that are used to transform the raw crude into useable and valuable products such as LPG[22], gasoline, kerosene, jet fuel, diesel and fuel oils. In a nut-shell the refining of crude oil can be talked of as a three step process involving separation, transformation and after treatment.

The Holy Grail of any refining process is the production of desirable products and most importantly gasoline due to the plain reason that 50% of the crude oil needs to be converted to gasoline in order to satisfy the transportation demands whereas the normal delivery from one barrel of crude oil is between 30 – 40% gasoline [27].

With increased development and a bourgeoning population there will be a commensurate increased demand for transportation fuels the world over. The bulk of the transportation that will be needed to serve this purpose will be mainly diesel and gasoline types of fuel and this where the significance of the FCC unit comes to the fore.

Fluid catalytic cracking is a process that converts the heavy distillates into lighter, higher-value components such as gasoline and olefin gases. The principle of the FCC process is based on the circulation of the coke laden catalyst and regenerated catalyst between the reactor and regenerator zones as depicted in Figure 2.11.

[22] Liquefied Petroleum Gas

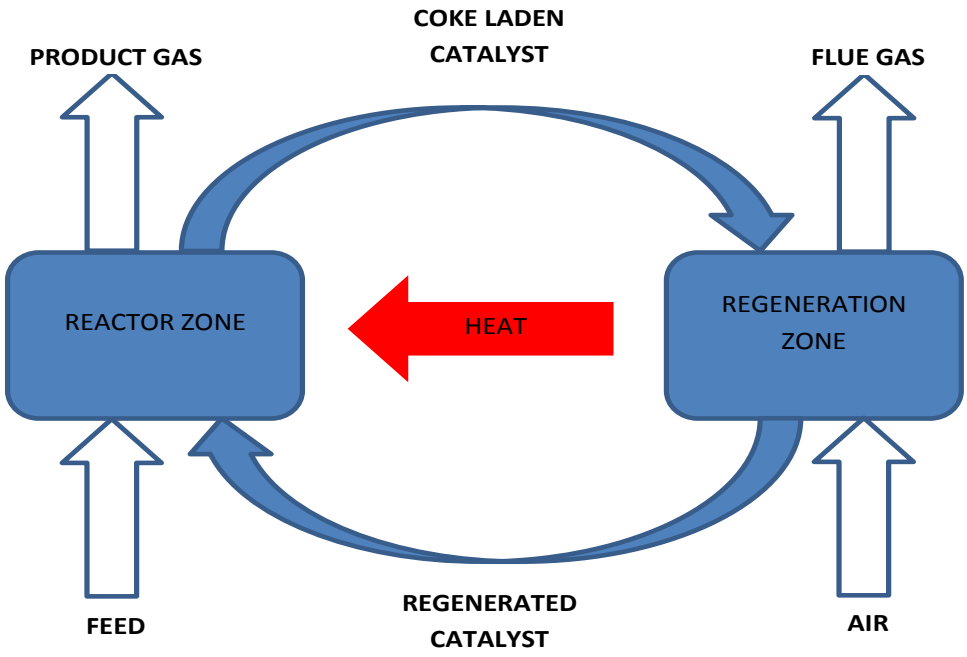

Figure 2.11 *FCC process principle.*

Ever since its invention and introduction into the refinery process, the Fluid Catalytic Cracking unit continues to be at the forefront in the conversion of crude oil, VGO[23] and other oils to lighter components of petroleum with more than 300 crackers worldwide currently [28]. It is envisaged that the FCC process will play a key role in providing the fuels needed to drive the future economies. It is thus no wonder that some have called it the mainstay of the refinery. Simply put the FCC is the heart of the refinery process.

In the coming years there will be a need to adapt the FCC unit to emerging feedstocks aside from the conventional ones. This thesis thus dwells on vegetable oils as an alternative feedstock in the FCC unit.

2.3.2 FCC Process Description

The FCC unit is primarily composed of three major sections as enumerated below:

a) Reactor/ Regenerator

b) Main fractionator

c) Gas recovery unit

[23] Vacuum gas oil

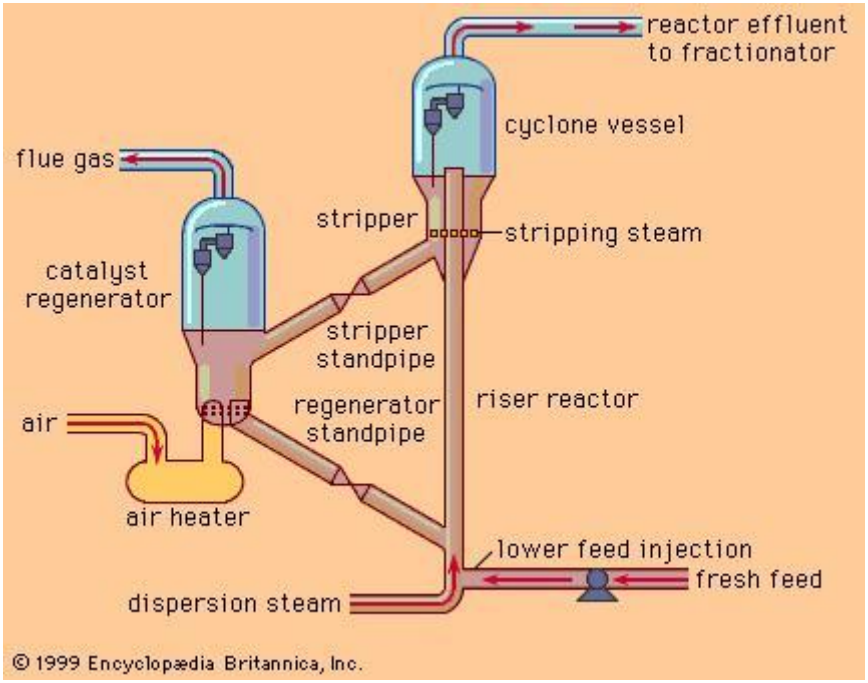

Figure 2.12 *Example of an FCC unit.*

A typical industrial FCC unit is captured in Figure 2.12. The cracking reactions of the feed occur in the reactor or the riser and during the course of these reactions the active sites in the catalyst surface are deactivated due to the formation of coke. Though coke deactivates the catalyst it is also a useful product since its combustion in the regenerator provides the heat for the cracking reaction and in the process the active sites of the catalyst are once again freed up.

From the riser the hydrocarbon product gases move to the fractionator. The functionality of the main fractionator is comparable to the distillation column save for the fact that the feed is superheated and therefore it needs to be desuperheated to enable the recovery of the products. The fractionator has the slurry oil as the bottoms product, three side cuts for HCO, LCO and heavy gasoline and finally unstable gasoline and light gases as the overhead product.

The unstabilized gasoline and light gases flow to the wet gas compressor which is the first device in the gas concentration unit. The function of the gas concentration unit is to separate the unstabilized gasoline and the light gases into the following products: fuel gas, C_3´s and C_4´s and C_5´s which is mainly gasoline range liquid [29].

A typical product distribution of the FCC process is captured in Table 2.4.

Table 2.4 *FCC product distribution [30].*

Product	C_1-C_2	C_3-C_4	Gasoline	LCO	Slurry	Coke
Yield	3-5	15-30	40-50	10-20	5-10	5-8

*LCO: Light cycle oil (B.P. 220-350°C), Slurry oil, B.P. 350°C^+)

2.3.3 Catalysts

Catalytic cracking employs a powdered catalyst known as a zeolite in the process. A zeolite according to the classical definition is a crystalline microporous oxide with a framework composed of adjacent silicon and aluminium tetrahedron forming channels of microporous dimensions, where alkali or alkali-earth cations and water molecules are situated [30].

The cracking reactions occur in the Brønsted and Lewis acid sites of the catalyst. Proton donors such as the hydroxyl group provide the Brønsted acid sites whilst the Lewis sites are generally electron acceptor centres.

The joining together of the silicon and aluminium tetrahedral forms a truncated octahedral which is a secondary building block for a number of zeolites. The stacking together of the truncated octahedra in turn leads to the formation of a sodalite. In faujasite-type zeolites, the octahedra are arranged like carbon atoms in diamond. As a result a supercage (sorption cavity) is formed surrounded by 10 sodalite units with the entrance into this cavity being bounded by 6 sodalite units. An example of the structure of a faujasite-zeolite type is shown in Figure 2.13.

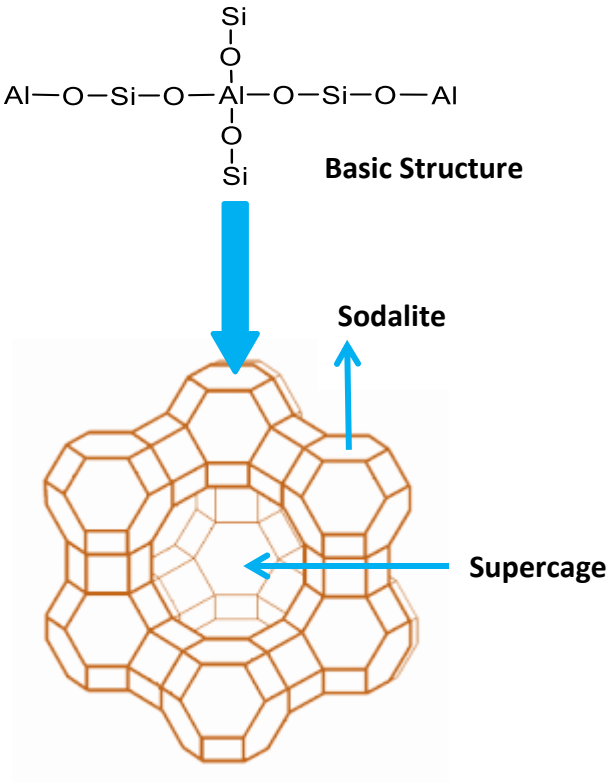

Figure 2.13 *Zeolite structure [31]*.

Aside from zeolite which accounts for 15 – 50 wt. % of the catalyst, other major components of a catalyst are the matrix, filler and binder. The matrix has alumina as its active ingredient whose sole purpose is to boost the bottoms conversion activity of the catalyst and it accounts for 0 – 20 wt. % of the catalyst. Fillers and binders are non-active constituents of the catalyst. Kaolin clay is commonly used as a filler to enhance the catalyst's physical properties such as surface area, pore volume and density. Binders have as their main task the binding together of the other constituents and can be made from silica compounds, aluminium compounds or clays.

2.3.4 Chemistry of FCC Reactions

Cracking of hydrocarbons as earlier stated entails the breaking up of large and heavy hydrocarbon molecules (long chain hydrocarbons) through a series of reactions into simpler, small and light hydrocarbon molecules (short chain hydrocarbons). The resultant products are more valuable and include gasoline and olefin gases such as propylene. The cracking process involves the rapture of the carbon-carbon bond and is favoured by high temperatures due to the fact that the reactions are endothermic.

Cracking of hydrocarbons can be achieved through two possible routes:

a) Thermal cracking
b) Catalytic cracking

Catalytic cracking is the predominant cracking route in an FCC unit with thermal cracking occurring as a consequence of several factors the main drivers being non ideal mixing in the riser and poor separation of cracked products in the reactor. Depending on the route used, different kinds of products may be arrived at as shown by Venuto PB [32].

2.3.4.1 Thermal Cracking

Thermal Cracking is carried out in the absence of a catalyst when the heavy hydrocarbons are processed at high temperatures (425 – 900˚C) and high pressures (up to about 70 atmospheres). This was the choice method by processors to obtain lighter hydrocarbons long before the development of the FCC unit. Delayed coking and Vis breaking are prime paradigms of processes that employ the thermal cracking principle. The latter is a mild form of thermal cracking with the residence time ranging from 1 – 3 minutes while the former is a moderate form of thermal cracking the residence time being 24 hours.

Thermal Cracking Mechanism

The cleavage of the carbon-carbon bond results in the formation of free radicals – extremely reactive – which is the first step in thermal cracking chemistry. The products obtained by the rapture process are uncharged and share a pair of electrons and based on the reaction path taken by the free radical, the product spectrum yielded will be different. The path taken could be one among alpha (α)-cleavage, beta (β)-cleavage or polymerization.

2.3.4.2 Catalytic Cracking

Catalytic cracking as the name suggests involves the use of catalysts where the reactions occurring are catalysed by acidic surfaces. The reactions can be classified into two categories:

a) Primary cracking of the vaporized feed
b) Secondary cracking and rearrangement of the products obtained from the first process

Catalytic Cracking Mechanism

The contacting of the hot regenerated catalyst with the oil feed causes the oil to vaporize leading to the intermediate formation of carbocations, i.e. positively charged carbon ions. Carbocations are composed of two groups of ions [33]:

a) carbenium ions
b) carbonium ions

The charge-carrying atom can be di- or tri-coordinated in the case of carbenium ions whereas it can be tetra or penta-coordinated in carbonium ions.

As pertains the stability of carbocations, it is worth noting that there is a decrease in the stability of the ions in the order: tertiary > secondary > primary. The kind of alkyl group attached to the positive charge also has an effect on the stability with the methyl group being the least stable. The stability can be depicted as follows.

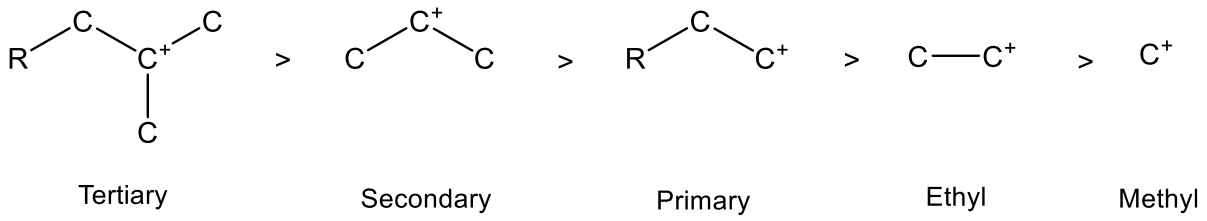

On the contrary, the energy of formation for the carbocations increases with an increase in the number of H atoms attached to the carbon atom from which the hydride ion is abstracted.

The fact that the primary carbocations are less stable explains their tendency to isomerize yielding secondary and tertiary carbocations in the process. The increased proportion of tertiary carbocations is one of the benefits of catalytic cracking since an increase of tertiary carbocations implies a corresponding increase in the branching degree.

Carbenium Ion Intermediate Mechanism

The initiation step of carbenium ion formation can occur at both Brønsted and Lewis acid sites. The Brønsted acid site reacts with an olefin leading to protonation of the olefin while on the other hand Lewis acid site reacts with a paraffin the result of which is hydrogen abstraction.

The formation of the carbenium ion marks the start of the propagation step which can proceed via two pathways. The first pathway which is also a cracking reaction may involve the cleavage of the carbon-carbon bond at the beta position with this monomolecular reaction yielding an olefin and a carbenium ion both of which will be of a smaller size. The second pathway is a bimolecular reaction involving the carbenium ion and a neutral paraffin molecule. This reaction results in hydrogen abstraction the products of which are a paraffin and a carbenium ion. The carbenium ions formed propagate the reaction by reacting with other paraffin molecules.

Chain termination of the carbenium ion occurs when either there is a loss of a proton to a catalyst the product of which is an olefin or when a hydride ion is added leading to the formation of a paraffin; the hydride ion is obtained from a donor such as coke. These reactions are shown below.

Initiation Reactions

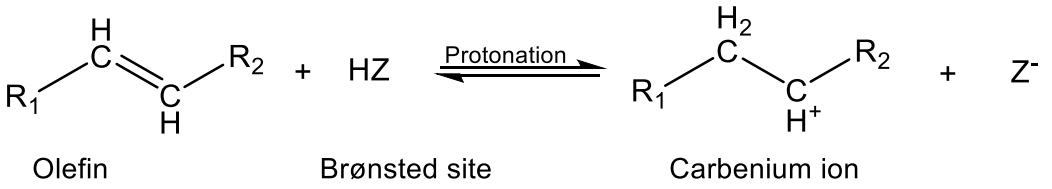

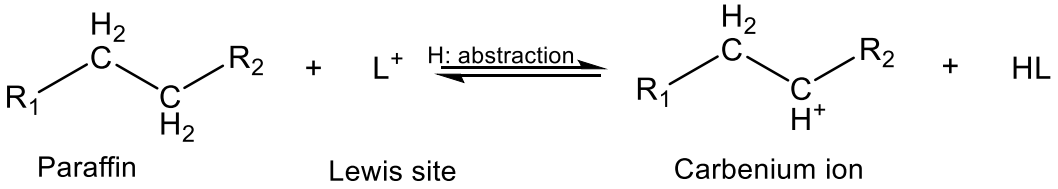

Propagation Reaction

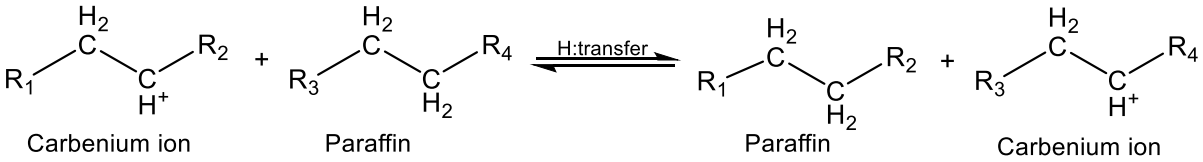

Cracking Reaction

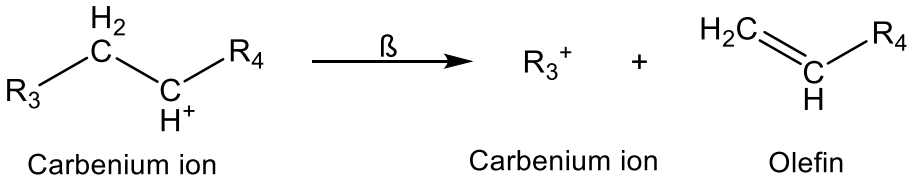

Carbonium Ion Mechanism

This cracking mechanism proceeds via a monomolecular reaction pathway and was proposed by Haag and Dessau [33]. The mechanism is favoured by high temperatures of over 500˚C and involves the penta-coordinated carbonium ions intermediates. The beta cleavage of these carbonium ions yields carbenium ions and paraffins. The carbonium ions may also suffer the loss of hydrogen yielding a carbenium ion and a hydrogen molecule lending credence to this mechanism since hydrogen is one of the cracking products.

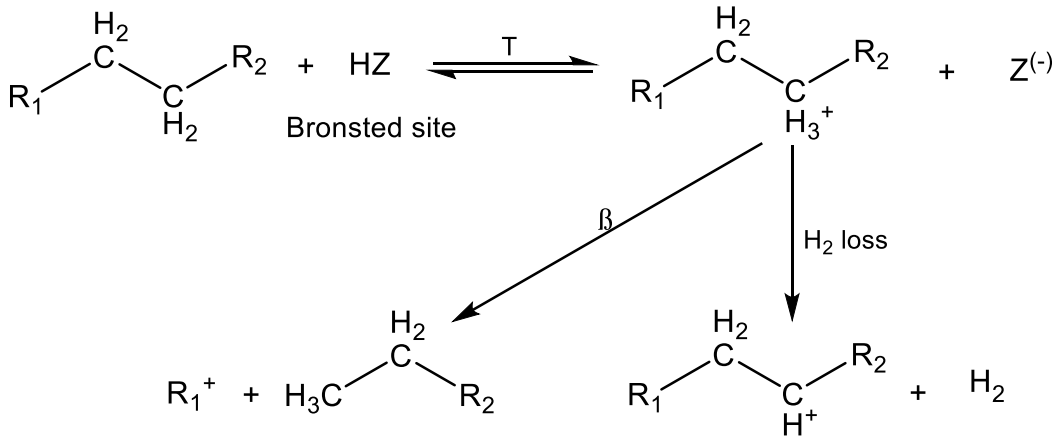

Aside from the main cracking reactions, other reactions may accompany the catalytic cracking of hydrocarbons such as isomerization, hydrogen transfer and coke formation.

2.3.5 Vegetable Oil Cracking

Leng TY et al. [34] proposed a reaction pathway as captured in Figure 2.14 for the catalytic cracking of palm oil over a zeolite catalyst, HZSM-5. The first step is the conversion of palm oil into heavy hydrocarbons and oxygenates via thermal and catalytic cracking. These reactions occur on the external surface of the catalyst. Deoxygenation and secondary cracking of the products obtained in the previous step is the follow up reaction with the reactions yielding light olefins (alkenes), light paraffins (alkanes), carbon dioxide, carbon monoxide, alcohol and water. Two different reaction pathways have been proposed for the deoxygenation step [35]:

a) Decarboxylation
b) Decarbonylation

The decarboxylation pathway involves the removal of the carboxyl group from the fatty acid, thereby releasing a molecule of carbon dioxide and a paraffin molecule. The second reaction pathway, the decarbonylation route, is the basis for the production of carbon monoxide, water and most importantly olefins through the removal of the carbonyl group. Both reaction pathways, decarboxylation and decarbonylation, may occur simultaneously during the cracking of the triglycerides or depending on the catalyst used, a certain reaction pathway could be favoured leading to a shift in the product spectrum.

a) Decarboxylation

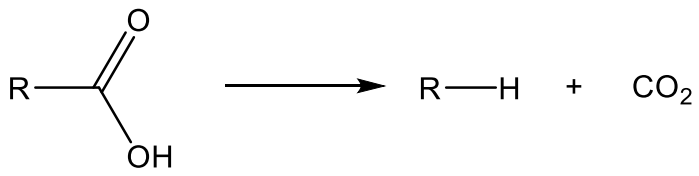

b) Decarbonylation

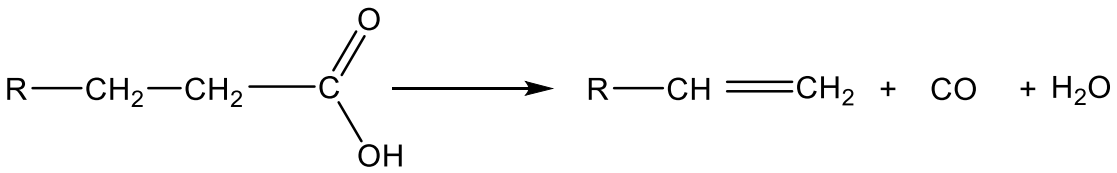

Deoxygenation is a critical process in the catalytic cracking of triglycerides since oxygen ought to be removed and substituted with hydrogen to be able to yield liquid fuels without any oxygenates.

The oligomerization of light alkenes is a possibility with the process leading to the production of heavier alkenes and alkanes, the alkanes being composed of fractions of gasoline, diesel and kerosene. The alkylation, aromatization and isomerization of the heavier alkenes and alkanes on the other hand yield aromatic hydrocarbons as the products. In this reaction pathway, coke formation was explained by the condensation of palm oil and polymerization of the aromatic hydrocarbons.

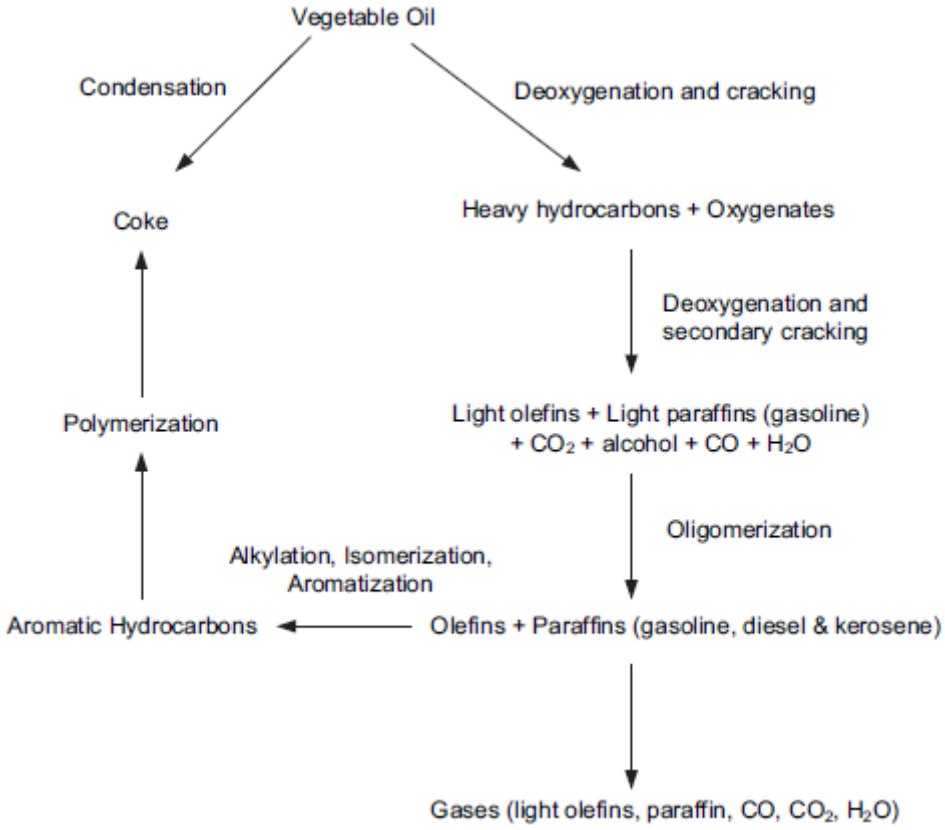

Figure 2.14 *Vegetable oil reaction pathway [34].*

3 FCC PILOT PLANT

3.1 Introduction

The Vienna University of Technology has two small scale FCC pilot plants that are employed to make test runs on various feedstocks. Unlike the industrial FCC plants which consist of two separate units of the riser and the regenerator, the plants at the university are a single unit. The first FCC plant was designed by Reichhold and Hofbauer in the mid-1990s with the support of OMV AG [36]. The principal driving force behind the development of the pilot plant was to have a flexible unit that could be used to process a wide range of feedstock based on the same process parameters as at the OMV refinery based in Schwechat.

As stated above, the design of the FCC pilot plant varies from the conventional industrial designs used the world over. The underlying difference lies in the fact that whereas the industrial plants involve the external circulation of the catalyst from the reactor to the regenerator, the plants at the university employ internal circulation of the catalyst from the riser to the regenerator. The internal circulating fluidized bed is achieved by having the riser concentrically located within a radially symmetrical regenerator. This design thus eliminates the need for two separate units. The major advantages of this design over the other industrial designs are optimal heat transfer and its compact design. The optimal heat transfer is achieved by the heat generated in the regenerator through the combustion of coke in the catalyst (exothermic reaction) being simultaneously used by the reactor (riser) for the cracking reactions (endothermic reaction).

The first plant or the old plant, was used to make various test runs ranging from VGOs, admixtures of refinery products to admixtures of VGO and vegetable oils with the first runs with pure vegetable oil being conducted by Schablitzky [37] and Schönberger[38].

The need to have a pilot plant capable of processing larger volumes and with better process parameters measurement necessitated the construction of a second plant, herein christened the new plant. The new plant has improved automation with an increased number of measuring points and a much larger regenerator capacity so as to enable the processing of heavier feedstock which yields more coke.

Vegetable oils have also successfully been processed using the new plant and the results published by Bielansky [39]. Figure 3.1 depicts the general flow sheet diagram for the processing of feedstocks in the pilot plant whereas the new plant´s specifications and key data are tabulated in Table 3.1 with the plant´s schematic being captured in Figure 3.2.

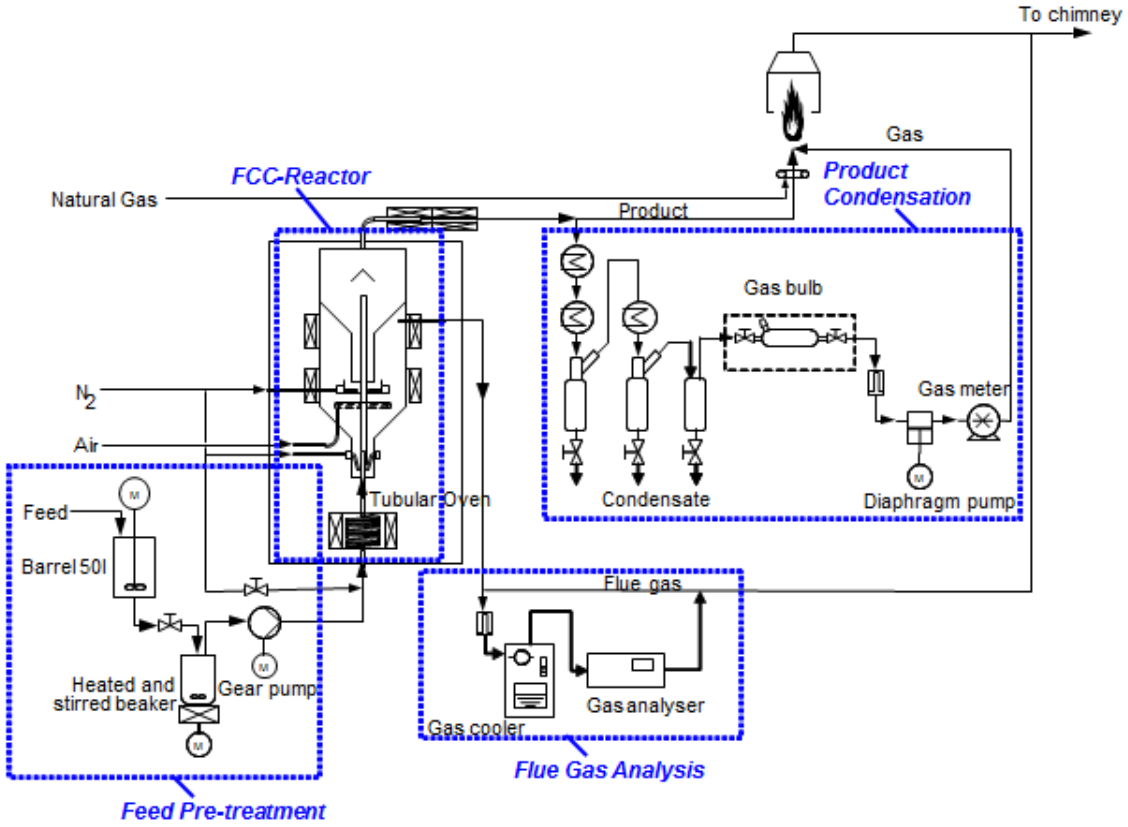

Figure 3.1 *Flow sheet diagram for pilot plant.*

Table 3.1 *Pilot plant key data and specifications.*

Total Height	2,900 mm
Riser Length	2,505 mm
Riser diameter	21.5 mm
Riser Temperature	420 – 650°C
Residence time	1 – 2 s
Regenerator diameter	330 mm
Regenerator temperature	500 – 800°C
Catalyst mass	40 – 75 kg
Feed rate	1.5 – 4 kg/h
C/O Ratio	6 – 60
Pressure	Atmospheric

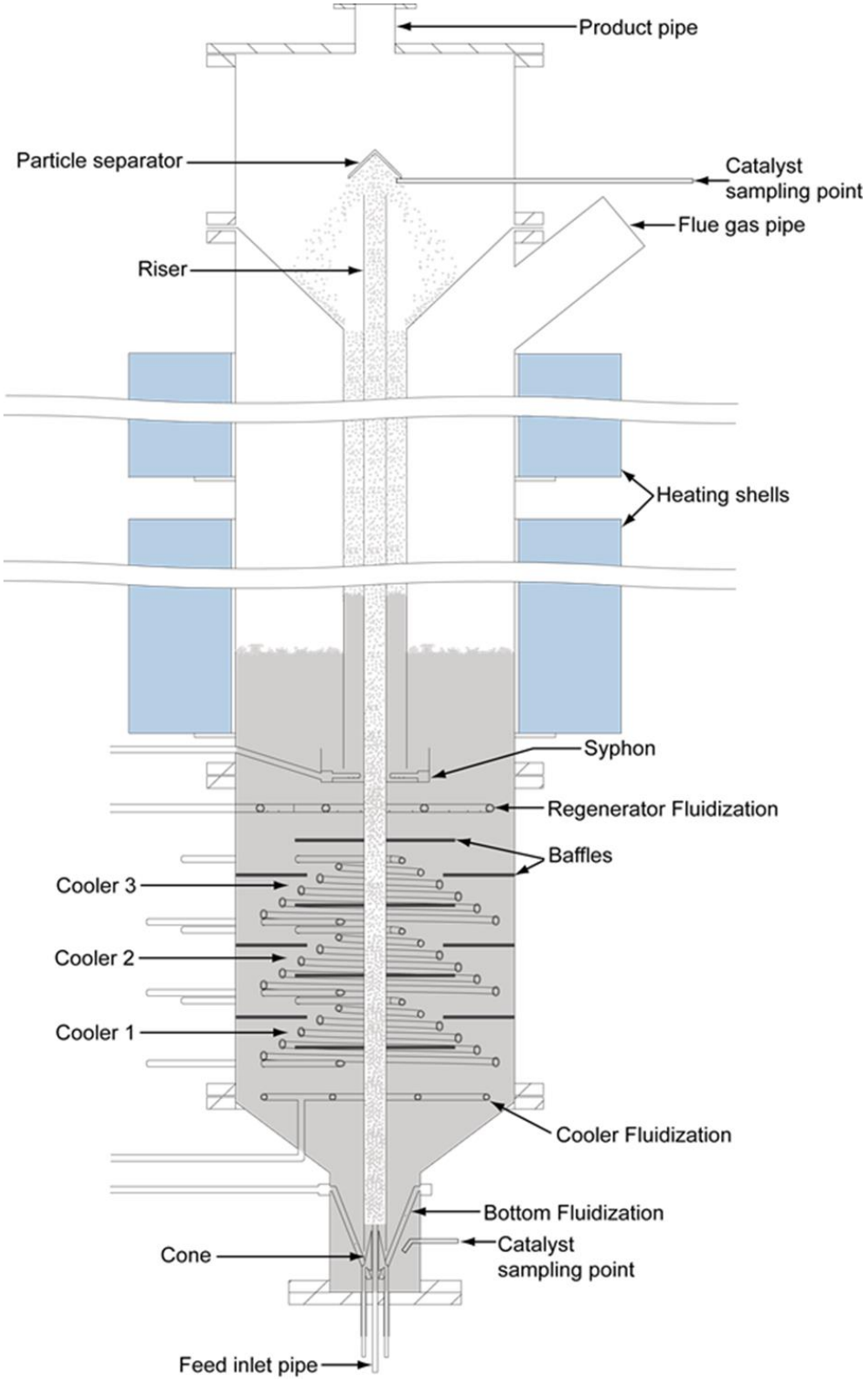

Figure 3.2 *Pilot plant schematic.*

3.2 Feedstock

The specifications for the two vegetable oils processed shown below were taken from literature since no detailed ones were available. Vegetable oils are primarily made up of three main fatty acids namely: palmitic, oleic and linoleic. A brief comparison of the two vegetable oils processed during this study shows that the highest composition of fatty acid in palm oil is palmitic acid while soybean oil is majorly made up of the fatty acids oleic and linoleic. The denotation of fatty acid is generally by their carbon chain length followed by the number of double bonds. The effect of the high presence of double or triple bonds in soybean oil will be brought to light in RESULTS AND DISCUSSION.

3.2.1 Soybean Oil

Soybean oil is liquid at room temperature and is majorly composed of polyunsaturated fatty acids. The fatty acid composition in soybean oil [40] and other key data [41] are shown below.

Table 3.2 *Soybean oil fatty acid composition.*

Fatty acid		Weight %
Myristic	14:0	0.1
Palmitic	16:0	11.0
Palmitoleic	16:1	0.1
Stearic	18:0	4.0
Oleic	18:1	23.4
Linoleic	18:2	53.2
Linolenic	18:3	7.8
Arachidic	20:0	0.3
Behenic	22:0	0.1

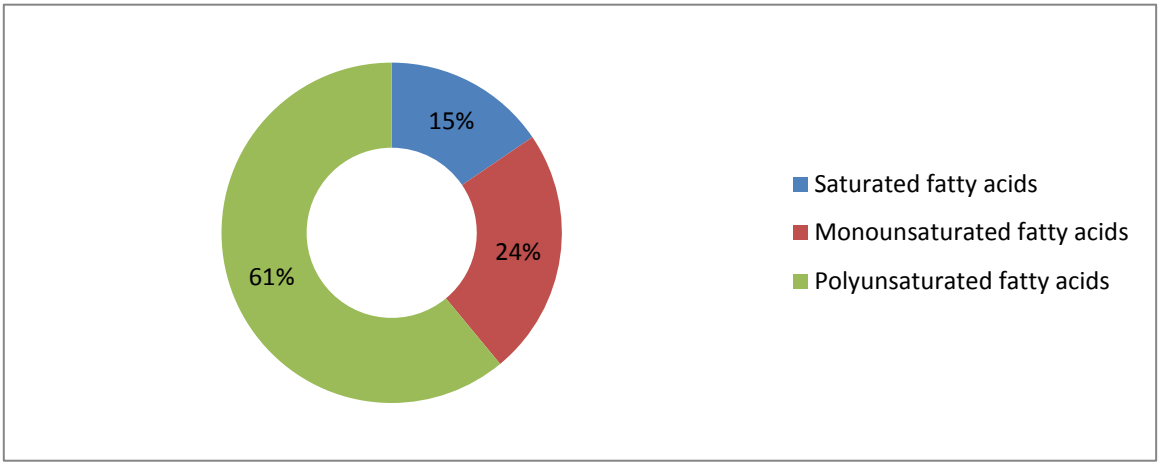

Figure 3.3 *Soybean oil fatty acid share.*

Table 3.3 *Soybean oil elemental composition.*

Element	Weight %
Carbon	77.59
Hydrogen	11.6
Oxygen	10.8
Others	0.01

3.2.2 Palm Oil

Palm oil is semi-solid at room temperature and can be easily separated into two products – palm olein and palm stearin – by fractionation. Palm olein is the liquid fraction whereas palm stearin is the solid fraction. It is majorly composed of saturated acids. The fatty acid composition [40] and other key data [41] are as tabulated.

Table 3.4 *Palm oil fatty acid composition.*

Fatty acid		Weight %
Lauric	12:0	0.2
Myristic	14:0	1.1
Palmitic	16:0	44.1
Palmitoleic	16:1	0.2
Stearic	18:0	4.4
Oleic	18:1	39.0
Linoleic	18:2	10.6
Linolenic	18:3	0.3
Arachidic	20:0	0.2

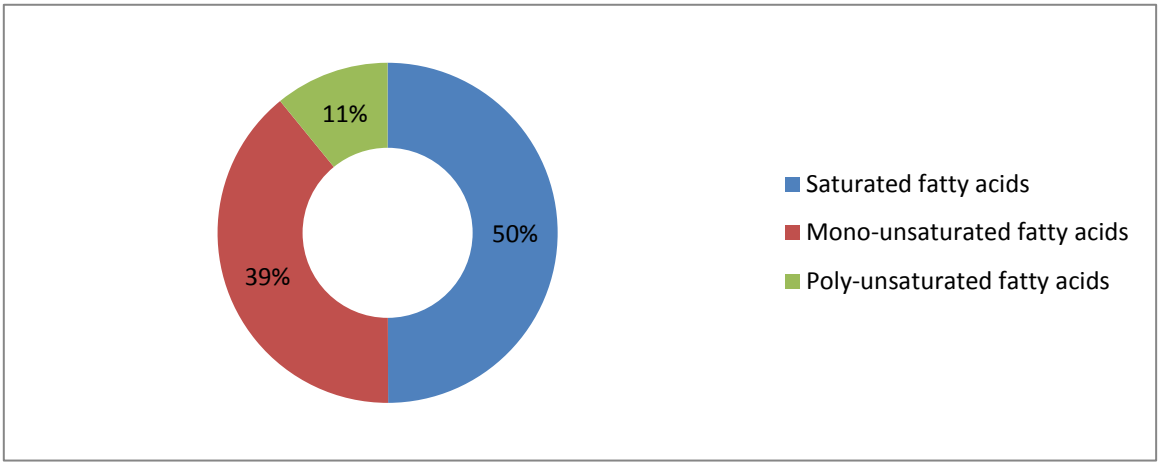

Figure 3.4 *Palm oil fatty acid share.*

Table 3.5 *Palm oil elemental composition.*

Element	Weight %
Carbon	76.79
Hydrogen	12.0
Oxygen	11.1
Others	0.11

Boiling Point Distribution

The boiling range distribution of the two vegetable oils based on the D2887 procedure is captured in Figure 3.5 [42]. From the curves it is evident that soybean oil has a higher IBP[24] (372°C) than palm oil (329°C) and this can be attributed to the fact that soybean oil has a higher molecular mass (≈900 g/mol) than palm oil (≈850 g/mol); both oils however have a similar FBP[25] value of 705°C.

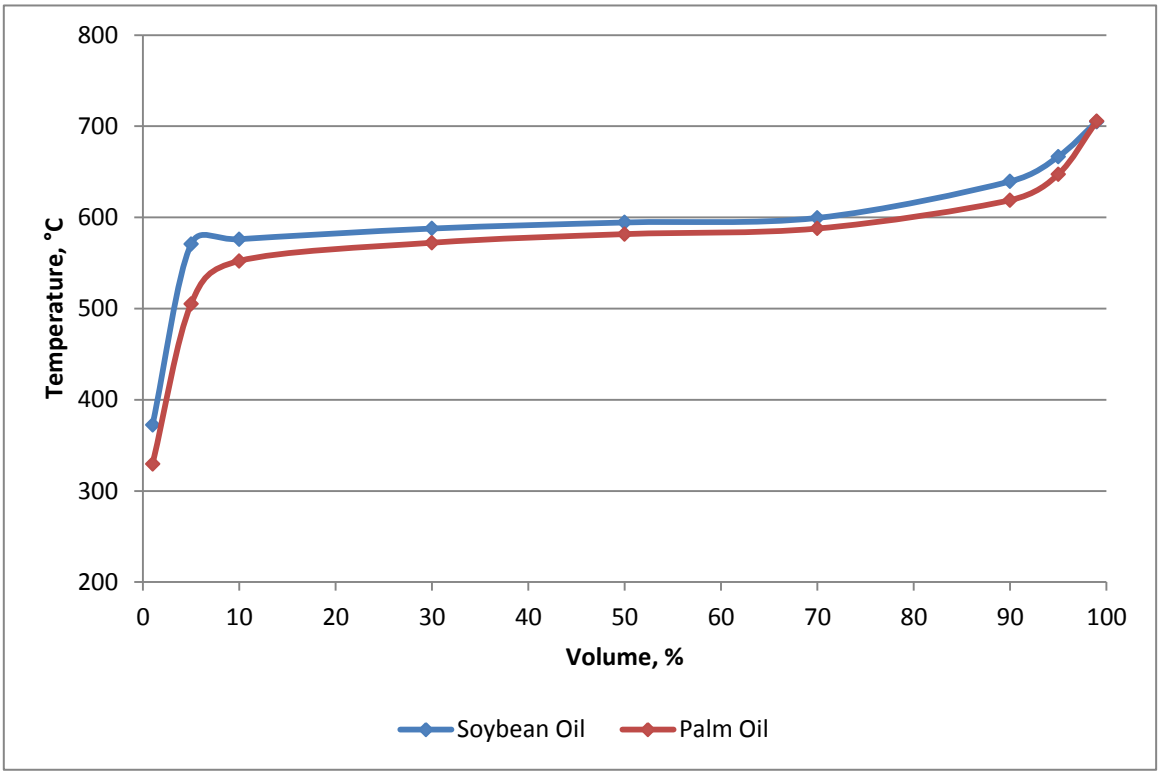

Figure 3.5 *Boiling point distribution for soybean oil and palm oil.*

3.3 Catalyst

The catalyst that was employed for the cracking process was obtained from the OMV AG Refinery. This therefore enables a good prognosis to be made for the trial runs in an

[24] Initial Boiling Point
[25] Final Boiling Point

industrial scale. Due to the fact that the catalyst was drawn from the cracking process at the refinery, steam pre-treatment to reduce its activity was not requisite.

The catalyst used goes by the trade name NEKTOR and is developed by Grace Davison Company. NEKTOR is one of the portfolio of FCC catalysts – others being NOMUS, NACER and NEKTOR-ULCC – developed by Grace Davison through its EnhanceR Technology Platform [43].

EnhanceR Pore Restructuring (EPR) and EnhanceR Metals Resistance (EMR) are the two technologies deployed in the formulation of NEKTOR. EPR as the name indicates involves the restructuring of mesopores physically which exerts an influence on pore connectivity and pore size distribution the end result being a deeper bottoms cracking coupled with improved coke selectivity. On the other hand, EMR is useful in processing metal-containing heavy feed molecules by facilitating an improved contact with metal-passivation catalyst sites. Through this EnhanceR technology, metal contaminants are chemically passivized thus enabling the protection of the zeolite and matrix functions whilst preserving the excellent physical properties of the catalyst.

A summary of the catalyst details and size distribution are depicted in Table 3.6 and Table 3.7 respectively.

Table 3.6 *Catalyst details.*

Manufacturer	Grace Division
Catalyst name	NEKTOR
Type	EnhanceR – based zeolite
Average particle diameter	81 µm
Bulk Density	0.91 g/cm³
Porosity	0.34 cm³/g

Table 3.7 *Catalyst size distribution.*

Size Class, µm	Percentage, p3[%]	Cumulative percentage, Q3[%]
0-20	1	1
20-40	4	5
40-60	19	24
60-80	25	49
80-105	24	73
105-149	20	93
149>	7	100

3.4 Plant Operation

The working principle of the pilot plant is more or less similar to that in oil refineries save for its compact design as has been mentioned.

Depending on the type of feed that is to be processed it may need to be preheated in the storage container before being transferred to a preheated beaker. It is placed on a precision weighing balance that is used to determine the feed rate. Palm oil for instance is semi-solid and forms two phases at room temperature unlike soybean oil and thus has to be preheated and mixed well to ensure the two phases are evenly distributed.

Once the oil is fluid enough to be pumped and after ensuring that the flare is burning smoothly, the processing of the feed can be commenced.

From the preheated beaker the feed is fed to the tubular oven by means of a gear pump. The principal purpose of the oven is to heat the feed to below boiling point and is thus operated at a temperature of between 250 – 330˚C depending on the type of feed. It is worth noting that the oven should not be operated at very high temperatures since higher temperatures will lead to pre-cracking of the feed resulting in clogging of the feed inlet pipe as a consequence of coke formation.

The heated oil then enters the reactor at the bottom and subsequently comes into contact with the hot regenerated catalyst. The vaporizing of the feed causes a corresponding expansion of volume which together with the help of the bottom fluidization aids in sweeping the mixture of the catalyst and oil vapours up the riser. The cracking reactions occur as the mixture is transported up the riser. The reaction temperature lies in the region 420 – 565°C whilst the residence time for the reaction is between 1 – 2 seconds. Due to the fact that the riser is a vertical pipe, an ideal plug flow reactor is simulated as the mixture of the catalyst and vapour travel up the riser with minimum back mixing.

The riser fluidization is turned off once it is observed that the plant is running smoothly leaving the vaporizing feed to act as a fluidization medium by means of its own expansion.

On exiting riser, the hydrocarbon vapours and the catalyst come into contact with the particle separator an equivalent of the RTD[26] used in industrial plants whose function is to separate the hydrocarbon vapours from the catalyst. The increase in diameter of the plant from the riser causes a decrease in the fluidization velocity thus making the separation effective. Expedient separation is done so as to deter additional – and undesirable – reactions from occurring which may include the non-selective catalytic secondary cracking of the desirable products. This is due to the plain reason that the catalyst leaving the riser still retains some activity.

[26] Riser Termination Device

The hydrocarbon vapours exit at the top of the plant and are then directed to the flare device where they are burned off whereas the separated catalyst flows down the return flow tube to the siphon. The return flow tube and the siphon fluidization provide a disengagement space for the remaining hydrocarbon vapours and those entrained with the catalyst. This in a way can be compared to a stripper found in industrial plants thus avoiding the burning off of these hydrocarbon vapours in the regenerator. Unlike in the industrial set up where steam is employed for the stripping action, at the pilot the siphon fluidization medium is technical nitrogen. Over and above that, the siphon fluidization (nitrogen) acts as a buffer zone between the regenerator and the hydrocarbon vapours thus avoiding any explosion risk besides helping in ensuring that the return flow tube is not blocked with catalyst.

During the cracking reactions, catalyst activity and selectivity is reduced as a consequence of coke deposition on the catalyst thus the term spent catalyst and the process is known as catalyst deactivation. From the stripper, the spent catalyst is then transferred to the regenerator where the catalyst activity is restored by burning off of the coke by contacting with air – oxygen – thus the term catalyst regeneration. The regenerator can be described as a steady state bubbling fluidized bed. Besides the restoration of the catalyst, the regenerator supplies heat for the cracking reactions: the regeneration of the catalyst is an exothermic reaction which raises the temperature of the catalyst. The flue gas from the combustion process of coke is channelled out of the regenerator through the flue gas exit which is located close to the top of the plant.

From the regenerator the catalyst flows down to the riser via a cooling system which aids in lowering the catalyst temperature with the bottom fluidization providing the aeration needed to ensure smooth flow of the catalyst down to the riser.

Table 3.8 shows the fluidization gas for the various fluidizations undertaken in the plant.

Table 3.8 *Pilot plant fluidization.*

Fluidization	Gas medium	Function
Bottom	N_2	Catalyst transportation Riser and regenerator separation
Riser	N_2	Catalyst transportation
Siphon	N_2	Catalyst transportation from the return flow tube to the regenerator Stripping effect Regenerator and return flow tube separation Riser and regenerator separation
Regenerator	Air	Combustion of coke for catalyst regeneration

From Table 3.8 one can evidently see that save for the regenerator that requires the oxygen for combustion the rest of the fluidization in the plant is primarily undertaken using nitrogen.

3.5 Low Temperature Cracking

During the course of the project, some cracking reactions were done at low riser temperatures not previously performed. Soybean oil was cracked at a low temperature of 430°C with palm oil being cracked at a temperature of 460°C.

Low temperature cracking brings with it some challenges by the very fact that the compact design of the plant implies that the riser and regenerator are thermally coupled: As a result, a lower riser temperature is contingent on having a lower regenerator temperature. Thus it is critical to ensure that a good balance is maintained to avoid lowering the regenerator temperature to a value below that required for regeneration of the catalyst leading to incomplete combustion of the coke.

The low riser temperatures were made possible by the use of the cooling system – three conical helix designed coolers – which uses either water or air as a cooling medium and by means of the cooler fluidization. The cooling thus aids in thermally decoupling the regenerator and the riser by cooling the catalyst as it flows down to the riser.

When using water as a cooling medium, distilled water is first pumped through the cooling system before turning on the faucet for the normal water. When the cracking process is over, the distilled water is again pumped in and then air is let in to ensure that no water remains in the system for safety reasons.

To reduce the effects of back mixing during the cooler fluidization, baffles were added to the cooler with holes drilled on the plates to avoid the formation of dead zones within the cooling region. The new distribution system thus ensured homogeneous fluidization over the cross sectional area.

A schematic of the cooling system is shown in Figure 3.6.

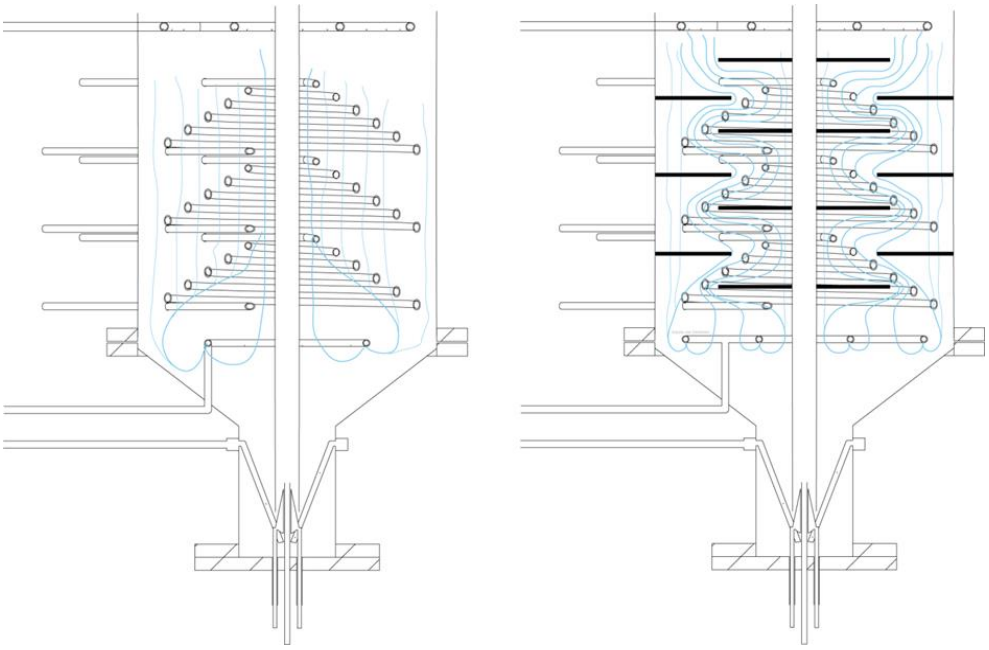

Figure 3.6 *Pilot plant cooling system.*

3.6 Analysis

In order to obtain samples for analysis of the product spectrum, extraction is achieved by means of a diaphragm pump which is used to extract a fraction of the gas and the rest is channelled onwards to the flare. A water cooling system and a cryostat having a set temperature of –15˚C are used to condense the various components with the latter aiding the condensation of the C_5 and C_6 components. The lighter components C_1 – C_4 are collected by means of a gas sampling bulb whilst the liquid product that has been condensed is collected in a glass bottle.

Figure 3.7 shows the liquid product sample extracted from the pilot plant with the two phases comprising the organic liquid product and water visible.

Figure 3.7 *Liquid product sample.*

A seven lump model is used for the characterization of the products. The various products obtained from the cracking of vegetable oil are featured in Figure 3.8.

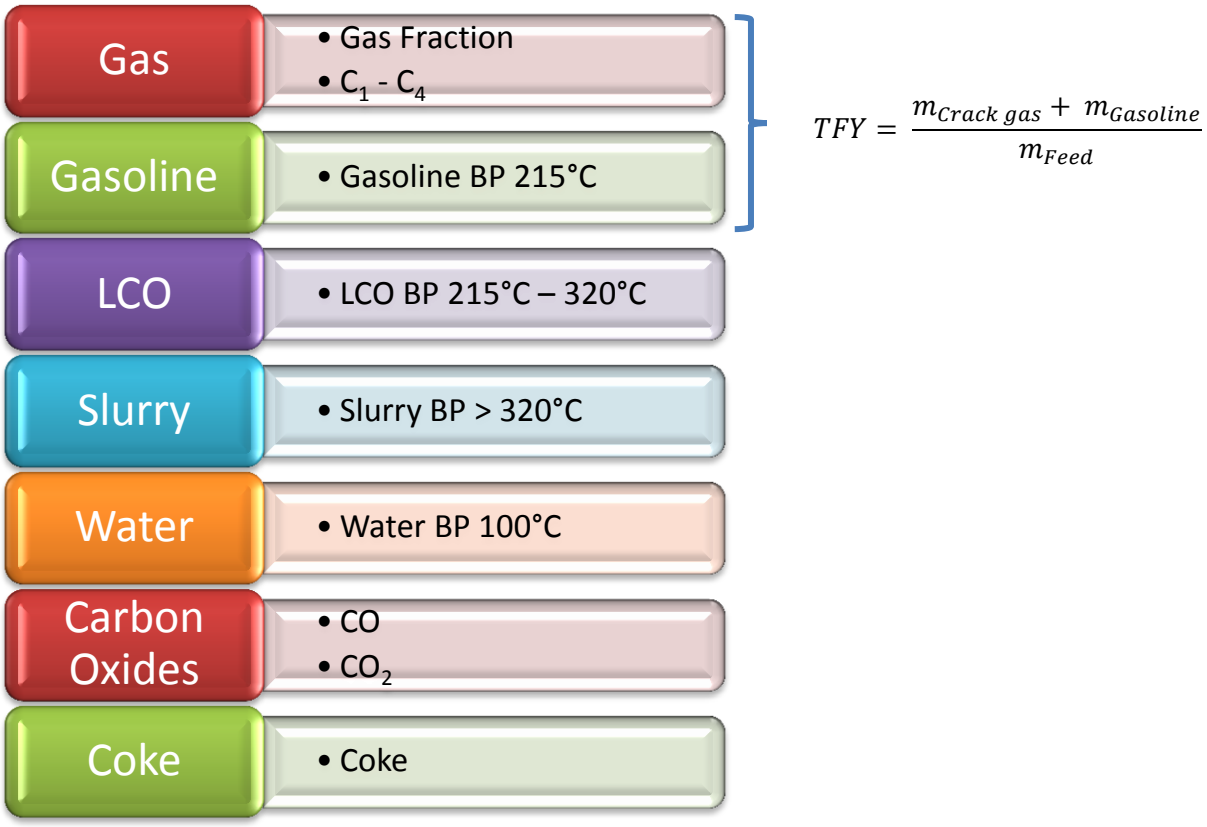

Figure 3.8 *Products obtained from the cracking process.*

The model lumps the different hydrocarbon products of the cracking process based on distillation cuts. Water yield is obtained by gravimetric analysis of the water obtained from the phase separation of the product sample while CO, CO_2 and coke a solid by-product of the cracking reactions are obtained from product gas and flue gas analysis respectively.

3.6.1 Total Fuel Yield

The total fuel yield also known as the conversion, is obtained from the following equation,

$$TFY = \frac{m_{Crack\ gas} + m_{Gasoline}}{m_{Feed}} \quad (3.1)$$

As can be noted, the total fuel yield takes into consideration the products considered as valuable.

3.6.2 Gas Analysis

For the purposes of the product gas analysis, a 50 µl probe is extracted from the gas bulb and injected into the instrument a Shimadzu G17 A GC, which uses a capillary column.

For the gas analysis case, the splitless mode is utilized. When the sample contains small amounts of the target analyte i.e. trace analysis, such that splitting the sample at the injection port will lead to an inadequate signal from the detector, then the splitless mode is employed. This technique of injection involves flipping of the split valve and as a consequence all of the sample analyte vaporized is transferred to the column for detection.

The chromatogram is then obtained and from it the various components present in the sample can be known. The carrier gas used is helium and the detection is achieved by both FID[27] and TCD[28]. FID is used for the detection of organic compounds with a hydrogen-carbon bond whereas TCD is used for detection of inorganic gases and concentrated organic compounds and in the processing case in this study, nitrogen and carbon dioxide; the gas used for the FID process is hydrogen while helium is used for the TCD process. The operation details for the Shimadzu G17 A GC are tabulated in Table 3.9.

Table 3.9 *Gas chromatography operation details.*

Carrier gas	Helium
Injection	Splitless mode, 200°C, 50 µl
Column 1	Varian CP-Al_2O_3/$NaSO_4$ 50 m * 0.25 mm * 4 µm
Detector 1	Flame Ionization Detector (FID), 200°C
Column 2	Carboplot P7 27.5 m * 0.53 mm * 25 µm
Detector 2	Thermal Conductivity Detector (TCD), 105°C

3.6.3 Simulated Distillation

Simulated Distillation utilizes the split mode system of injection. In the split mode, a fraction of the vaporized sample is transferred to the column with the remainder exiting from the injection port via a split vent. This mode of injection is employed when the sample concentration is high such that discarding some during the injection process will not make any difference to the analysis.

With respect to the simulated distillation procedure, a probe of 1.6 µl is injected into the instrument also a Shimadzu G17 A GC, which is likewise vaporized below the septum and separated into the various components in the column. A split ratio of 1:30 is used with the detector employed being the FID type. The chromatograph is obtained and in addition a

[27] Flame Ionization Detector
[28] Thermal Ionization Detector

boiling curve is also produced. The carrier gas is hydrogen and this also used for the FID process.

A summary of the operation details for the Shimadzu G17 A GC SimDist are captured in Table 3.10.

Table 3.10 *SimDist operation details.*

Carrier gas	Hydrogen
Injection	Split mode 1:30, 325°C, 1.6 µl
Column	Zebron ZB-1 30 m*0.32 mm*0.25 µm
Detector	Flame Ionization Detector (FID), 350°C

Figure 3.9 shows a sample distillation curve obtained from the SimDist analysis for the organic liquid product.

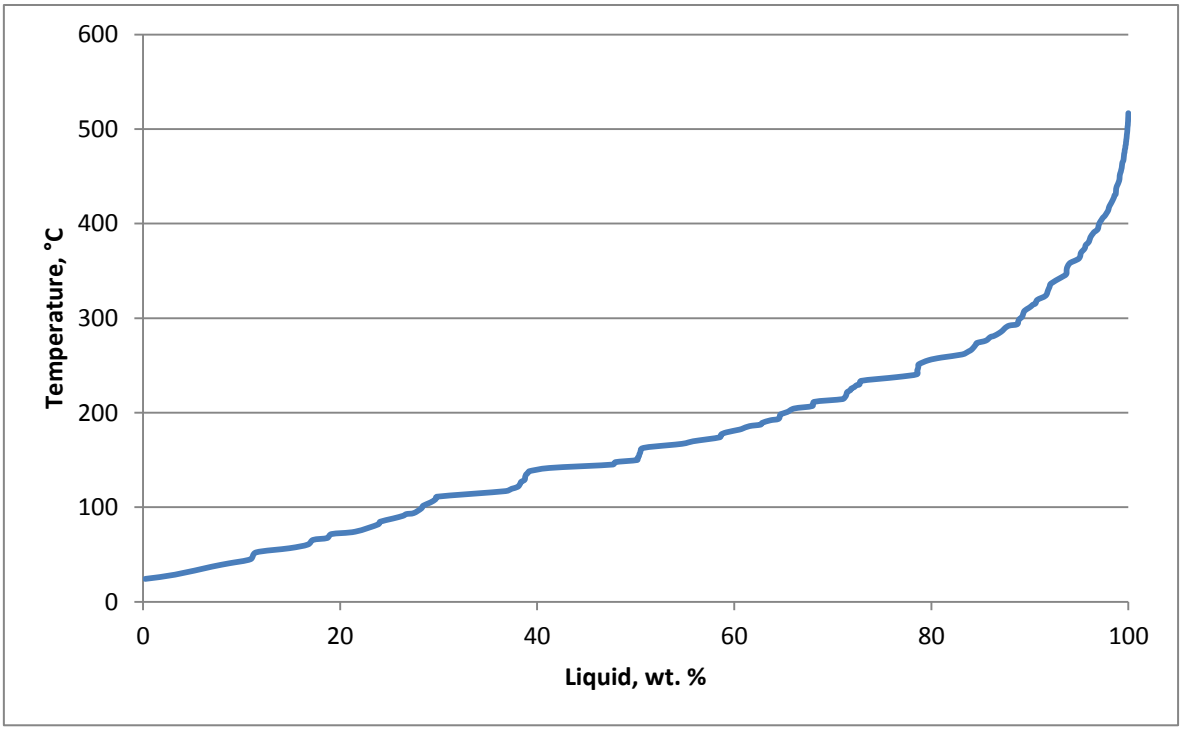

Figure 3.9 *Distillation curve for the liquid organic product obtained.*

3.6.4 Flue Gas Analysis

During the operation of the plant, continuous analysis of the flue gas is undertaken by means of a Rosemount NGA2000 gas analyser. It is imperative to determine the amount of O_2, CO and CO_2 so at to be able to keep tabs on the combustion process of coke and subsequently from the analysis of the flue gas composition the yield of coke can be determined. The values of O_2, CO and CO_2 will indicate to what extent the combustion of

coke goes and if need arises some parameters may need to be adjusted to facilitate good combustion.

The measuring principle of oxygen contained in the flue gas is based on paramagnetism, i.e. the paramagnetic properties of oxygen are exploited as a basis of measurement since it is attracted to a strong magnetic field while most gases are not.

For CO and CO_2 measurement, NDIR[29] is used. The type of gas is characterised by the gas specific wavelength absorption bands whilst the concentration of the gas being measured is derived from the strength of the absorption.

3.6.5 Gasoline Analysis

Gasoline analysis is undertaken by means of an IROX 2000 instrument which is a Mid-FTIR[30] spectrophotometer that automatically measures the concentration of the most important gasoline components. The inbuilt density meter and a mathematical model aids in determining key properties of gasoline such as octane numbers, aromatics, olefins, oxygenates, distillation properties and vapour pressure.

Gasoline octane numbers give a measure of its knocking – maximum compression ratio – characteristics; the higher the octane numbers the lower tendency for the gasoline to self-ignite or knock. There are two types of octane numbers based on the severity of the operation of the engine. The Research Octane Number (RON) is used to simulate the performance of gasoline under low-severity engine operation with the engine speed for its measurement being pegged at 600 rpm whereas the Motor Octane Number (MON) simulates gasoline performance at high-severity engine operation or at high loads thus the engine speed is set at 900 rpm.

Determination of the octane numbers is based on the blending of *n*-heptane (0 octane) and iso-octane (100 octane). Thus an octane number of say 90 implies that the gasoline knocks at the same compression ratio as that of a blend of 90% iso-octane and 10% *n*-heptane.

The Michelson interferometer principle which is depicted in Figure 3.10 is used for the analysis of the various components of gasoline. The absorption spectrum is then evaluated after the scan from the different intensity values stored by performing a Fourier transform.

[29] Non-Dispersive Infrared
[30] Fourier Transform Infrared

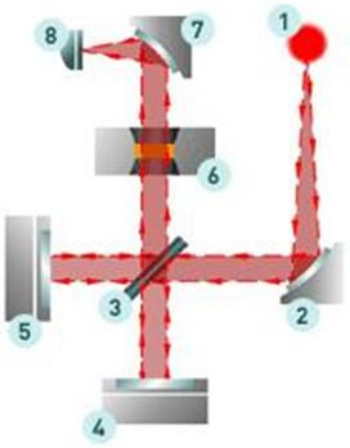

Figure 3.10 *IROX measuring principle [44].*
Legend: *(1)Infrared source, (2)Collimation mirror, (3)Beam splitter, (4)Fixed mirror, (5)Scanning mirror (6)Measuring cell (7)Collimation mirror, (8)Infrared detector.*

3.7 Computation

3.7.1 Feed Rate

The feed rate is calculated by determining the rate of decrease of the feed in the pre-heat flask over a time interval. The determination of the feed rate during the extraction of the product is vital due to the fact that from it the various mass balances especially on coke can be calculated.

It is thus obtained by,

$$\dot{m}_{Feed} = \frac{\Delta m_{Pre-heat\ flask}}{\Delta t} \tag{3.2}$$

3.7.2 Circulation Rate

For a circulating fluidized bed, the circulation rate is a pivotal parameter and can be used to deduce on whether the plant is coked or if in case the fluidization orifices have been clogged by the catalyst. The method of the circulation rate was developed by Reichhold [36].

In the pilot plant, the circulation rate is determined by switching off the siphon fluidization for a short interval of time. The switching off of the siphon fluidization implies that the catalyst ceases to be transported from the siphon to the regenerator but it does not affect the cracking process. Since the catalyst continues to be sucked in through the riser, the level of the catalyst in the regenerator decreases and this decrease causes a corresponding decrease in the pressure drop at the bottom of the bed. Thus the hydrostatic pressure drop in the regenerator as a consequence of the siphon being switched off becomes the basis for

the calculation of the circulation rate of the catalyst given that the geometry of the regenerator and the catalyst properties are known.

The regenerator pressure drop is calculated by,

$$\Delta(\Delta p_{Reg}) \approx \frac{\Delta m_{Catalyst} * g}{A_{Reg}} \tag{3.3}$$

On rearranging, the correlation yields,

$$\Delta m_{Catalyst} \approx \frac{\Delta(\Delta p_{Reg}) * A_{Reg}}{g} \tag{3.4}$$

Whereby the area of the regenerator A_{Reg} is given by the correlation,

$$A_{Reg} = \frac{\pi}{4} * \left(d_{Reg,i} - d_{Return,o}\right) \tag{3.5}$$

Dividing through equation 3.3 by the time the siphon is switched off yields the correlation that is used to determine the circulation rate.

$$\dot{m}_{Catalyst} = \frac{\Delta m_{Catalyst}}{\Delta t} \approx \frac{\Delta(\Delta p_{Reg}) * A_{Reg}}{\Delta t * g} \tag{3.6}$$

Figure 3.11 depicts the pressure drop behaviour when the siphon is switched off for a short interval of time.

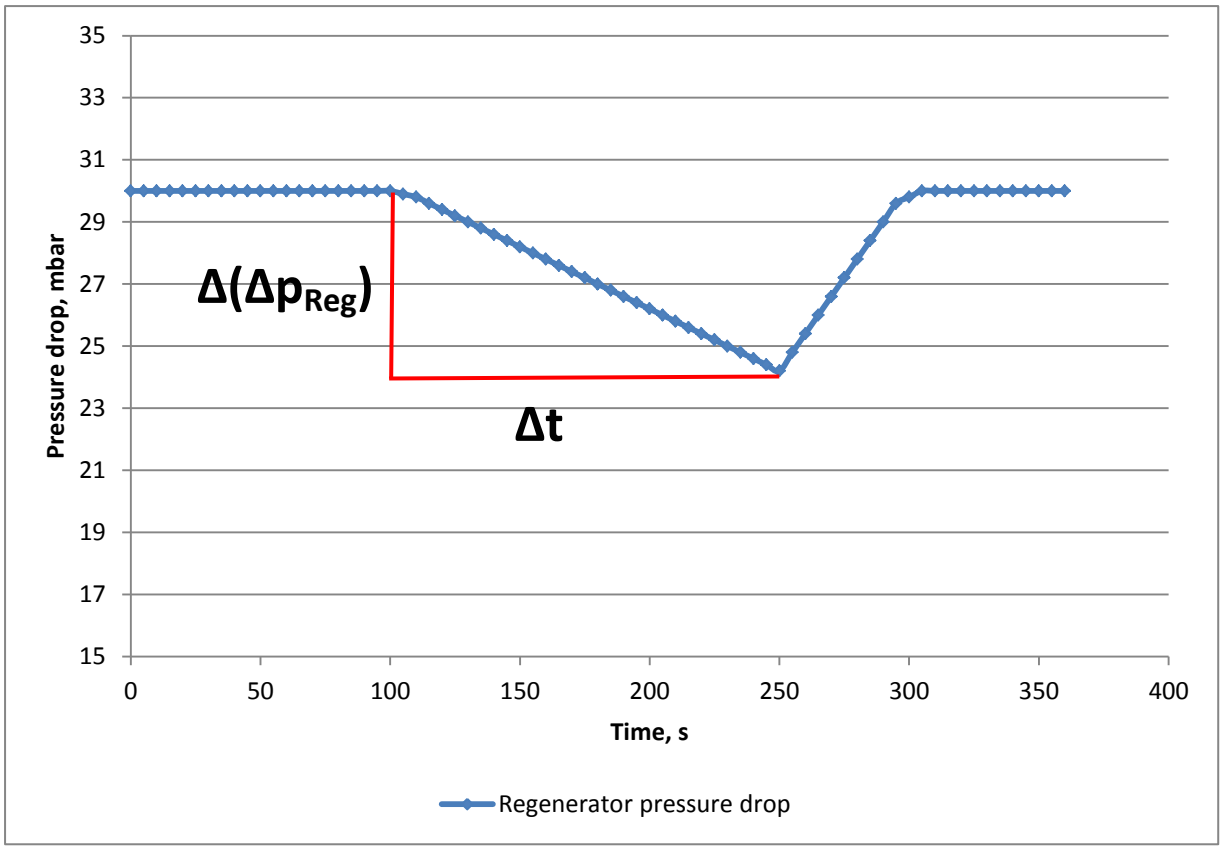

Figure 3.11 *Regenerator pressure drop changes when siphon fluidization is switched off.*

3.7.3 Catalyst to Oil Ratio

The Catalyst to Oil ratio or in abbreviation C/O ratio is an important parameter in ascertaining the severity of the cracking process. Using the catalyst circulation rate, equation 3.6, and feed flow rate, equation 3.2, the correlation for the C/O ratio for the pilot plant can be obtained.

$$C/O = \frac{\dot{m}_{Catalyst}}{\dot{m}_{Feed}} \tag{3.7}$$

The C/O ratio and its influence on the product spectrum when varied, for the FCC pilot plant, was extensively studied by Hofer [45]. In the industrial plants the C/O ratio is usually in the range of 5 – 8 with its variation being achieved by regulation of the stripper and regenerator slide valves. In the pilot plant, the C/O ratio may be varied by adjusting the cone height, feed inlet pipe height, the mass of the catalyst and also by means of the bottom fluidization.

3.7.4 Coke

Coke composition is obtained by means of a carbon and hydrogen balance of the flue gas by calculation of mass flow rates as shown in the equations that follow.

$$\dot{m}_{C\_coke} = M_C * \left(\frac{\rho_{CO} * \dot{V}_{CO}}{M_{CO}} + \frac{\rho_{CO_2} * \dot{V}_{CO_2}}{M_{CO_2}} \right) \quad (3.8)$$

$$\dot{m}_{H\_coke} = M_{H_2} * \left(\frac{\rho_{H20} * \dot{V}_{H2O}}{M_{H2O}} \right) \quad (3.9)$$

The coke´s C/H mass ratio is then determined by dividing the flow rates in equation 3.8 and 3.9.

$$\frac{C}{H} = \frac{\dot{m}_{C\_coke}}{\dot{m}_{H\_coke}} \quad (3.10)$$

4 RESULTS AND DISCUSSION

4.1 Soybean Oil

The cracking of soybean oil was undertaken with the main parameter variation being the riser temperature which involved temperatures ranging from 430°C to 550°C. The feed rate for the processing at this range of riser temperature was set at 2.5 kg/h. The product spectrum of the total conversion and the different lumps within these range of temperatures are depicted in the graphs that follow.

4.1.1 Total Conversion, Gasoline and Gas

From Figure 4.1, the conversion curve exhibits a steady increase with a corresponding upping of the riser temperature until a temperature of about 520°C. The lowest conversion, 51.3%, is recorded at the lowest temperature during the experiment, i.e. 430°C. From then henceforth, the conversion starts to pick with the highest conversion, 65.4%, being attained at a temperature of 550°C – highest riser temperature during the trial. It is worth noting that the conversion increases minimally once a temp of about 520°C is reached since the conversion at a riser temperature of 518°C is 65% implying that from 520°C to 550°C a meagre gain of 0.4% is realized whereas from 430°C to 520°C a gain of 13.7% is achieved.

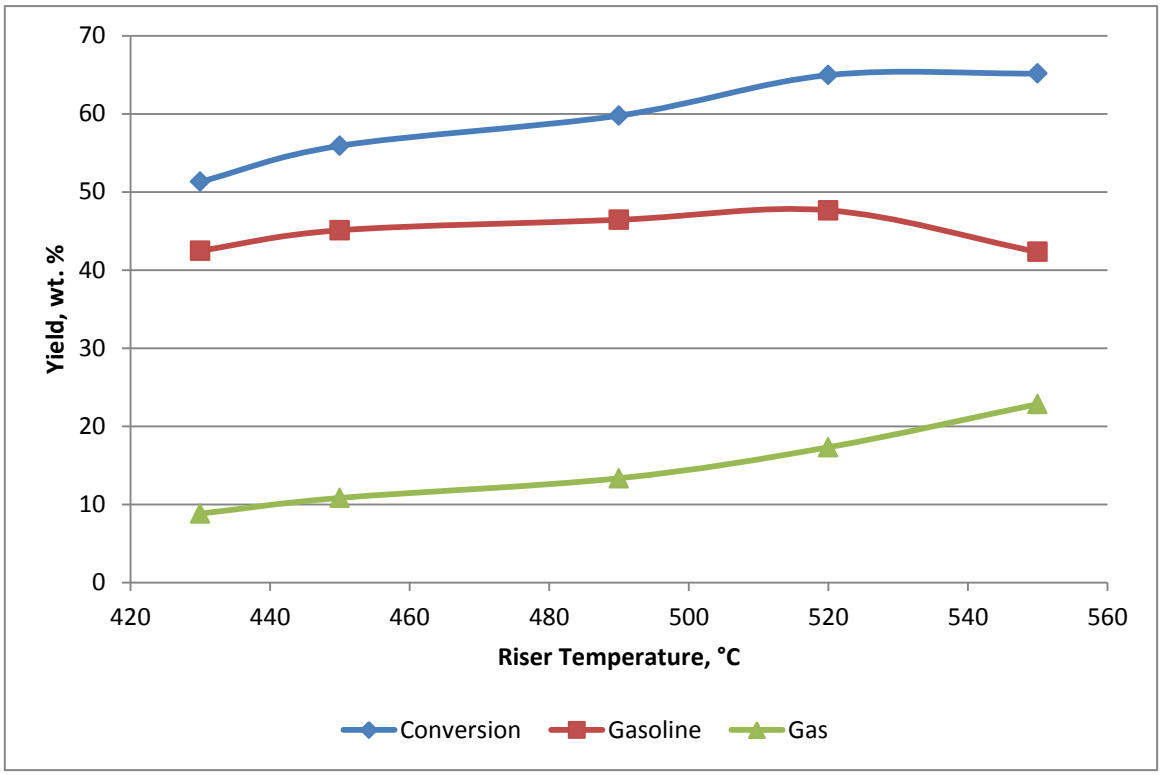

Figure 4.1 *Soybean oil conversion, gasoline and gas yields over riser temperature range trends.*

Gasoline shows a gradual increase in yield from 42.5% at a riser temperature of 430°C to a maximum yield of 47.6% attained at a riser temperature of 520°C – a gain of 5.2% as seen in Figure 4.1. From then on a tendency is observed where with an increase in the riser temperature the gasoline yield exhibits a sharp decline with a riser temperature of 550°C having an output of 42.3%; a value lower than that obtained at the lowest riser temperature of 430°C, a drop of 5.3% for a 30° rise in temperature. The decrease in yield can be attributed to further cracking of the gasoline.

At the lowest riser temperature, 430°C, the gas yield is 8.8% and as captured in Figure 4.1, with a rising riser temperature comes with it a rise in the gas yield with the value peaking at temperature a of 550°C where a yield of 22.8% is achieved. Between the riser temperatures of 490°C and 550°C, a sharp increase in the gas yield is exhibited with a gain of 9.5% being recorded. Of interest though is that contrary to the gasoline trend, there is an increase in the yield from the riser temperature of 520°C to 550°C, with a rise of 5.5% being noted; quite the opposite with gasoline which exhibits a 5.3% drop in yield, an almost equivalent value. These results lend credence to the argument advanced previously that the gasoline is converted to gas due to further cracking reactions.

The graph also paints a picture that the gas yield from the cracking process racks up the conversion.

4.1.2 LCO, Slurry and Coke

As can be deciphered from the graph in Figure 4.2, both LCO and slurry evince a gradual decline in the yield with a rising riser temperature. Both coincidentally have a drop in yield of roughly 8% with the highest LCO yield, 19.8%, being recorded at the lowest temperature, 430°C. Conversely the highest riser temperature, 550°C, has the lowest return of LCO, 11.2%. The same scenario is exhibited by the slurry with the highest return, 12.5%, being attained at the lowest temperature 430°C whereas the highest riser temperature has a meagre output of 4.7%.

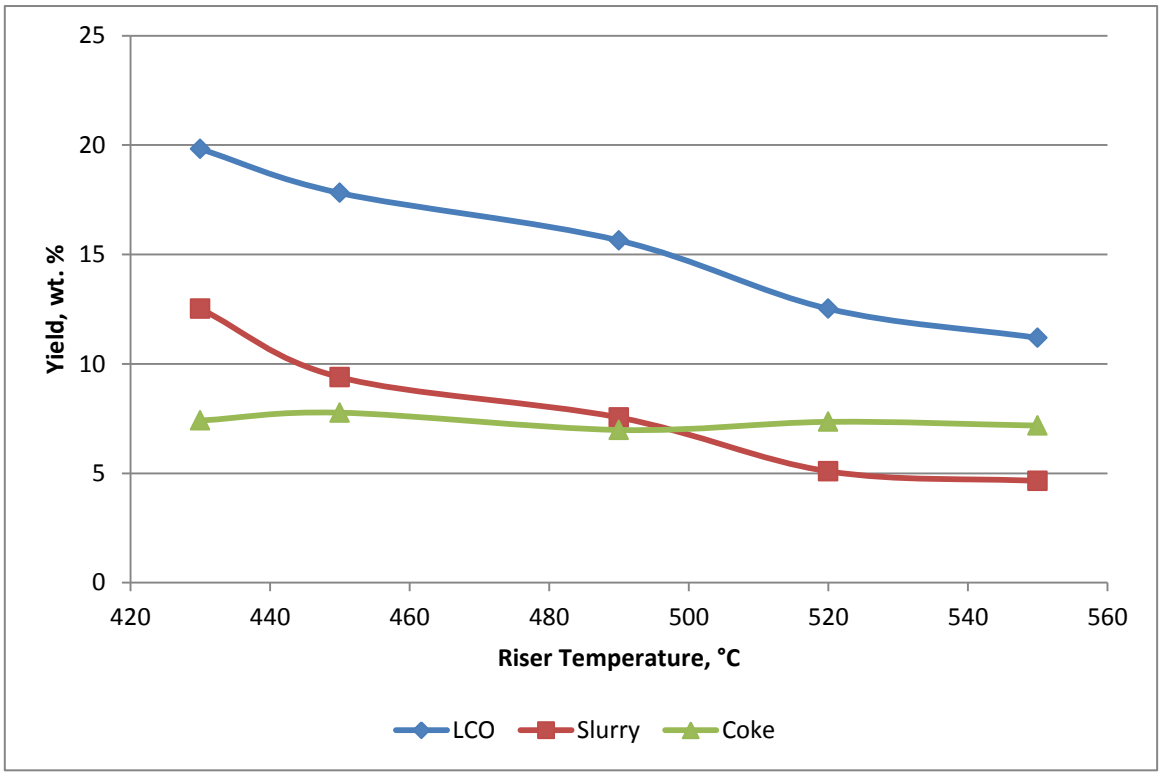

Figure 4.2 *Soybean oil conversion, LCO, slurry and coke yields over riser temperature range trends.*

It is worth pointing out that from a comparison with the total yield curve, once the total conversion starts to increase minimally between the temperatures 520°C and 550°C, both LCO and slurry seem to exhibit a minimal decline in the yield, with a drop of 1.3% being observed as in the case of the LCO and 0.4% in the case of the slurry.

Coke yield is relatively constant throughout with output averaging 7.3% in the riser temperature range of 430 – 550°C.

4.1.3 Water, CO and CO_2

As can be noted from the graph depicted in Figure 4.3, the water curve ascends with a rise in temperature with a yield of 10.5% being recorded at the highest riser temperature up from 8.4% at a riser temperature of 430°C – a gain of 2.0%.

As noted earlier on, unlike the conventional crude oil processed in the FCC plants, vegetable oils yield water when catalytically cracked and this results justify this point. The results corroborate the theory presented on the mechanism of the catalytic cracking of vegetable oil that the deoxygenation process leads to the formation of water, CO and CO_2.

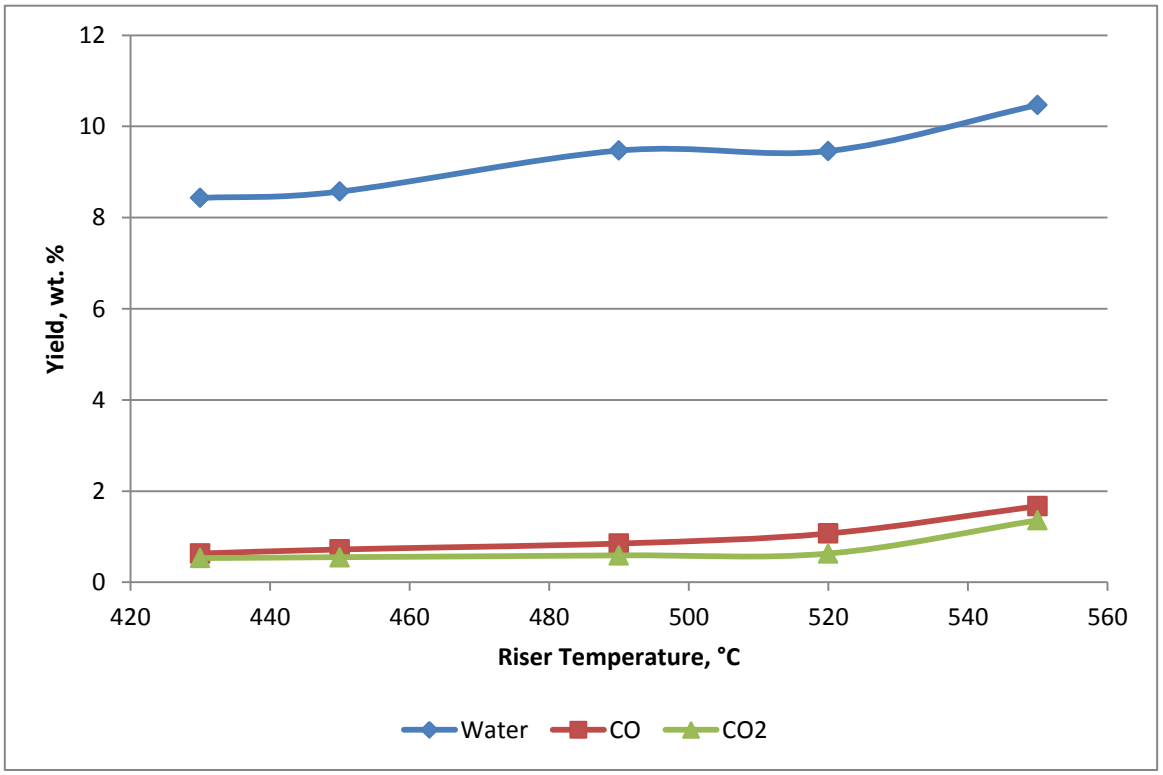

Figure 4.3 *Soybean oil water, CO and CO_2 yields over riser temperature range trends.*

Both CO and CO_2 project a similar trend of curves with CO recording a paltry gain of 1% from a value of 0.6% at the lowest riser temperature of 430°C to a peak value of 1.7% at 550°C riser temperature. CO_2 on the other hand records a 0.8% gain with a peak yield of 1.4% being recorded at a riser temperature of 550°C whilst the lowest yield 0.53% being obtained at the lowest riser temperature of 430°C.

The curves also paint a picture of a sharp rise in the yield of both CO and CO_2 from the temperature of 520°C a similar scenario portrayed previously by the gas yield in Figure 4.1.

4.1.4 Product Gas Spectrum

The product gas spectrum for the cracking of soybean oil over the various riser processing temperatures is depicted in Figure 4.4. As had earlier been explained in section 4.1.1, it is evident that the gas yields increase with a corresponding rising riser temperature. Propylene and isobutane register the highest yields with the yield of propylene gaining 4.9% to a final value of 7.7% whereas the highest output of Isobutane is 3.3% corresponding to 1.9% increase in yield. The high yield of propylene and isobutane can be attributed to the carbenium ion theory whereby the β-cleavage of the hydrocarbon molecule implies that the smallest molecule formed in this cracking reaction will be composed of three carbon atoms. This thus explains the high yield of the C_3 and C_4 gases while the C_1 and C_2 gases gain minimally.

The two gases obtained in large quantities are important gases with isobutane being increasingly preferred instead of CFCs[31] as a refrigerant and propellant in aerosol sprays in a bid to stem the spiralling of GHG emissions.

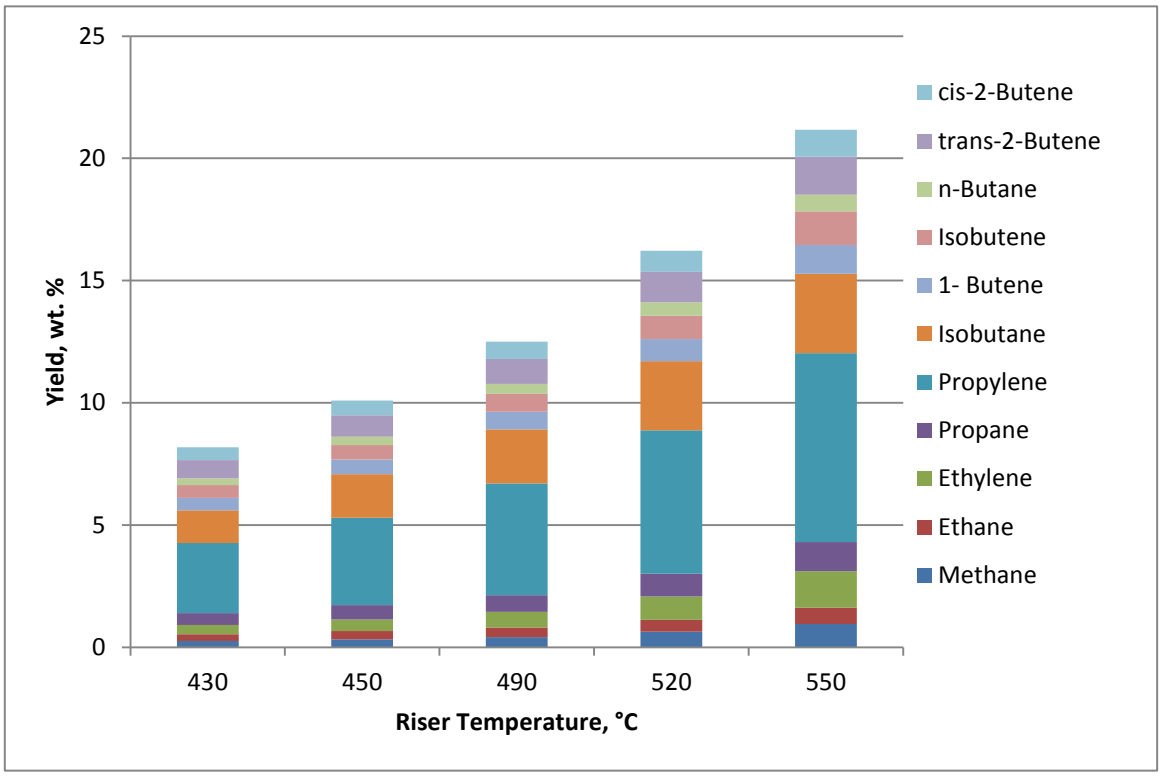

Figure 4.4 *Product gas spectrum obtained from soybean oil over riser temperature range.*

The olefin gases which are valuable products obtained in an FCC process are compared with the rest of the gases. Propylene which is a major component of a wide array of end use

[31] Chlorofluorocarbons

products is compared with the most important chemical block ethylene and the butenes which are normally used as copolymers.

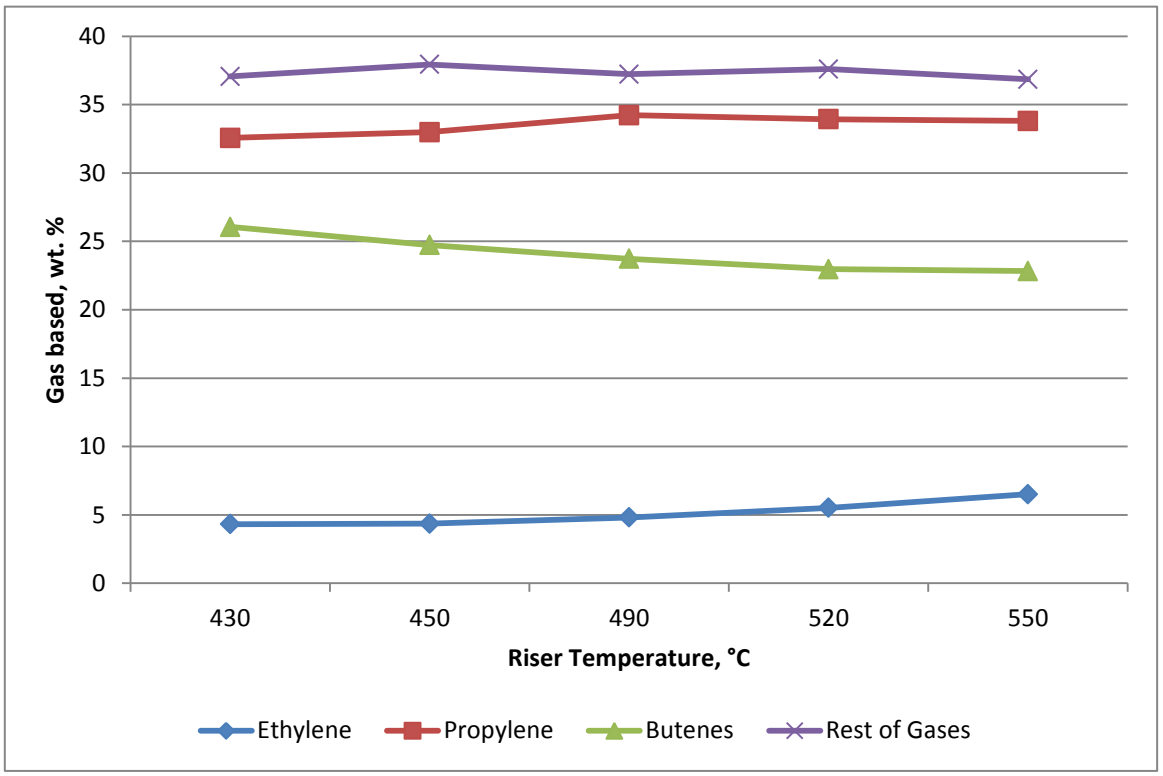

Figure 4.5 *Comparison of ethylene, propylene and butenes with the rest of the gases obtained from soybean oil.*

From Figure 4.5, it can be inferred that of the three important olefin gases, propylene yield increases by 1.2% to 33.8% while ethylene posts the most gain, an increase of 2.2% the final value standing at 6.5%. However, though there is an increase in the yield of the butenes, it experiences a percentage drop when compared to the other gases to a final value of 22.8% from 26.1% – comparable to a 3.3% decrease. The percentage drop is almost comparable to the total increase of ethylene and propylene.

4.2 Palm Oil

Palm oil was cracked with the riser temperature being varied from 460°C to 540°C. The feed rate for the processing at this range of riser temperature was also set at 2.5 kg/h. The results obtained are captured in the graphs that follow.

4.2.1 Total Conversion, Gasoline and Gas

The palm oil conversion curve projects the same trend as that of soybean oil with the conversion increasing with a corresponding rise in riser temperature as captured in Figure 4.6. At the lowest riser temperature, 460°C, a conversion of 55% is obtained and this value

rises to 67.6% at the highest riser temperature, 540°C. Just like as was the case for soybean oil, the conversion gains minimally at the higher temperatures.

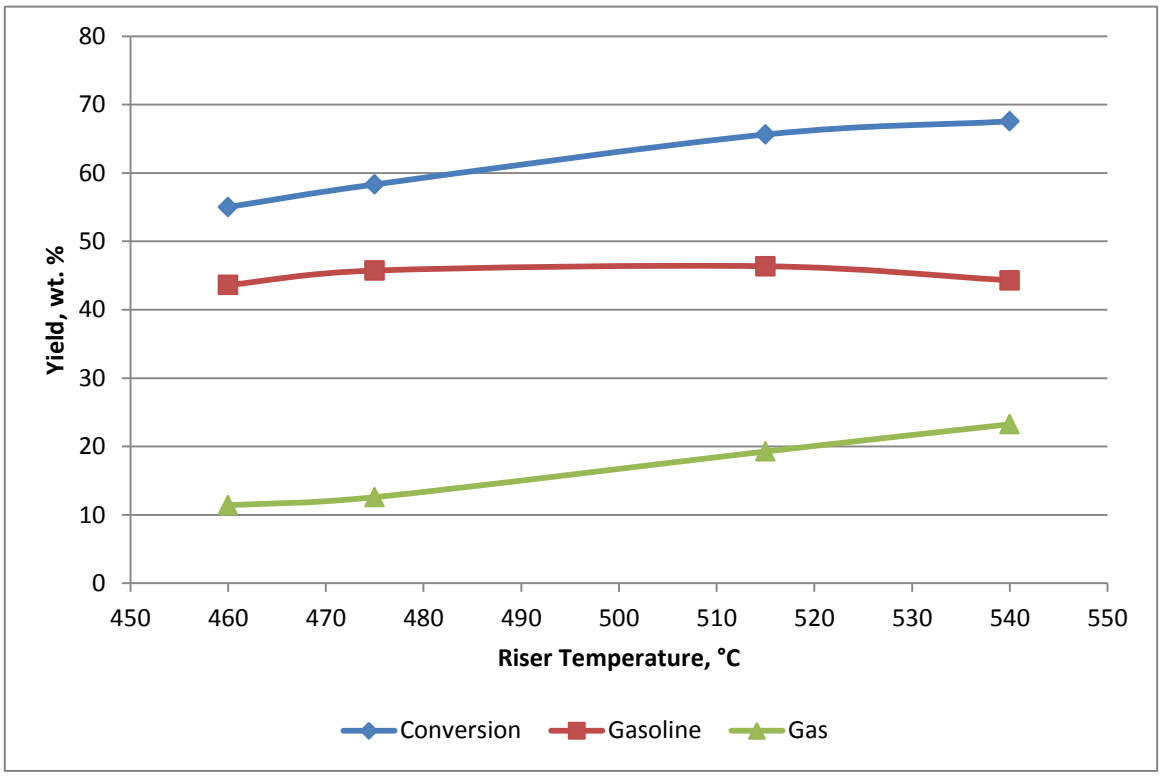

Figure 4.6 *Palm oil conversion, gasoline and gas yields over riser temperature range trends.*

As pertains to gasoline, a scenario similar to that of soybean oil in Figure 4.1 is replicated with the yield increasing from 43.6% at the lowest riser temperature to a peak value of 46.4% at 515°C. Thereafter the yield begins to show a decline with the highest riser temperature 540°C posting a yield of 44.3%. The same reason advanced earlier for the decline in soybean oil gasoline – further cracking of the gasoline – also plays a role in the decrease in yield.

The gas yield curve projects a similar trend as that previously observed for soybean oil case in Figure 4.1. The yield rises from a low of 11.4% at riser temperature 460°C, to a maximum value of 23.3% at 540°C. As had been stated in section 4.1.1, the gas yield increases at the higher temperatures as a consequence of the cracking of gasoline.

4.2.2 LCO, Slurry and Coke

The curves in Figure 4.7 purvey a picture similar to that observed in Figure 4.2. The LCO and the slurry yield decrease with an increasing riser temperature with LCO yield suffering a drop of 6.3% from a high of 15.7% obtained at riser temperature 460°C to a low of 9.4% at 540°C. On the other hand the yield of the slurry drops from 9.2% to 4.3%, a 4.9% drop within the same temperature range.

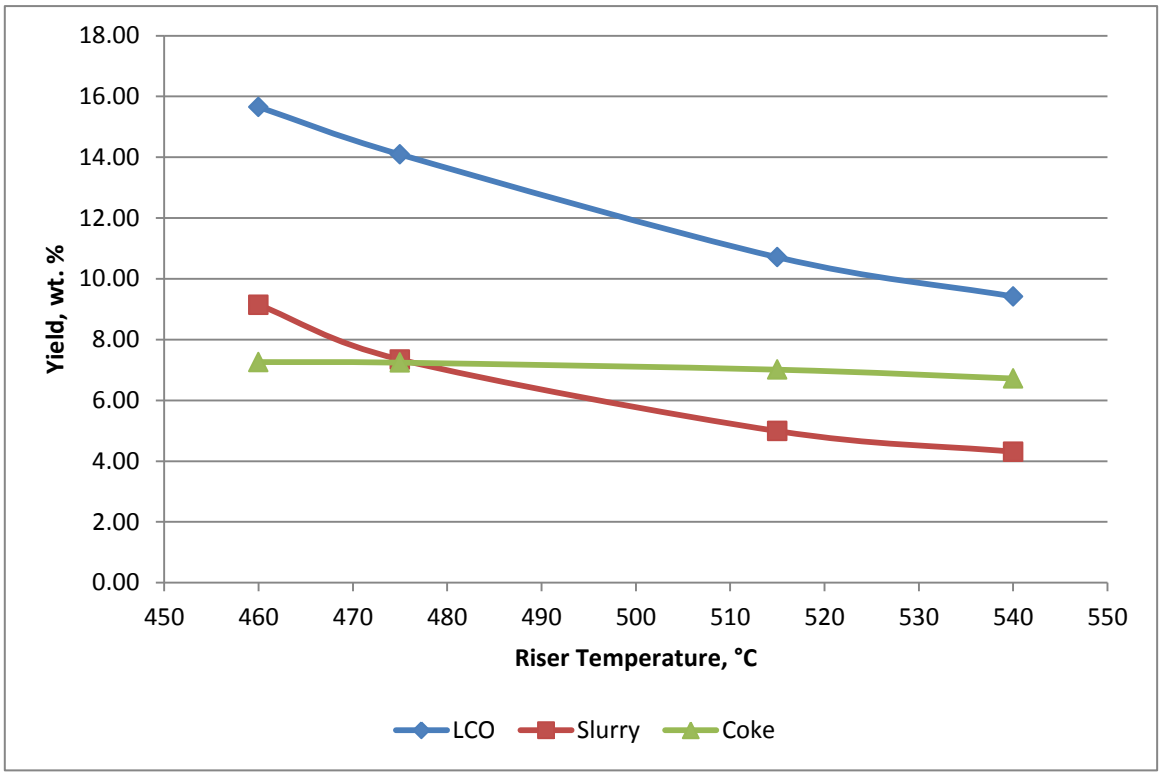

Figure 4.7 *Palm oil conversion, LCO, slurry and coke yields over riser temperature trends.*

Coke yield remains pretty much constant over the same range of temperature as can be noted from the curve with an average yield of 7.1% being posted.

4.2.3 Water, CO and CO_2

Unlike the water curve for soybean oil in Figure 4.3, the water curve for palm oil in Figure 4.8 does not evince a rising trend. At low riser temperature, a high yield of water, 10.9% is recorded and this yield suffers a decrease to 10.6% at a riser temperature of 515°C. From riser temperature 515°C to 540°C, the yield posts an increase to a final value of 10.9% again. Thus it may be said that the water yield roughly stays the same.

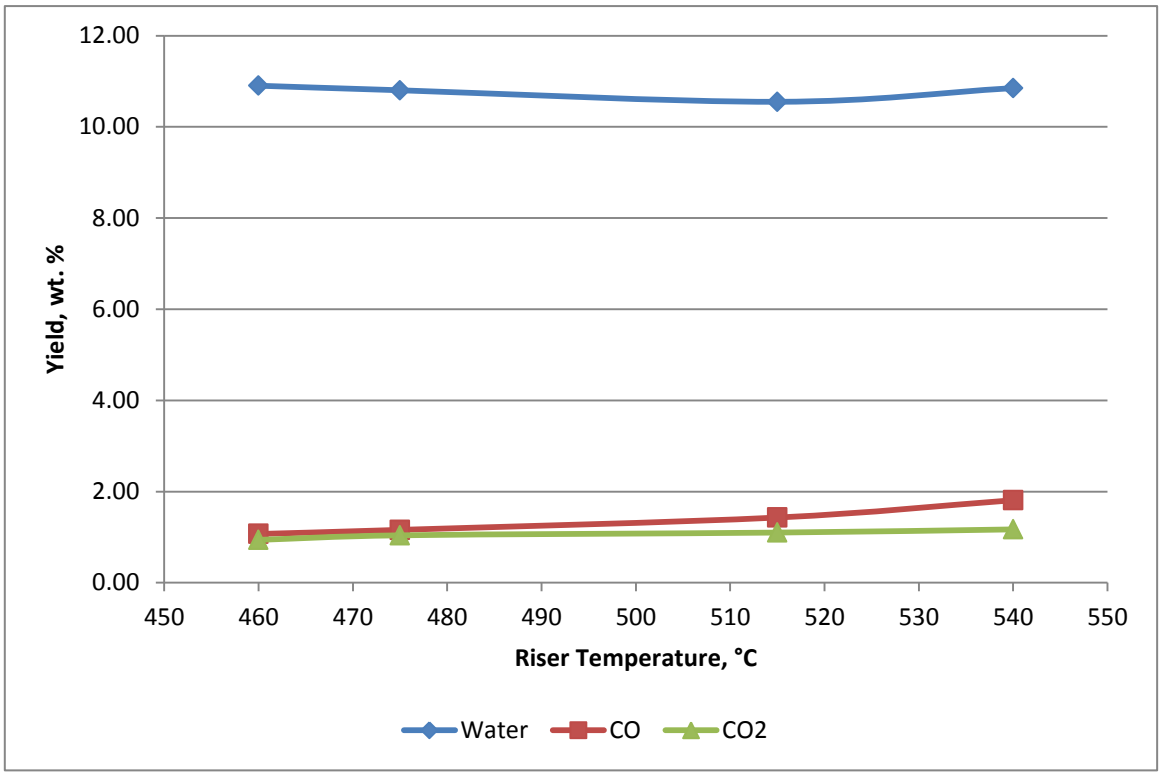

Figure 4.8 *Palm oil water, CO and CO_2 yields over riser temperature trends.*

Both CO and CO_2 yield increase with an increase in riser temperature though minimally with the CO yield posting a bigger increase as compared to CO_2 gaining 0.7% to stand at 1.8% at the highest riser temperature. CO_2 on the hand gains a meagre 0.2% ending with a paltry value of 1.2% at the final riser temperature. It is worth noting also that the CO yield posts a higher increase between the riser temperature 515°C and 540°C.

4.2.4 Product Gas Spectrum

The cracking of palm oil over the various riser processing temperatures yielded a spectrum of product gases as depicted in Figure 4.9. As previously noted in section 4.1.1, the gas yields increase with a corresponding rising riser temperature and just like in section 4.1.4, propylene and isobutane register the highest yields with the yield of propylene gaining 3.5% to a final value of 7.6% whereas the highest output of isobutane is 3.4% corresponding to a 1.7% increase in yield. The reasons for the high yields of propylene and isobutane expounded in section Product Gas Spectrum hold here also.

A match up of the three most important olefin gases with the rest of the gases depicts minimal gains and losses as is evident in Figure 4.10. Ethylene yield though posting a lower yield is on an upward in terms of percentage gain posting an increase of 1.1% whereas propylene more or less stays constant losing 0.3% to a final value of 32.6%. Conversely, the butenes record a drop of 1.6% with a final value of 27.8% being posted.

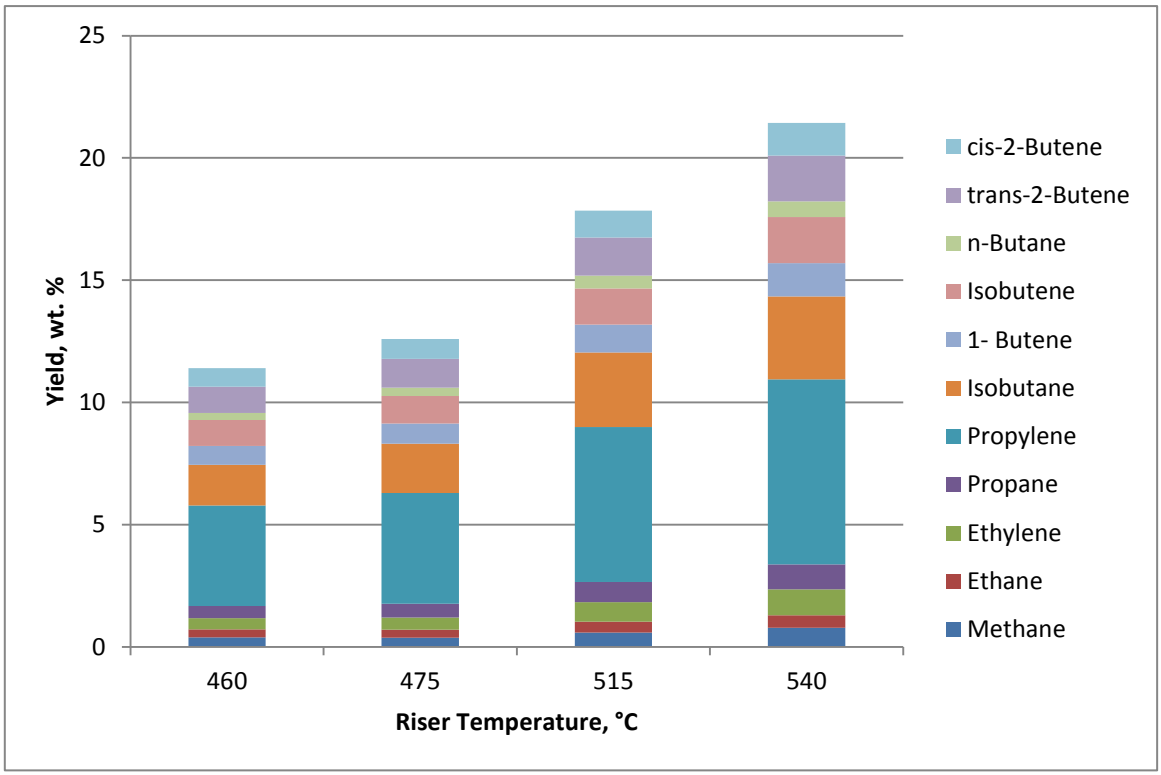

Figure 4.9 *Palm oil product gas spectrum.*

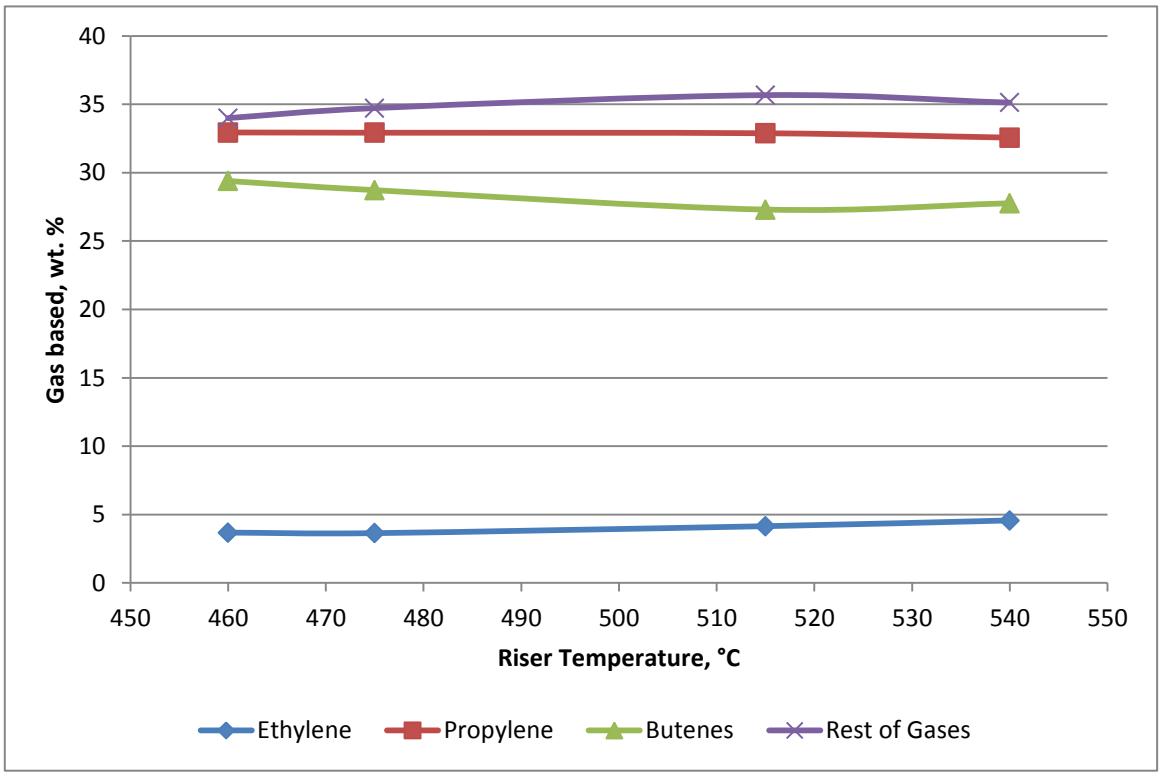

Figure 4.10 *Comparison of ethylene, propylene and butenes with the rest of the gases obtained from palm oil.*

4.3 Comparison of Soybean Oil and Palm Oil

A juxtaposition of the two vegetable oils processed is captured in the sub-sections that follow.

4.3.1 Conversion

On comparison of the two curves in Figure 4.11 for soybean oil and palm oil, it is quite evident that palm oil has a slight upper edge in terms of conversion. Palm oil has as its highest conversion a value of 67.6% at 540°C riser temperature while soybean posts a conversion of 65.4% at 550°C.

From the riser temperature 520°C, the soybean oil conversion seems to gain minimally unlike that of palm oil. It can also be noted that at the lower temperatures up to about 485°C, soybean oil performs better in terms of conversion than palm oil. This scenario paints a picture of soybean oil conversion being affected by higher temperatures and a good presumption would be that the higher the saturation content of a vegetable oil the higher its conversion at higher temperatures.

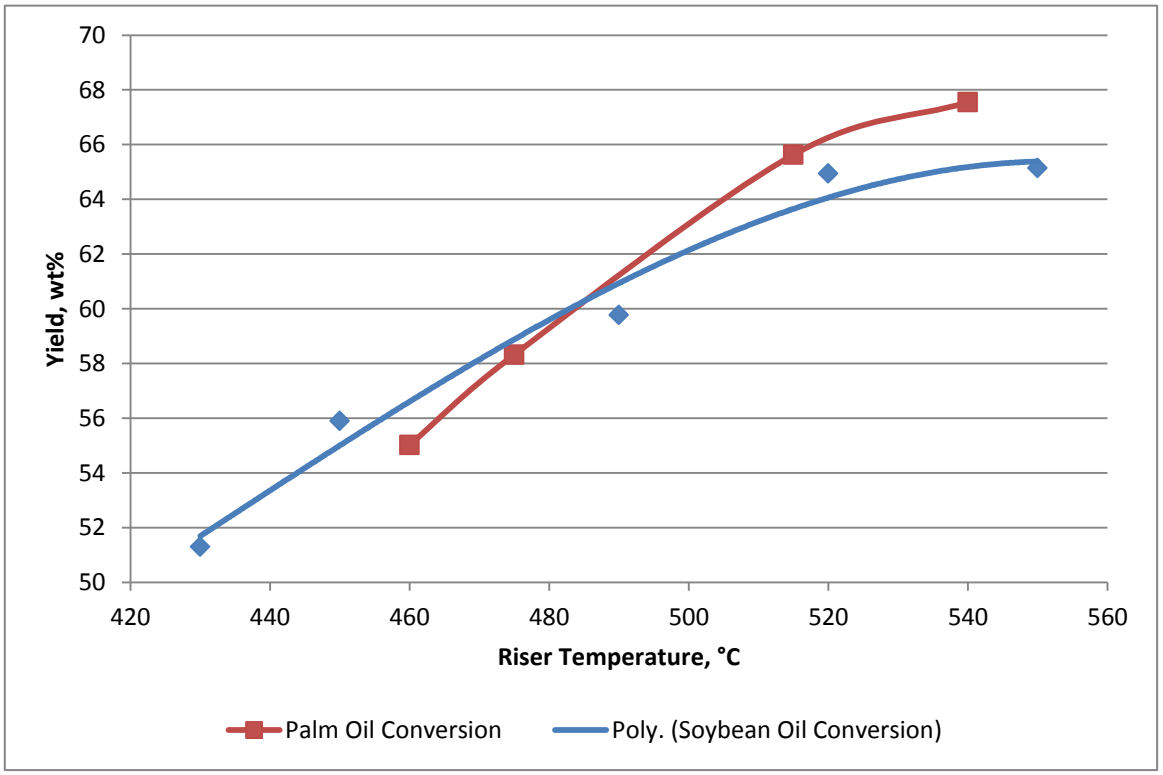

Figure 4.11 *Soybean oil and palm oil conversion trends.*

4.3.2 Gasoline

From Figure 4.12, one can evidently note that soybean oil has a better turnover of gasoline than palm oil; soybean oil posts a yield of 47.6% at 520° while palm oil posts a yield of 46.3% at a riser temperature of 515°C.

As was previously stated, both soybean and palm oil have a gasoline optimum and from a closer look at the graph this optimum value is recorded at a riser temperature of about 515°C.

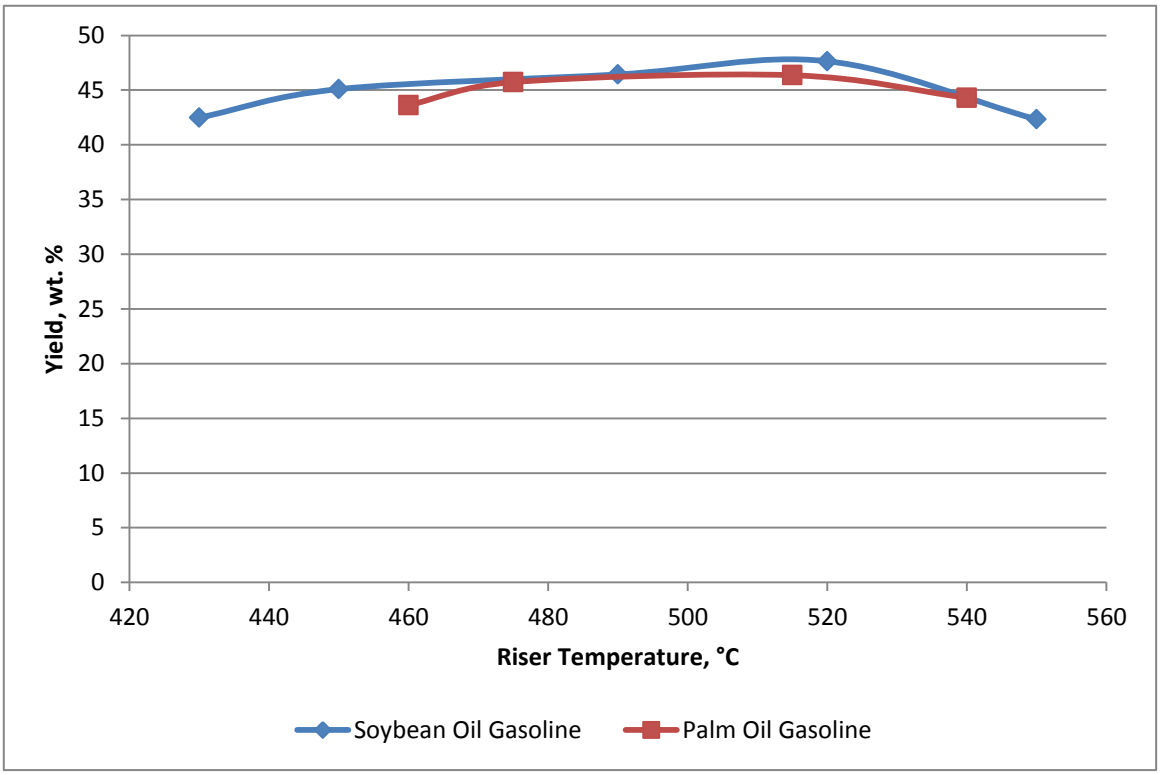

Figure 4.12 *Soybean oil and palm oil gasoline trends.*

With increase in temperature the yield of gasoline begins to decline and this is most pronounced in soybean oil than in palm oil. This is due to the fact that at higher temperatures the reactivity of olefins increases and with it comes more secondary transformations leading to the cracking of the gasoline already formed: Olefins are easily cracked than paraffins and when they are cracked the double bond is protonated forming carbenium ions which are more energetically suitable for the β-cleavage of the carbon-carbon bond. Soybean oil being more unsaturated thus suffers the brunt of the reactivity of the olefins and hence an increase in the unsaturation content of a vegetable increases the cracking of gasoline at higher temperatures.

4.3.3 Gas

A match-up of the gas yield from the two vegetable oils shows that palm oil has the upper edge with the yield of palm oil at the highest riser temperature of 540°C being 23% while that of soybean oil at the same riser temperature stands at 21% as captured in Figure 4.13. From the curves it can be drawn that an increase in unsaturation results to a decrease in the gas yield.

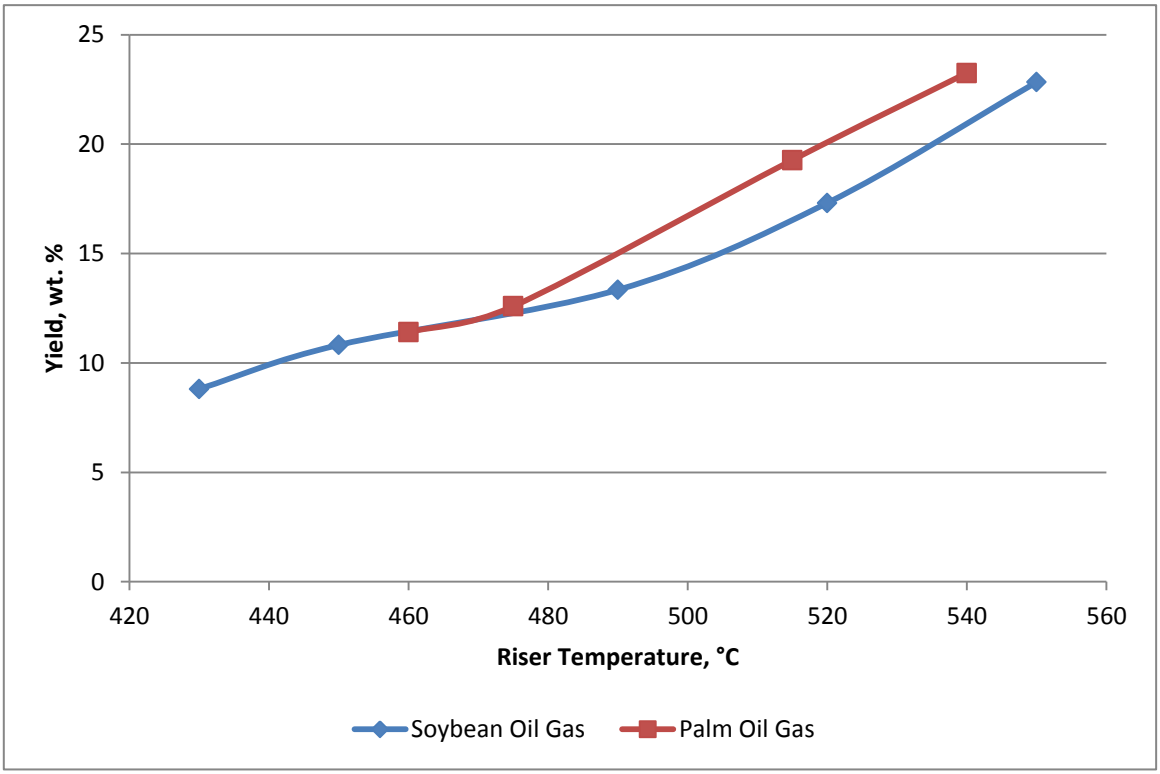

Figure 4.13 *Soybean and palm oil gas trends.*

4.3.3.1 Olefin and Paraffin Gases

A stacking up of palm oil product gas olefin yield against soybean oil product gas olefin yield purveys a picture of less output for soybean oil. At the riser temperature 540°C, palm oil has a yield of 15% olefins whilst soybean oil posts a yield of 13% which attests to the theory advanced earlier that the olefins have a higher reactivity. Hence from these observations it is clear that the higher the unsaturation content, the lower the olefin yield. These trends are shown in Figure 4.14.

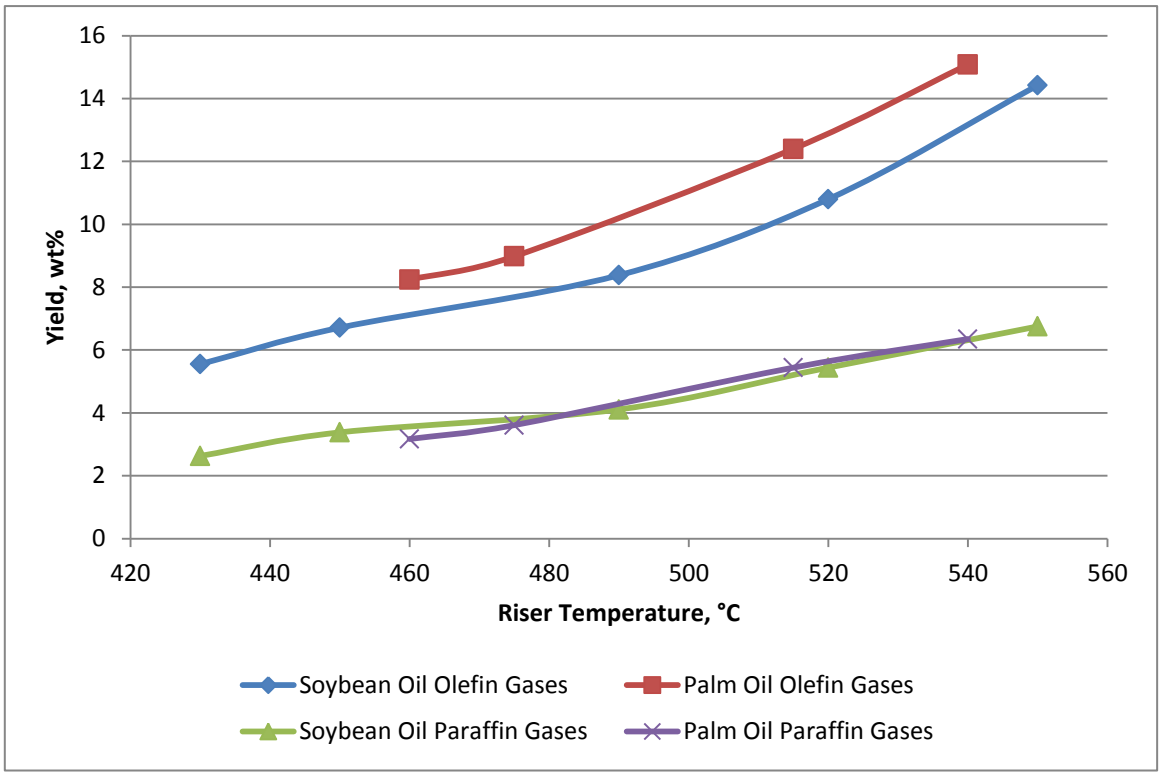

Figure 4.14 *Soybean oil and palm oil olefin and paraffin gases trends.*

A glimpse at the paraffin yield in the product gases shows no effect of unsaturation content on the yield for both soybean oil and palm oil. Both feedstocks have almost a similar value of yield with an increase in temperature translating to increased yield.

4.3.3.2 Quality of Gases

The cracking process yields industrially useful olefins which are important basic chemical building blocks as previously mentioned. These significant products are compared in Figure 4.15.

From Figure 4.15, we can draw that palm oil has got an upper edge when it comes to the yield of propylene and butene with ethylene yielding almost the same amount for palm oil and soybean oil.

Palm oil returned a propylene yield of 7.6% at a riser temperature of 540°C with soybean oil posting an output of 7.0% at the same processing temperature while the yield at riser temperature 460°C is 3.8% and 4.1% for soybean and palm oil respectively. On the other hand the yield for butene is 6.5% for pam oil and 4.8% for soybean at 540°C while at 460°C a return of 3.7% and 2.8% was posted for palm oil and soybean oil respectively.

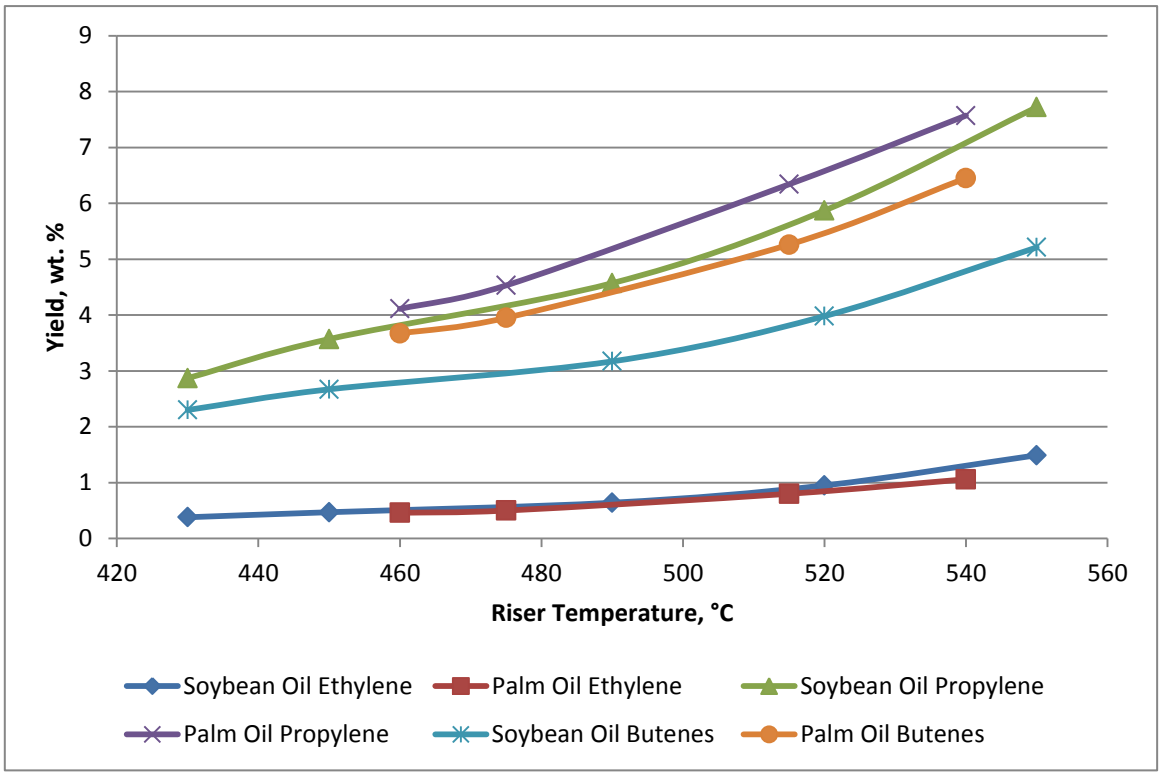

Figure 4.15 *Soybean oil and palm oil ethylene, propylene and butenes trends.*

Based on these results it can be concluded that the more unsaturated a vegetable oil is, the less the yield of the important olefin gases.

4.3.4 LCO, Slurry and Coke

It is plain to see in Figure 4.16 that soybean oil posts a higher output of LCO than palm oil. At the lowest processing temperature for palm oil, 460°C, LCO yield is 15.7% whereas at the same temperature the soybean oil yields 17%. These yields decrease with increase in riser temperature and the yield for palm oil LCO at 540°C – highest palm oil riser temperature – is 9.4% while soybean oil has an output of 11.7% at the same temperature.

A comparison of the slurry and coke curves show that both vegetable oils yield pretty much the same yield at the same riser temperature.

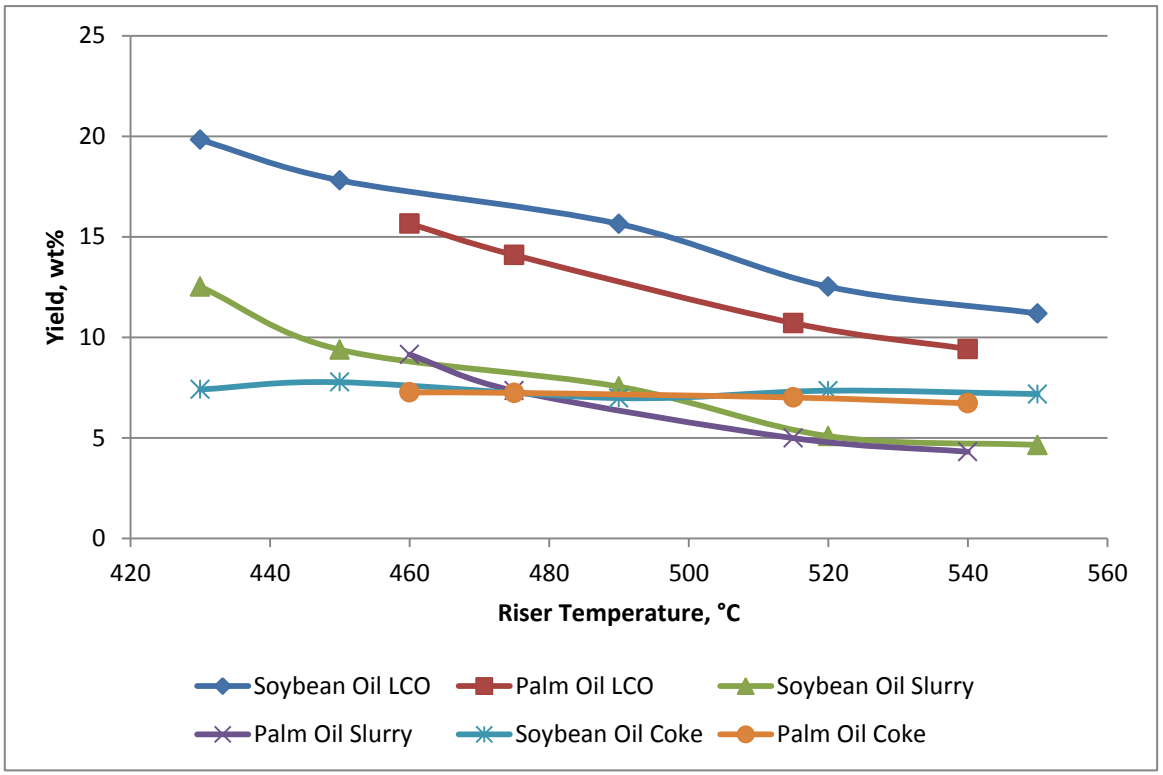

Figure 4.16 *Soybean oil and palm oil LCO, slurry and coke trends.*

It follows then that it would be safe to say that as the unsaturation content increases so does the yield of the LCO fraction. The effect of the catalyst also cannot be ignored in trying to justify the declining yield of the LCO and the slurry. This is because NEKTOR enhances the cracking of the bottoms product thus a decrease in the yield of the bottoms product is to be expected. In relation to the cracking temperature, it can be argued based on these results that low temperatures favour a higher output of the bottoms product.

4.3.5 Water, CO and CO_2

A match-up of the water curves in Figure 4.17 shows the soybean oil water curve is on an upward trend with an increasing riser temperature whereas the palm oil water curve more or less stays the same. Palm oil has the upper hand in terms of water yield throughout the processing temperatures.

A few plausible reasons could perhaps help in unravelling these trends. The increase in water yield with increase in temperature can be attributed to the hydrogen loss experienced at high temperatures by the carbonium ion. This leads to the formation of the carbenium ion as pointed out earlier on in the catalytic cracking mechanism. Hence the tendency to form water increases due to the availability of hydrogen and the oxygen available from the triglycerides. Thus it can be said that the hydrodeoxygenation reaction pathway is witnessed when vegetable oils are catalytically cracked at high temperatures. It may also be argued

that the decarbonylation route is the dominant pathway over decarboxylation since the decarbonylation route favours water formation.

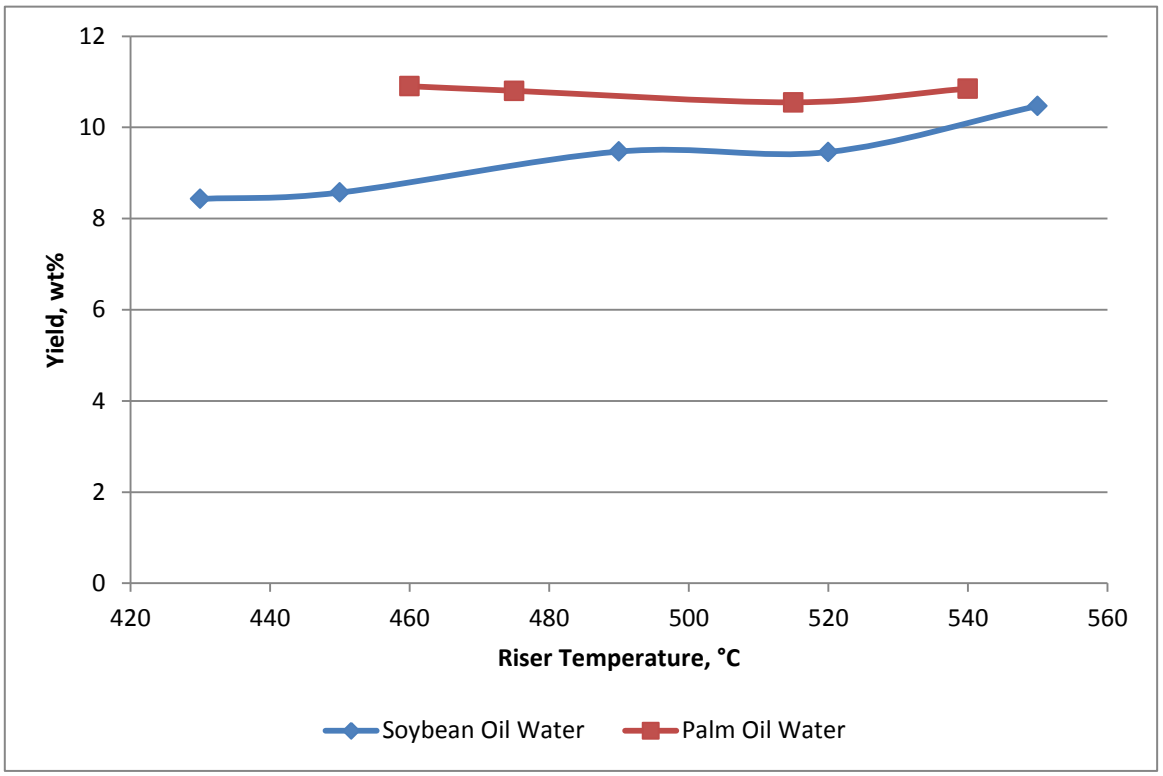

Figure 4.17 *Soybean oil and palm oil water trends.*

On comparing the yield of CO and CO_2 for soybean oil and palm oil in Figure 4.18, it is plain to see that palm oil posts a higher yield of the two gases than soybean oil with the output increasing with an increasing riser temperature. A trend can be observed for soybean oil whereby from a riser temperature of about 520°C there is a sharp increase in the yield of both CO and CO_2. This trend is not conclusive enough to be attributed to the reactivity of the unsaturated vegetable oils; as to whether there is any relationship is subject to further analysis.

What is without doubt though, is that as pertains to the reaction mechanism for the catalytic cracking of vegetable oil, one can argue based on these results that the decarbonylation pathway is the dominant one as compared to the decarboxylation pathway based on the premise that a higher percentage of CO is yielded.

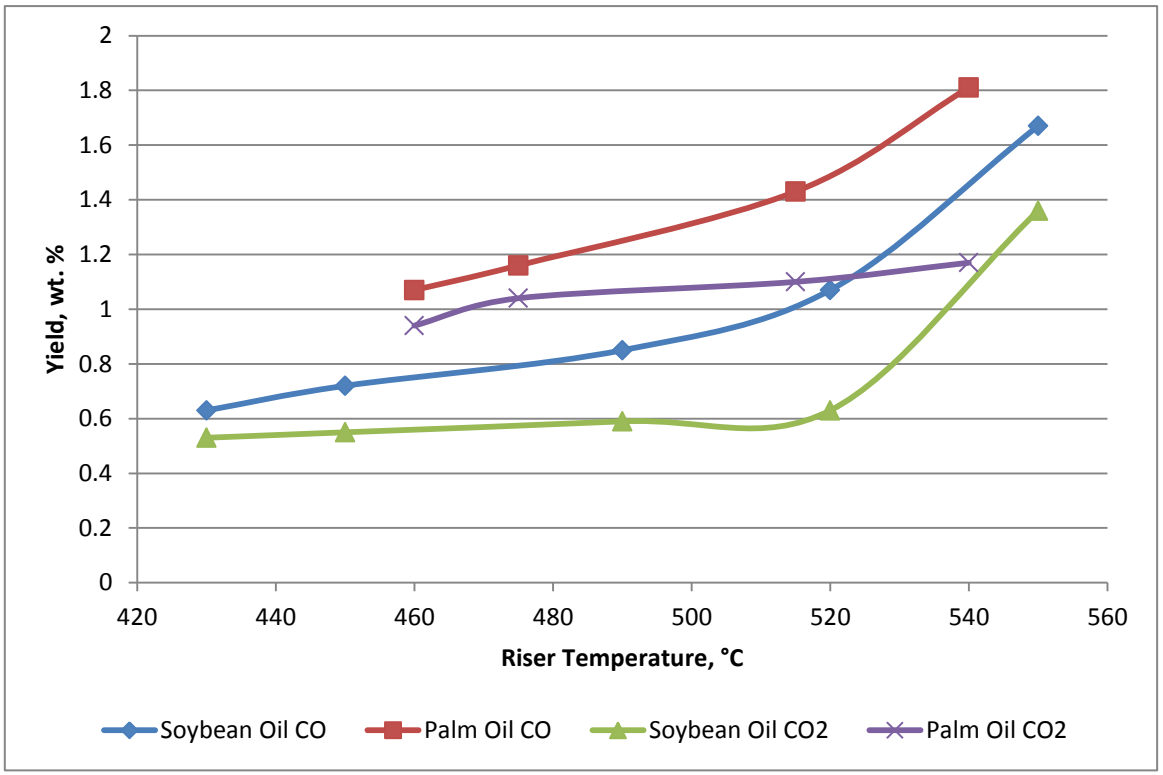

Figure 4.18 *Soybean oil and palm oil CO and CO_2 trends.*

4.4 Gasoline Quality

The quality of gasoline obtained from the two oils were analysed in the following sections on the basis of the octane numbers and the constituents in the gasoline.

4.4.1 Octane Numbers

The RON and MON values obtained from probes of palm oil and soybean oil are plotted against various parameters in the graphs that follow.

4.4.1.1 Riser Temperature

Figure 4.19 purveys a picture of increasing octane numbers with an increase in the riser temperature. The rise of the RON and MON values is a consequence of the increase in the aromatics with RON gaining more than MON. Both soybean and palm oil register an increase of roughly 0.8 RON units for an increase of 10°C riser temperature whilst the MON increase for both soybean oil and palm oil is about 0.5 units for an increase in 10°C riser temperature. The RON and MON values for soybean oil are 90 and 81 respectively at the lowest riser temperature of 430°C. At the riser temperature of 550°C the RON and MON values are 98 and 86. This corresponds to 8 RON units and 5 MON units increase. Palm oil on the hand has a lower increase in the octane numbers when compared to soybean oil. RON increases by 6 units whereas MON by 4 units. At 460°C the RON and MON values are 90 and

81 respectively whilst the RON and MON values are 96 and 85 respectively at the highest riser temperature of 540°C.

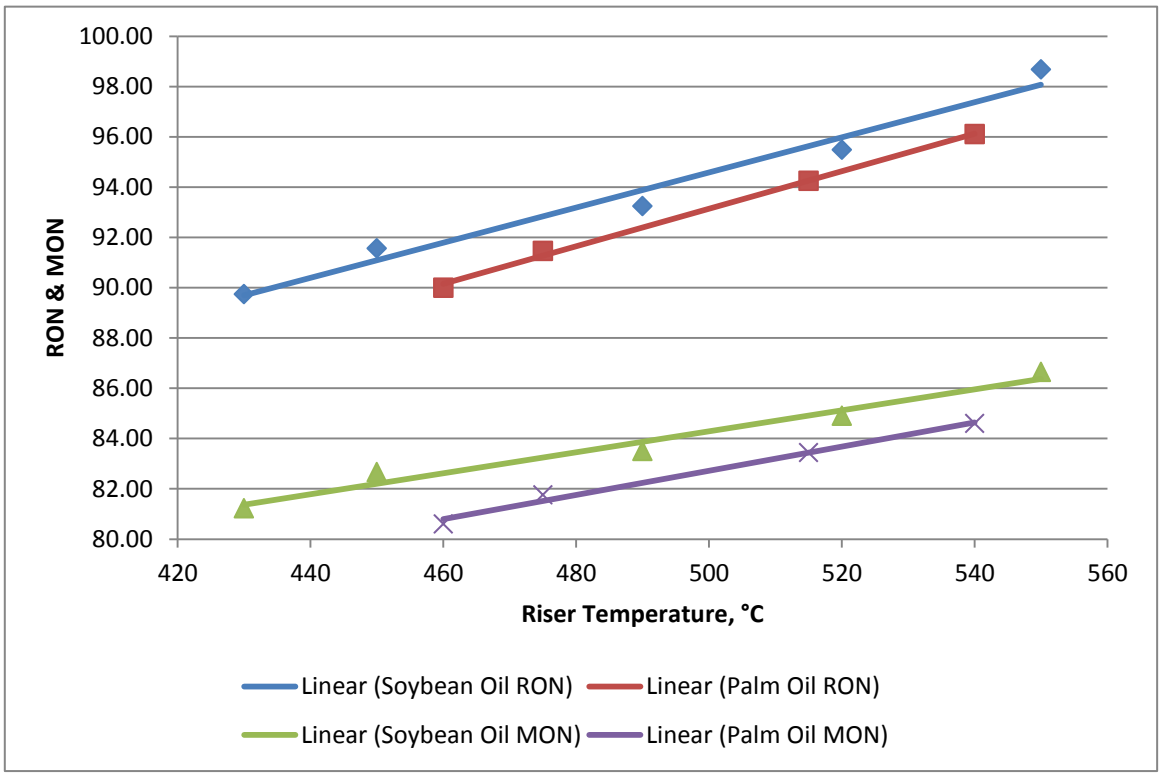

Figure 4.19 *Soybean oil and palm oil RON and MON over riser temperature trends.*

4.4.1.2 Conversion

It can be drawn from Figure 4.20 that both RON and MON increase with conversion. The higher conversion causes an increase in the RON and MON values as a consequence of the increase in the aromatic contents and a decrease in the paraffinic contents which are considered octane depressors. The reactivity of the vegetable oils plays a key role in the RON and MON values as is quite evident since soybean oil posts higher values for both RON and MON respectively. The change observed is roughly 4 RON units for a 10% conversion for both soybean oil and palm oil while about 2 MON units for a 10% conversion is noted for soybean and palm oil.

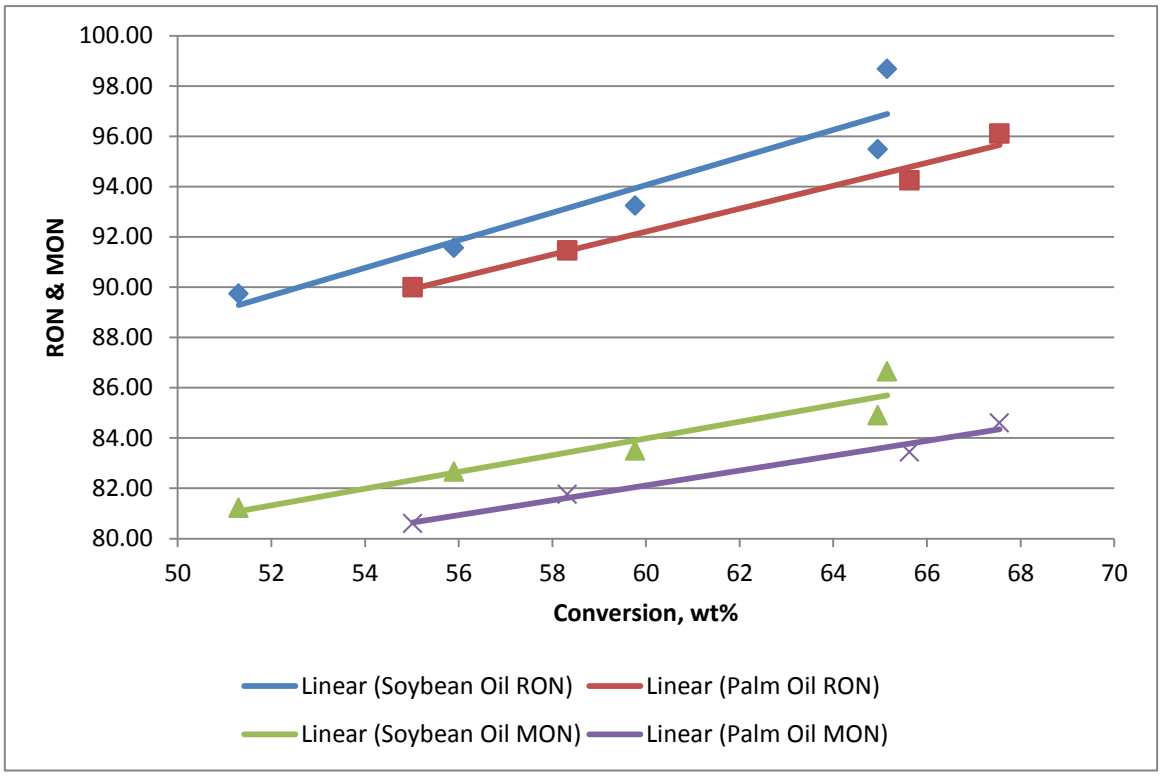

Figure 4.20 *Soybean oil and palm oil RON and MON trends with respect to conversion*.

4.4.1.3 Aromaticity

As has been mentioned in section 4.4.1.1, the principal driving force for the rise in the octane numbers is the increase in aromatics. From Figure 4.21, the RON values for both oils project a similar and almost equivalent trend. For 1 unit gain of soybean oil RON there is a 4.1% increase in the aromatic content whereas a 3.5% increase is recorded for palm oil. In the case of MON, a 6.9% increase leads to a gain of 1 unit for soybean oil while for palm oil a unit gain is due to a 5.6% rise in aromatics.

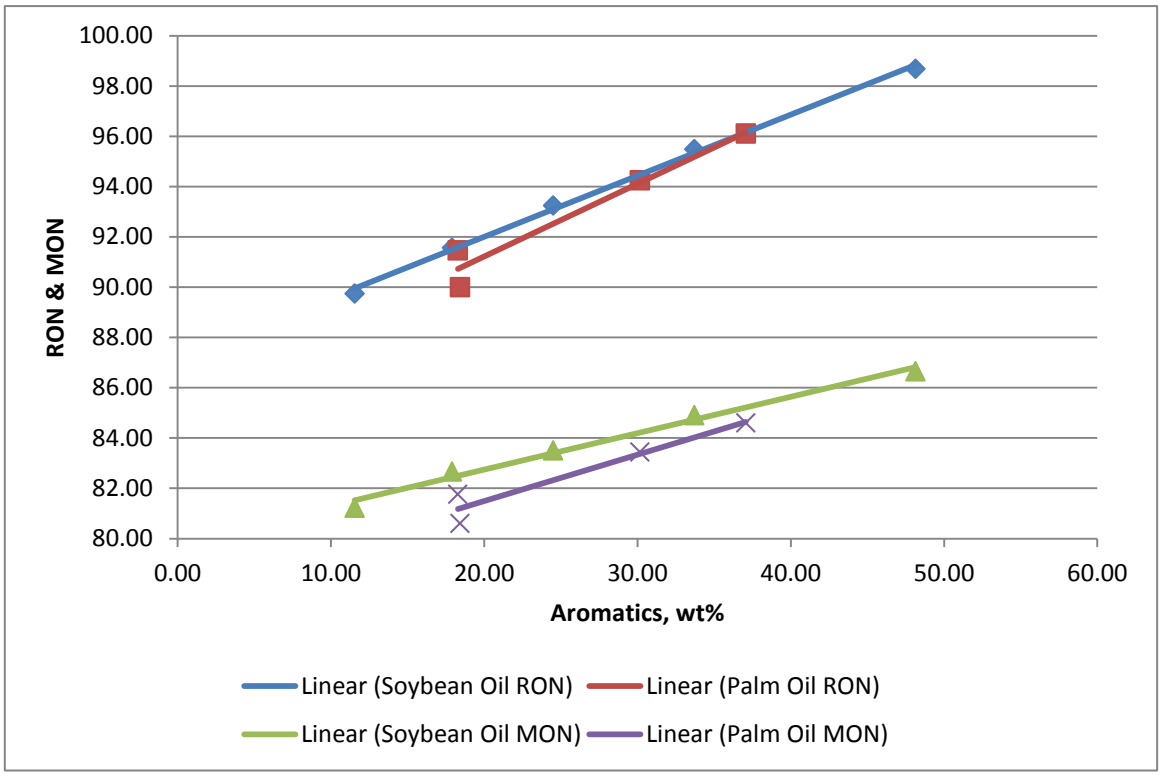

Figure 4.21 *Soybean oil and palm oil RON and MON trends with respect to aromatics.*

4.4.2 Gasoline Constituents

From Figure 4.22, it can be noted that the aromatic content of soybean increases from 11% to 45% whereas that of palm oil increases from 17% to 37%. This increase of the aromatic contents occurs at the expense of the olefins and the paraffins. As can be deciphered, the increase in soybean oil is more pronounced than in palm oil. This can be correlated to the fact that as the degree of unsaturation increases in a vegetable oil so does the aromatic content in the product.

The reason for this being that the reactivity of triglycerides increases with a commensurate increase in their unsaturation content as earlier expounded. Hence soybean oil having a higher unsaturation content than palm oil will have more aromatic content due to the role of secondary transformations. The rationale behind this argument is that the olefins produced by the cracking of the double bonds in the soybean oil take part in aromatization reactions as depicted in the reaction mechanism pathway in Figure 2.14.

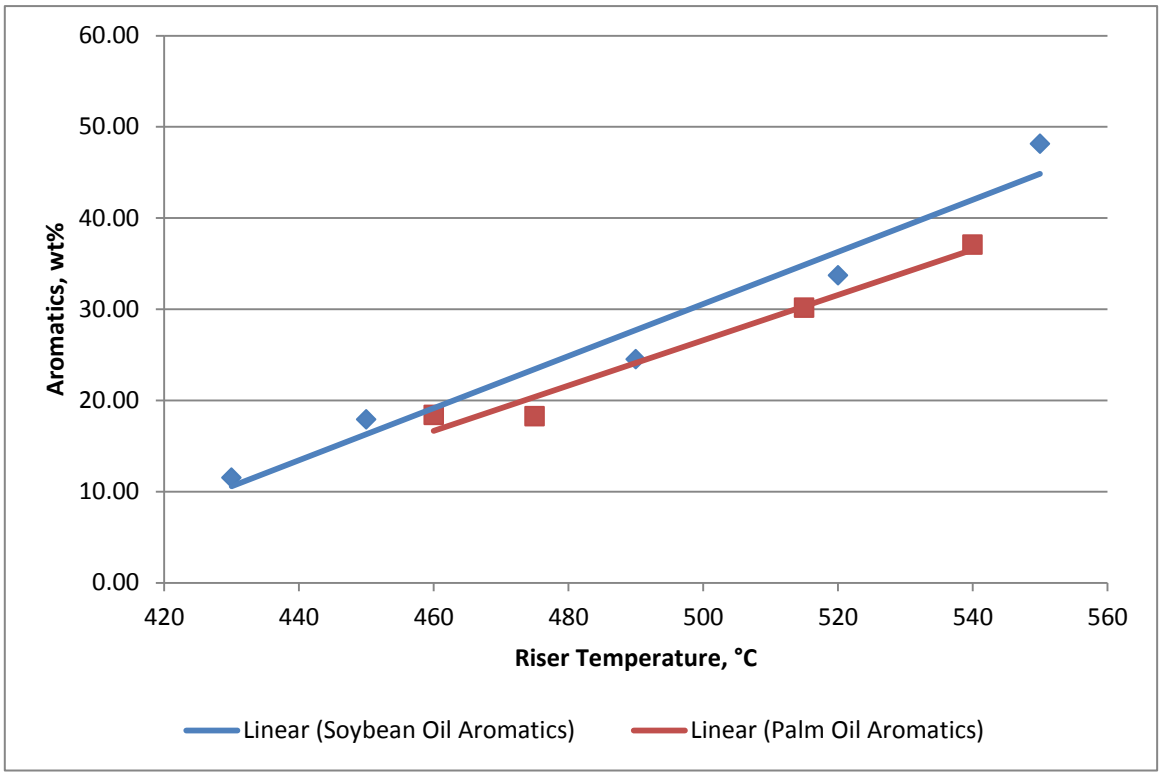

Figure 4.22 *Soybean oil and palm oil gasoline aromatic content trends.*

The effect of the reactivity of the olefins is plain to see in Figure 4.23. From the graph, we can deduce that the yield of olefins of soybean oil in gasoline is less than that of palm oil with the output decreasing with an increase in riser temperature. Soybean oil posts an olefin yield of 23% at a riser temperature of 430°C and this yield slumps down to a value of 16% at 550°C. On the other hand palm oil has got an olefin yield of 31% at its lowest riser temperature of 460°C with this output declining to 22% at 540°C; a value almost close to the value obtained by the lowest soybean oil riser temperature. Hence the higher the unsaturation content the lower the olefin yield.

The paraffins content in the gasoline obtained from both oils as had been noted earlier also suffer a decrease in yield as can be deciphered from Figure 4.23. The soybean oil paraffins yield drops from 66% to 39% – a 27% slump – from a riser temperature of 430°C and 550°C respectively while that of palm oil suffers a drop of 12% to a final value of 41% at a riser temperature of 540°C. Though soybean oil gasoline has a higher content of paraffins initially than palm oil gasoline, it suffers the brunt of the reactivity of the olefins. The carbenium ion intermediates from the olefins are responsible for the further cracking of the paraffins. Thus the higher the unsaturation content of a vegetable oil the greater will be the influence of the olefin reactivity on the gasoline paraffins yield.

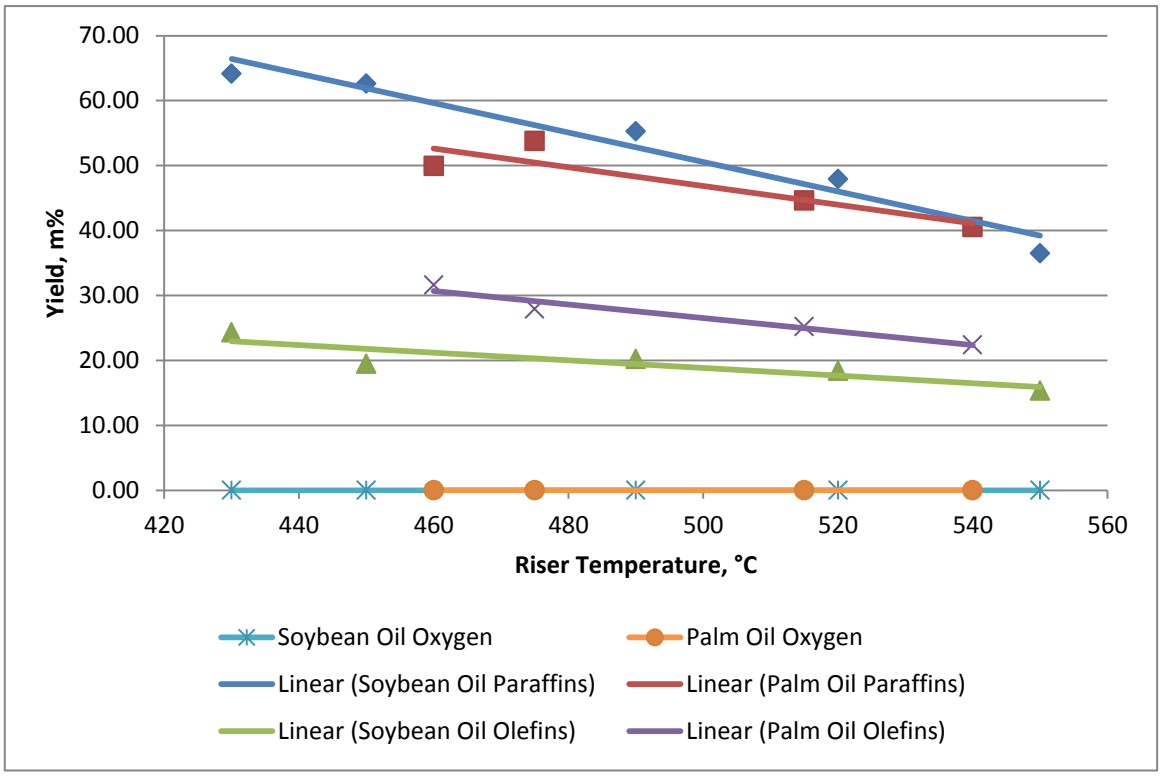

Figure 4.23 *Soybean oil and palm oil gasoline constituents' trends.*

As can be noted in Figure 4.23, the oxygen content in both oils is zero throughout the trials implying that there are no oxygenates in the gasoline product due to the complete conversion of the oxygen in the oils to the inorganic products comprising water, CO and CO_2 through the deoxygenation process.

5 CONCLUSION AND OUTLOOK

The damning ICCP synthesis report behoves all stakeholders to work towards decarbonizing the transport sector and one way of achieving this goal is to embrace the biofuels sector. Granted, the biofuels sector cannot ultimately compete on the same plane with the petroleum fossil fuel but will nonetheless go a long way in helping to bring down the greenhouse gas emissions to manageable levels.

Though different in structure – unsaturation content – palm oil and soybean oil which account for over 60% of the total vegetable oil production, both posted good conversion rates. The effect of the unsaturation content of the vegetable oil was brought to the fore during the trials with a higher conversion obtained by palm oil than soybean oil implying that conversion decreases with an increase in the unsaturation content.

Higher unsaturation content was also shown to have a corresponding effect on the product spectrum by raising the reactivity of the vegetable oils. Both oils posted a gasoline optimum at a temperature of about 515°C a phenomenon explained by the reactivity of the olefins. Given the fact that soybean oil has higher unsaturation content, it thus showed a greater decline in gasoline yield due to higher reactivity of the olefins.

An increase in the number of double or more bonds in the vegetable oil structure also had an impact on the gas yield with palm oil recording a better output than soybean oil; soybean oil also saw its olefin gases yield decrease as compared with palm oil implying that with an increase in unsaturation comes with it a drop in the yield of olefin gases. Substantial amounts of the industrially important olefin gases comprising ethylene, propylene and butene were recorded during the trial with yields increasing with a corresponding rising riser temperature.

The LCO and slurry yields were also subject to the influence of the unsaturation content with soybean oil posting higher yields of the two products. The low riser temperatures showed a propensity for a higher yield of LCO and slurry and hence given a scenario whereby diesel is the desired product then cracking at low temperatures should suffice.

High RON and MON values were also recorded during the trials; values comparable to commercial values. Oxygen containing compounds were completely transformed to CO, CO_2 and water as attested to by the lack of oxygenates in the IROX analysis while an increase in secondary transformations as a consequence of an increase in the unsaturation content was the reason behind the increase in the aromatic content in soybean oil.

Environmental concerns currently dictate the quality of gasoline that ought to be sold at the pump and as per the European Commission Gasoline Specifications, the gasoline should have a RON of 95 and an aromatic level less than 35% volume. Given the results obtained in

the trials, one can say that processing the vegetable oil at a temperature of 520°C would yield the gasoline that meets the desired standards.

A roadmap for the future would perhaps involve trying to crack vegetable oils using other catalysts. For instance it would be interesting to find out how the product spectrum looks like when vegetable oil is cracked using Protagon; a catalyst which is geared towards the maximization of propylene. Another interesting venture would be a trial of diesel maximisation catalysts such as NOUMUS – Dmax and DieseliseR in a bid to check if there will be any significant increase in the middle distillate outputs. This is due to the plain reason that these catalysts are geared towards the bottoms maximization.

An in-depth analysis of the deoxygenation process would also offer a comprehensive understanding of the various routes with the effect of catalyst type being investigated to ascertain the routes they promote based for instance on their acidity. There is also a need to establish if there are any oxygenates such as alcohols, aldehydes, ketones and phenolic components present in the LCO and the slurry so as to know if all the oxygen in the vegetable oils are converted in the deoxygenation process. An analysis to determine the aromatic contents of the LCO is also paramount in order to establish the quality of the LCO which is normally used as a diesel blend.

Finally, the Ecofining process is a trailblazer in proving that existing refinery units such as the FCC unit can be put to use in the production of biofuels. Hence it is high time a leap is made from the pilot plant scale to an industrial scale with the FCC unit offering the advantage that there is no consumption of hydrogen gas when compared to the Ecofining process. The projected fall in world vegetable oil prices should also offer impetus to their use in the FCC units and thus refinery companies should leverage on this.

BIBLIOGRAPHY

1. World Population Prospects: The 2012 Revision: UNPD; 2013 [cited 2014 December]. Available from: http://esa.un.org/unpd/wpp/Documentation/publications.htm.
2. Key World Energy Statistics: IEA; 2014 [cited 2014 December]. Available from: http://www.iea.org/publications/freepublications/publication/KeyWorld2014.pdf.
3. BP Energy Outlook 2035 2014 [cited 2014 December]. Available from: http://www.bp.com/content/dam/bp/pdf/Energy-economics/Energy-Outlook/Energy_Outlook_2035_booklet.pdf.
4. Eyton D. Strategic role of technological advances in unlocking available and affordable oil and gas supplies: BP; 2014 [cited 2014 December]. Available from: http://www.bp.com/en/global/corporate/press/speeches/international-petroleum-week-2014.html.
5. Trends in Atmospheric Carbon Dioxide: Earth System Research Laboratory, Global Monitoring Division; 2015 [updated January 15, 2015; cited 2015 January]. Available from: http://www.esrl.noaa.gov/gmd/ccgg/trends/weekly.html.
6. World Energy Outlook 2012 [press release]. Paris: IEA2012.
7. Fifth Assessment Report (AR5) - Climate Change 2014 Synthesis Report: IPCC; 2014 [cited 2014 December 2014]. Available from: https://www.ipcc.ch/pdf/assessment-report/ar5/syr/SYR_AR5_SPM.pdf.
8. Speight JG. The Biofuels Handbook: Royal Society of Chemistry; 2011.
9. OECD-FAO Agricultural Outlook 2014: OECD-FAO; 2014.
10. Major Vegetable Oils: United States Department of Agriculture - Foreign Agricultural Service [cited 2014 December]. Available from: http://apps.fas.usda.gov/psdonline/psdReport.aspx?hidReportRetrievalName=Table+03%3a+Major+Vegetable+Oils%3a+World+Supply+and+Distribution+%28Commodity+View%29&hidReportRetrievalID=533&hidReportRetrievalTemplateID=5.
11. FAOSTAT [Internet]. FAO Statistics Division. [cited December 2014]. Available from: http://faostat3.fao.org/home/E.
12. Codex Alimentarius Fats, Oils and Related Products: Codex Alimentarius; 2001.
13. Facts about palm oil and rainforests [cited 2014 December]. Available from: https://www.rainforest-rescue.org/topics/palm-oil.
14. Palm Oil-Specification Department of Standards Malaysia (Standards Malaysia); 2007.
15. Sustainable Palm Oil: Round Table on Sustainable Palm Oil (RSPO); [cited 2014 December]. Available from: http://www.rspo.org/.
16. Demirbas A. Biorefineries: For Biomass Upgrading Facilities. London: Springer - Verlag; 2010.
17. Production Process: Biox Corporation; [cited 2014 December]. Available from: http://www.bioxcorp.com/production-process/.
18. Fuel properties comparison: Alternative Fuels Data Centre; [cited 2014 December]. Available from: http://www.afdc.energy.gov/fuels/fuel_comparison_chart.pdf.
19. Biodiesel: Alternative Fuels Data Centre , U. S. Department of Energy; [cited 2014 December 2014]. Available from: http://www.afdc.energy.gov/fuels/biodiesel_blends.html.
20. Höfer R. Sustainable Solutions for Modern Economies. Cambridge: Royal Society of Chemistry; 2009.
21. Hydroprocessing - Ecofining: UOP; [cited 2014 December]. Available from: http://www.uop.com/hydroprocessing-ecofining/.
22. Green Refinery: Bio-based News; [cited 2014 December]. Available from: http://bio-based.eu/news/green-refinery/.
23. Fabrizio Cavani GC, Siglinda Perathoner, and Ferruccio Trifiró. Sustainable Industrial Processes. Weinheim: WILEY-VCH Verlag GmbH & Co. KGaA; 2009.

24. Honeywell Green Jet Fuel™ To Power Flights Transporting The Brazil National Soccer Team During The 2014 FIFA World Cup™2014 December 2014. Available from: http://honeywell.com/News/Pages/Honeywell-Green-Jet-Fuel-To-Power-Flights-Transporting-The-Brazil-National-Soccer-Team-During-The-2014-FIFA-World-Cup.aspx.
25. Renewable Fuel Standard (RFS): United States Environmental Protection Agency (EPA); [cited 2014 December 2014]. Available from: http://www.epa.gov/otaq/fuels/renewablefuels/.
26. Renewable Energy - Biofuels: European Commission; [cited 2014 December]. Available from: http://ec.europa.eu/energy/renewables/biofuels/biofuels_en.htm
27. The Refinery Process: American Fuel & Petrochemical Manufacturers (AFPM); [cited 2014 December 2014]. Available from: (http://www.afpm.org/The-Refinery-Process/) . .
28. Sadeghbeigi R. Fluid Catalytic Cracking Handbook. Third ed. Waltham, MA: Butterworth Heinemann; 2012.
29. Wilson J. Fluid Catalytic Cracking Technology and Operation. Tulsa, Oklohoma: PennWell Publishing Company; 1997.
30. Zeolites in Chemical Engineering: Verlag Process Engineering GmbH; 2011.
31. Zeolites [Internet]. [cited 2014]. Available from: http://zeoliteandcatalysis.blogspot.co.at/.
32. Paul B. Venuto and E. Thomas Habib J. Fluid Catalytic Cracking with Zeolite Catalysts. New York and Basel: Marcel Dekker, INC; 1979.
33. Scherzer J. Octane-Enhancing Zeolitic FCC Catalysts. New York and Basel: Marcel Dekker, INC.; 1990.
34. TY Leng AM, S Batia. Catalytic conversion of palm oil to fuels and chemicals. The Canadian Journal of Chemical Engineering. 1999;77(1):156-62.
35. Kostas Triantafyllidis AL, Michael Stöcker. The Role of Catalysis for the Sustainable Production of Bio-fuels and Bio-chemicals. Oxford: Elsevier; 2013.
36. Reichhold A. Entwicklung von Reaktions / Regenarationssystemen für Adsorptions / Desorptionsprozesse und für katalytisches Cracken auf der Basis von intern zirkulierenden Wirbelschichten [Dissertation]: Vienna University of Technology; 1996.
37. Schablitzky H. Katalytische Konversion pflanzicher Öle in Kohlenwasserstoffe mittels vollkontinuierlicher FCC- Pilotanlage [Dissertation]: Vienna University of Technology; 2008.
38. Schönberger C. Fischer-Tropsch und Fluid Catalytic Cracking: Zwei alternative Technologien zur Herstellung von flüssigen Treibstoffen aus Biomasse [Dissertation]: Vienna University of Technology; 2010.
39. Bielansky P. Alternative Feedstocks in Fluid Catalytic Cracking [Dissertation]: Vienna University of Technology; 2012.
40. Gunstone FD. Vegetable Oils in Food Technology. Second ed: Wiley Blackwell; 2011.
41. Vegetable oils data: GEMIS - Globales Emissions-Modell integrierter Systeme; [cited 2014 December]. Available from: http://www.iinas.org/gemis-de.html.
42. New opportunities for co-processing renewable feeds in refinery process 2008 [cited 2014 December]. Available from: https://grace.com/catalysts-and-fuels/en-us/Documents/103-New%20Opportunities%20for%20Co-Processing%20Renewable%20Feeds.pdf.
43. NEKTOR-ULCC Catalysts: Grace Refining Technologies

[cited 2014 December]. Available from: https://grace.com/catalysts-and-fuels/en-us/Documents/Nektor%20PDS%20Final%20050114.pdf.
44. IROX 2000 Gasoline Analyzer: Grabner Instruments; [cited 2014 December]. Available from: http://www.grabner-instruments.com/products/fuelanalysis/irox2000.aspx.
45. Hofer G. Steuerung des Katalysator / Öl-Verhältnisses einer FCC-Pilotanlage mit intern zirkulierender Wirbelschicht [Masterarbeit]: Vienna University of Technology; 2014.

TABLE OF FIGURES

TABLE OF TABLES

ABBREVIATIONS

AR5	Fifth Assessment Report
ASTM	American Society for Testing and Materials
BP	British Petroleum
C/O	Catalyst / Oil
EISA	Energy Independence and Security Act
EPA	Environmental Protection Agency
ETBT	Ethyl Tertiary Butyl Ether
FAME	Fatty Acid Methyl Ester
FAO	Food and Agriculture Organization
FBP	Final Boiling Point
FCC	Fluid Catalytic Cracking
FFA	Free Fatty Acid
FFB	Fresh Fruit Bunch
FFV	Flexible Fuel Vehicles
FID	Flame Ionization Detector
FTIR	Fourier Transform Infrared
GC	Gas Chromatography
GHG	Greenhouse Gas
HCO	Heavy cycle oil
HCV	High Conservation Value
HVO	Hydrotreated Vegetable Oil
IBP	Initial Boiling Point
IEA	International Energy Agency
IPCC	Intergovernmental Panel on Climate Change
KOH	Potassium Hydroxide
LCO	Light cycle oil
LPG	Liquefied Petroleum Gas
MERCUSOR	*Mercado Común del Sur*
NaOH	Sodium Hydroxide

NDIR	Non-Dispersive Infrared
OECD	Organisation for Economic Co-operation and Development
RED	Renewable Energy Directive
RFS2	Renewable Fuel Standard 2
RSPO	Roundtable on Sustainable Palm Oil
RTD	Riser Termination Device
SimDist	Simulated Distillation
TFY	Total Fuel Yield
TID	Thermal Ionization Detector
UNPD	United Nations Population Division
USD	United States Dollar
VGO	Vacuum Gas Oil

NOTATIONS

A_{Reg}	Area of regenerator
$d_{Reg,i}$	Diameter of regenerator, inside
$d_{Return,o}$	Diameter of return flow tube, outside
g	Gravitational force
M_C	Molecular weight of carbon
$\dot{m}_{C\_coke}$	Mass flow of carbon in coke
$\Delta m_{Catalyst}$	Mass change in catalyst
M_{CO}	Molecular weight of carbon monoxide
M_{CO_2}	Molecular weight of carbon dioxide
$m_{Crack\ gas}$	Mass of crack gas
m_{Feed}	Mass of feed
$\dot{m}_{Feed}$	Mass flowrate of feed
$m_{Gasoline}$	Mass of gasoline
$\dot{m}_{H\_coke}$	Mass flowrate of hydrogen in coke
M_{H_2}	Molecular weight of hydrogen
M_{H2O}	Molecular weight of water
$\Delta m_{Pre-heat\ flask}$	Mass change of pre-heat flask
n_D	Refractive index
$\Delta(\Delta p_{Reg})$	Pressure drop change in regenerator
ρ_{CO}	Density of carbon monoxide
ρ_{CO_2}	Density of carbon dioxide
ρ_{H20}	Density of water
Δt	Time change
$\dot{V}_{CO}$	Volume flowrate of carbon monoxide
$\dot{V}_{CO_2}$	Volume flowrate of carbon dioxide
$\dot{V}_{H2O}$	Volume flowrate of water
Wijs	Iodine value

APPENDIX A: NEW PILOT PLANT PHOTO

APPENDIX B: NEW PILOT PLANT P&ID